FINAL REPORT –

RESEARCH PROGRAM ON SEALED CELLS

UNDER NATIONAL AERONAUTICS
AND SPACE ADMINISTRATION

GOULD-NATIONAL BATTERIES, INC.
RESEARCH AND ENGINEERING CENTER
MINNEAPOLIS 14, MINNESOTA

RESEARCH AND DEVELOPMENT PROGRAM ON SEALED NICKEL-CADMIUM CELLS FOR SPACE USE

FINAL REPORT

RESEARCH AND DEVELOPMENT PROGRAM ON SEALED NICKEL-CADMIUM CELLS FOR SPACE USE

Under National Aeronautics and Space Administration
Contract No. NAS 5-1045

Report by William Jakobi

On contributions by:

Claude Menard, John Walsh,
and Everette Burkholder
SEPARATOR STUDY

Raymond Schenk, Roy Zikmund
CELL CLOSURE

Raymond Schenk, Ken Wallgren
SEAL TESTING

Released April 30, 1963

Gould-National Batteries, Inc.
Research and Engineering Center
Minneapolis 14, Minnesota

TABLE OF CONTENTS

ABSTRACT 1

SEPARATOR STUDY

I. Introduction 3
II. Mechanical Strength 5
III. Porosity 7
IV. Oxygen Permeability 8
V. Absorbency 10
VI. Rate of Absorption 12
VII. Reactivity in KOH 13
VIII. Reactivity with KOH in the Presence of Oxygen 26
IX. Electrical Performance in Sealed Cell 29
X. Special Cell Investigation of Polypropylene 39
XI. Cell Internal Pressure on Overcharge 39
XII. Performance in Cell Under Acceleration 40
XIII. Conclusions — Areas for Future Study 42

CELL CLOSURE

I. Introduction 47
II. Prevention of Corrosion of the Glass 48
III. Projection Weld 54
IV. Heli-Arc Weld 64
V. Conclusions 70

SEAL TESTING

I. Introduction 71
II. Development of Test Apparatus 72
III. Alternative Test Methods — Calibration 76
IV. Experimental Test Performance 79
V. Conclusions — Areas for Future Study 84

APPENDIX 85

LIST OF FIGURES

FIG. NO.	TITLE	PAGE NO.
SEPARATOR STUDY		
1-6	Material Weight Loss VS. KOH Concentration	16-21
7	Discharge Curves of Separator Materials	34
8	Material Absorbency VS. Capacity	38
9	Effect of Acceleration on Discharge Performance	41
10	Separator Material Summary	44-46
CELL CLOSURE		
11	Cover and Inner Seal Configuration	49
12	Cross Section of Experimental Inner Seal/Cell Closure Weld	49
13	Inner Seal Diaphragm	50
14	Dies for Inner Seal Diaphragm	51-53
15	Developmental and Final Cover Projections	55
16	Developmental and Final Inner Diaphragm Projections	55
17	Welding Operations and Variables	56
18	Direction of Stresses in Drawn Flange Area	58
19	Possible Battery Arrangements with Flange Cells	59
20	Projection Weld Technic	60
21	Cover for Projection Weld	61
22	Forming and Coining Die for Projection Weld Cover	62
23	Projection Welding Electrodes	63
24	Heli-Arc Weld Technic	66
25	Cover for Heli-Arc Weld	67
26	Electrodes for Overlapping Spot Weld	68
27	Heli-Arc Welding Blocks	69
SEAL TESTING		
28	Ionization Pump Current VS. Pressure	73
29	High-Vacuum Test System	75
30	Idealized Pressure VS. Time Curve, Elevated Base Pressure Method	76
31	Idealized Pressure VS. Time Curve, Rate-of-Rise Method	76
32	Idealized Pressure VS. Time Curve, Pump-Down Method	77
33	Standard Curve, System Pressure VS. Leak Rate	78
34	Cell Charge Voltages and System Pressure on Overcharge	80
35	Test Curves Obtained by Rate-of-Rise Method	81
36	Test Curves Obtained by Pump-Down Method	83

LIST OF TABLES

TABLE NO.	TITLE	PAGE NO.
SEPARATOR STUDY		
1	Separator Materials Studied	3-4
1-A	Material Sources	5
2	Strength Averaged by Resin Type	6
3	Material Strength	6-7
4	Porosity Averaged by Resin	7
5	Material Porosity	8
6	Average Oxygen Permeability	9
7	Oxygen Permeability of Materials	9-10
8	Average Absorbency by Resin	10
9	Material Absorbency	11
10	Average Rate of Absorption	12
11	Material Rate of Absorption	12-13
12	Average Percentage Weight Loss	13
13	Weight Loss of Individual Samples	14-15
14	Percentage of Shrinkage or Stretch, Averaged by Resin Type	22
15	Percentage of Material Shrinkage or Stretch	22-24
16	Millequivalents KOH Lost, Averaged by Resin Type	24
17	Millequivalents KOH Lost with Individual Cells	24-26
18	Average Resin Reactivities with KOH and O_2	27
19	Material Reactivity with KOH and O_2	27-28
20	Average Capacities and Internal Resistances	30
21	Average Performance Spread	30
22	Initial Performance by Individual Cell	30-33
23	Capacities for Each Discharge	35
24	High Rate Discharge, Averaged for Resin Type	36
25	High Rate Discharge Performance	36
26	Average Absorbencies VS. Capacity	37
27	Material Absorbency VS. Capacity	37
28	Special Polypropylene Investigation, American Felt EX 635	39
29	Internal Pressure vs. Oxygen Permeability	40
SEAL TESTING		
30	Vacuum System Calibration Values	78
31	Seal Test Performance, Pump Down Method	82

ABSTRACT

This program involved 3 areas of study on the sealed nickel cadmium system: (1) separator materials; (2) cell closure and improvement in the performance of the glass-to-metal seal; and (3) a high vacuum method of testing cell seal.

Study of the basic physical, chemical, and electrical characteristics of separator materials was undertaken since it is known that separators are a weak element in present nickel cadmium design and that the information on the various types of separator material available, relative to their performance in sealed cells, is incomplete. Furthermore, battery manufacturers have not had complete understanding of the precise characteristics that a material must have in order to function well as a separator. The parameters studied are mechanical strength, porosity, permeability to oxygen, absorbency, rate of absorption, reactivity in KOH, reactivity with KOH in the presence of oxygen, electrical performance in the sealed cell, cell internal pressure on overcharge, and performance in the cell under acceleration.

Of the 3 general categories of tests — physical fiber characteristics (strength, porosity, absorbency, etc.), chemical reactivity, and electrical performance — the reactivity experiments produced by far the most uncertain results. The only materials that behaved with any consistency in the reactivity experiments were polypropylene. These materials ranged over no more than $^2/_3$ of the overall performance range; most other materials ranged from the lower third of the general performance range under one test condition, to the upper third under another.

Generally speaking, nylon, dynel, and polypropylene performed better than any of the other resin types tested. The nylon materials (most of which were Pellons) had the best general electrical performance of any resin. They had the highest capacities of all materials tested, good resistance to reactivity except at high temperatures, and had good body. Their fiber characteristics, though good in some respects, were only average in others. On the negative side, their absorbency was frequently poor. The dynel materials generally had good rate of absorption but average or poor performance in the other fiber characteristics, average resistance to KOH, and electrical performance ranging from low to high. Polypropylene consistently had the best resistance to KOH of any of the more common resins tested, and was the only important resin that did not exhibit increased reactivity at high temperature. On the other hand, the polypropylene materials generally had average strength and average to low absorbency and porosity, and exhibited a much wider spread of electrical performance values than other materials.

The work on cell closure revolved chiefly around means of protecting the glass seals from attack by the electrolyte, and improvement in the technology of cell weld closure. Several materials claimed to have good resistance to attack by alkali were evaluated as protective coatings for the underside of the cover seal assembly. These coatings all deteriorated very rapidly in sealed cells; it is likely that the existence of the cell Emf across the coatings is a major factor in their poor performance. An inner seal design was developed which provides a much more effective barrier between the glass and the electrolyte. The sealing element is a nylon gasket with an ID considerably smaller than the diameter of the positive terminal pin. The gasket is forced over the positive pin, and is supported by a metal diaphragm which is in turn welded to the underside of the cover.

Study of cell weld closure involved work with both the heli-arc and projection welding methods. With the projection welding, it was found that the geometry of the optimum weld bead when working with nickel differs considerably from that recommended for steels and similar metals; the bead which produced the most satisfactory welds with nickel had a base width roughly the same as that recommended for steels, but was more triangular than semicircular in cross-section, having considerably less mass. Similarly, optimum welding cycle characteristics for nickel differ considerably from those for steels; both the weld pulses and the cool pulses should be kept very short, and a large number of pulses used.

The heli-arc weld technic developed under this program is a very reliable technic; it has been used on a large number of cells, with a very small incidence of leakage and a low scrap rate. The method involves securing the cell cover to the can with a seam of overlapping spot welds prior to the heli-arc weld. Weld characteristics have been established which make it possible to form a remarkably smooth bead with exceptional finish, with a single pass of the electrode.

Considerable attention was given to developing an improved method of high-vacuum testing of sealed cells, since present radioisotope and helium leak detection methods have grave drawbacks, and most present high-vacuum test methods are very time consuming. A test unit was designed and built which makes it possible to read test chamber pressures by reading the current drawn by an ionization pump, rather than with some sort of gauge; this makes it possible to obtain pressure readings within a very short time (1-2 hrs.) after placing the test cell in the chamber, and without requiring that the test system be shut down or the test chamber sealed off. Three test technics were evaluated; the most satisfactory involves establishing the standard pump-down curve for the empty system, then comparing with this curve the slope of the pump-down curve obtained with a test cell in the chamber. The severity of leakage from the cell is indicated by the degree to which the pump-down curve of the system with test cell, differs from the standard curve. With this system, a complete test to a sensitivity of 1×10^{-6} atm. cc/sec. can be performed in 2 hours; within 4 hours, leaks of 5×10^{-7} atm. cc/sec. can be detected.

SEPARATOR STUDY

I. INTRODUCTION

There are at present many different materials available on the market that are worth considering as separator material. However, information on separator performance, with respect to the dozen or so material parameters now known to be vitally important in sealed cells, is incomplete or inconclusive even for the materials that are presently being used as separators. Information on the performance of the great number of materials that have not yet actually been used in storage batteries is sketchy at the best. In addition, it is felt that there are material parameters having a bearing on cell performance that have not yet been identified.

Furthermore, resin and fabric technology has been advanced to the point where great numbers of new materials, involving new fibers, new treatments of fibers presently known, or new combinations of two or more fiber types, can be developed. We are led to believe that in many cases, a developmental material can be closely tailored to the customer's requirements. However, so little is known of what precisely is required of the optimum separator material that resin and fabric manufacturers have thus far been able to do little more than supply the battery industry with samples of materials presently in their line, or being developed by them for other uses.

With these problems in mind, this phase of the program was intended to provide detailed performance information on a wide range of the materials presently available to us. The parameters studied are mechanical strength, porosity, permeability to oxygen, absorbency, rate of absorption, reactivity in KOH, reactivity in KOH in the presence of oxygen, electrical performance in the sealed cell, cell internal pressure on overcharge, and performance in the cell under acceleration.

Table 1 is the complete listing of all materials that were considered in any way for study under this program. The resin of which the material is composed is given in the second column; as will be seen, in some instances we were unable to learn the identity of the resin. Some of these materials were eliminated fairly early in the test program, due to poor performance under one important test parameter or other, or due to the fact that after it had been received, we learned of some characteristic that would make the material patently unsatisfactory as a separator. A summary of the performance of these materials under each test condition is given as Fig. 10, appearing at the end of this division of the report (pp. 44-46).

TABLE 1. SEPARATOR MATERIALS STUDIED

TRADE NAME	COMPOSITION	CONSTRUCTION	THICKNESS (on Ames comparameter No. 2)
1. VISKON 3406	35% Vinyon; 65% Cellulose	Non woven	.010
2. VISKON 25083-3	100% Dynel	Non woven	.006
3. PELLON T1800 (FT 2100)	100% Polyamide (nylon)	Non woven	.008-.010
4. PELLON V20815 (FT 2100G)	100% Polyamide (nylon)	Non woven	.008-.010
5. PELLON FT 2100K	100% Polyamide (nylon)	Non woven calendered	.005-.006
6. PELLON FT 2101	100% Polyamide (nylon)	Non woven	.006-.008
7. PELLON FT 2101K	100% Polyamide (nylon)	Non woven calendered	.0045-.0055
8. PELLON FT 2101 K/U	100% Polyamide (nylon)	Non woven calendered	.006-.007
9. PELLON FT 2110	100% Dynel	Non woven	.0015-.002
10. PELLON FT 2120	100% Polyvinylchloride	Non woven	.0045-.0055

TABLE 1. (Cont'd) SEPARATOR MATERIALS STUDIED

TRADE NAME	COMPOSITION	CONSTRUCTION	THICKNESS (on Ames compar-ameter No. 2)
11. PELLON FT 2121	100% Polyvinylchloride	Non woven	.005-.0055
12. PELLON N405A	100% Polypropylene	Non woven	.0035-.0045
13. PELLON N405B	100% Polypropylene	Non woven	.006-.007
14. PELLON 21342	100% Nylon	Non woven	.011
15. PELLON 2505	100% Nylon	Non woven	.011
16. WEBRIL EM 230	100% Dynel	Non woven	.0035
17. WEBRIL EM 309	100% Dynel	Non woven	.001
18. WEBRIL EM 403	100% Dynel	Non woven	.0008
19. WEBRIL EM 424	100% Dynel	Non woven	.007
20. WEBRIL EM 307	100% Dynel	Non woven	.007
21. WEBRIL EM 341	100% Dynel	Non woven	.004
22. WEBRIL EM 429	100% Dynel	Non woven	.004
23. WEBRIL EM 430	100% Dynel	Non woven	.005
24. WEBRIL EM 312	Nylon & Dynel	Non woven	.0035
25. WEBRIL EM 387	Nylon & Dynel	Non woven	.0025
26. WEBRIL EM 414	Nylon & Dynel	Non woven	.012
27. WEBRIL EM 444	Vinyon & Rayon	Non woven	.0025-.003
28. WEBRIL M 1401	100% Dynel	Non woven	.0035
29. PAPYLON FN 60	Polyvinyl alcohol fiber	Non woven	.007
30. PAPYLON FN 84	Polyvinyl alcohol fiber	Non woven	.010
31. PAPYLON FN 684	Polyvinyl alcohol fiber	Non woven	.010
32. PORON	Microporous Thermo-plastic	Non woven	.028
33. SYNPOR	Microporous Plastic Material	Non woven	.008-.010
34. AM. FELT EX 635	Polypropylene	Non woven	.008-.009
35. AM. FELT EX 636	Polypropylene	Non woven	.007-.008
36. AM. FELT EX 661	100% Polypropylene	Non woven	.011
37. AM. FELT EX 662	100% Polypropylene	Non woven	.010
38. AM. FELT EX 709	100% Polypropylene	Non woven	.008-.011
39. POLYPOR PVA	Nylon base	Non woven	.0045
40. POLYPOR WB	Nylon base	Non woven	.0055
41. POLYPOR ANGSTRA	Rayon base	Non woven	.0105
42. ROVYFASERPAPIER	Dynel	Non woven	.010
43. PERLONGEWEBE	Nylon	Woven	.0125
44. ONDULONGEWEBE	Nylon	Woven	.0335
45. NATIONAL LEAD POLYETHYLENE	Porous polyethylene	Sheet	.011-.013
46. RIEGEL DACRON	100% Dacron	Non woven	.016
47. NYLON CLOTH	Nylon	Woven	.0055
48. 3-M ACRYLIC, INNER	Acrylic fiber	Non woven	.015
49. 3-M ACRYLIC, OUTER	Acrylic fiber	Non woven	.020
50. 3-M	Nylon	Non woven fabric with binder	.011-.013
51. 3-M	Polypropylene	Non woven fabric with binder	.010-.013
52. 3-M	Dynel	Non woven fabric with binder	.015
53. ALDINE ALDEX 514	100% Cellulose	Non woven fabric	.007
54. EATON DIKEMAN 3042	Dacron	Non woven fabric	.0045
55. EATON DIKEMAN 791	Cellulose	Non woven fabric 30#	.007
56. EATON DIKEMAN 794	Cellulose	Non woven fabric 32#	.011
57. EATON DIKEMAN 938	Cellulose	Non woven fabric 25#	.013
58. EATON DIKEMAN 928	Cellulose	Non woven fabric 50#	.018
59. DORRON 37B		Non woven fabric	.005

TABLE 1-A MATERIAL SOURCES

VISKON	Chicopee Mills, Inc.	47 Worth Street New York 13, N. Y.
PELLON	Pellon Corporation	350 5th Avenue New York 1, N. Y.
WEBRIL	The Kendall Co. Fiber Products Division	Walpole, Mass.
PAPYLON	Seiwa Shoji K. K.	4, 2-Chome, Ohtemachi, Chiyoda Ku, Tokyo, Japan
PORON	Rogers Corporation	Rogers, Conn.
SYNPOR	Stokes Molded Products	Taylor St. at Webster P.O. Box 751 Trenton 4, N. J.
AM. FELT	American Felt Co.	Glenville, Conn.
POLYPOR	Niemand Brothers, Inc.	45-10 94th Street Elmhurst 73 Long Island, N. Y.
ROVYFASERPAPIER PERLONGEWEBE ONDULONGEWEBE	DEAC	Postfach 5029 Neue Mainzer Strasse 54 Frankfurt/Main 1, Germany
NATIONAL LEAD POLYETHYLENE	National Lead Co. Research Labs	105 York Street Brooklyn 1, N. Y.
RIEGEL DACRON	Riegel Paper Corporation	260 Madison Avenue New York 16, N. Y.
3-M	3-M New Product Development, Ribbon Laboratory	900 Bush Avenue St. Paul 6, Minn.
ALDINE ALDEX	Aldine Paper Co., Inc.	535 Fifth Avenue New York 17, N. Y.
EATON DIKEMAN	The Eaton-Dikeman Co.	Mount Holly Springs, Penna.

II. MECHANICAL STRENGTH

Mechanical strength, one of the most fundamental material properties, is very important in sealed cells, particularly in cylindrical cells with coiled plates. The material must be strong enough so that the plates can be coiled and the element inserted into the can without tearing. Through these operations, the material is subjected to both tensile and compressive forces — tensile along the long dimension of the strip, and compressive perpendicular to the face of the strip. In addition, the material must resist puncturing by loose particles of active material and loose ends of wire from the screen of the plaque. It is impossible to completely eliminate these loose particles and wire ends, no matter how carefully the plate processing is done — and any of them, if allowed to penetrate the separator, will short the cell.

Furthermore, the material must retain its strength to the greatest degree possible throughout the life of the cell. As the cell is cycled, the plates expand and contract, thus placing the separator under continued stress as long as the cell is used.

Tensile stress, tensile strain, and the elastic modulus were calculated from data taken from a Riehle tensile-compressive test machine, according to the following formulas:

$$\text{Tensile Stress} = \frac{\text{force}}{\text{cross-section area}} = \frac{F}{A}$$

$$\text{Tensile Strain} = \frac{\text{increase in length}}{\text{original length}} = \frac{\triangle L}{L_0}$$

$$\text{Elastic Modulus} = \frac{\text{tensile stress}}{\text{tensile strain}} = \frac{FL_0}{A\ \triangle L} = Y$$

During the course of the program, it developed that polypropylene, nylon, and dynel were the most promising resin types of the several studied. Therefore with this and with most of the following experiments, a table of average performances of the materials composed of each of these 3 resins is given prior to the performance values of the complete list of individual materials.

TABLE 2. STRENGTH AVERAGED BY RESIN TYPE

RESIN	TENSILE STRENGTH (lbs/in^2)	TENSILE STRAIN ($\Delta L/L_o$)	ELASTIC MODULUS (lbs/in^2)
Polypropylene (7 Mat'ls)	330.7	.060	1.05×10^4
Nylon (7)	1529.3	.394	9.25×10^3
Dynel (10)	918.4	.047	3.74×10^4

TABLE 3. MATERIAL STRENGTH

MATERIAL	TENSILE STRESS (lbs/in^2)	TENSILE STRAIN ($\Delta L/L_o$)	ELASTIC MODULUS (lbs/in^2)
1. VISKON 3406 cellulose & vinyon	1030	.028	3.7×10^4
2. VISKON 25083-3 dynel	1349	.038	3.6×10^4
3. PELLON T1800 (FT 2100) nylon	484	.188	2.6×10^3
4. PELLON V20815 (FT 2100G) nylon	484	.180	2.7×10^3
5. PELLON FT 2100K nylon	810	.025	3.3×10^4
6. PELLON FT 2101 nylon	98	.023	4.3×10^3
7. PELLON FT 2101 K/U nylon	259	.022	1.2×10^4
8. PELLON FT 2110 dynel	165	.059	2.8×10^3
9. PELLON FT 2120 pvc	346	.023	1.5×10^4
10. PELLON FT 2121 pvc	293	.035	8.5×10^3
11. PELLON N405A polypropylene	257	.030	8.6×10^3
12. PELLON N405B polypropylene	371	.037	1.0×10^4
13. WEBRIL EM 230 dynel	1640	.036	4.6×10^4
14. WEBRIL EM 424 dynel	490	.012	4.2×10^4
15. WEBRIL EM 307 dynel	1142	.024	4.7×10^4
16. WEBRIL EM 341 dynel	1860	.025	7.4×10^4
17. WEBRIL EM 429 dynel	0	.200	0
18. WEBRIL EM 430 dynel	534	.012	4.5×10^4
19. WEBRIL EM 312 nylon & dynel	71	.013	5.3×10^3
20. WEBRIL EM 387 nylon & dynel	360	.650	8.8×10^2
21. WEBRIL EM 414 nylon & dynel	39	.020	2.0×10^3
22. WEBRIL EM 444 vinyon & rayon	870	.042	2.1×10^4
23. WEBRIL M 1401 dynel	1910	.024	7.9×10^4

TABLE 3. (Cont'd) MATERIAL STRENGTH

MATERIAL	TENSILE STRESS (lbs/in²)	TENSILE STRAIN ($\Delta L/L_o$)	ELASTIC MODULUS (lbs/in²)
24. PAPYLON FN 60 pva	3976	.259	1.5×10^4
25. PAPYLON FN 84 pva	2655	.086	3.1×10^4
26. PAPYLON FN 684 pva	4870	.248	2.0×10^4
27. SYNPOR	225	.043	5.2×10^3
28. AM. FELT EX 635 polypropylene	500	.193	3.2×10^3
29. AM. FELT EX 636 polypropylene	235	.036	6.5×10^3
30. AM. FELT EX 661 polypropylene	346	.066	5.3×10^3
31. AM. FELT EX 662 polypropylene	253	.049	5.2×10^3
32. AM. FELT EX 709 polypropylene	353	.010	3.5×10^4
33. POLYPOR PVA nylon base	5813	.312	1.9×10^4
34. POLYPOR WB nylon base	7455	.454	1.6×10^4
35. POLYPOR ANGSTRA rayon base	1455	.042	3.5×10^3
36. ROVYFASERPAPIER dynel	94	.041	2.3×10^3
37. PERLONGEWEBE nylon	6000	.718	8.4×10^3
38. ONDULONGEWEBE nylon	2570	1.60	1.7×10^3
39. NATIONAL LEAD POLYETHYLENE	76	.028	2.7×10^3
40. RIEGEL dacron	37	.021	1.8×10^3
41. EATON DIKEMAN 3042 dacron	1220	.051	2.4×10^4

III. POROSITY

Porosity, another of the more fundamental material parameters, is intimately related to absorptivity and to gas permeability both of which are critical in the sealed cell. For the purpose of this study, porosity is defined as the percentage of material volume which consists of void space. It was determined by observing the amount of water displaced by a measured specimen of the material, and calculating according to the formula:

$$\text{Porosity} = \frac{V_1 - V_2}{V_1} \times 100$$

where V_1 = volume of specimen (length × width × thickness)
V_2 = volume of H_2O displaced

Two specimens of each material were tested and the results averaged.

TABLE 4. POROSITY AVERAGED BY RESIN

RESIN	POROSITY, %
Polypropylene (7 mat'ls)	54.83
Nylon (11)	75.42
Dynel (12)	58.55

TABLE 5. MATERIAL POROSITY

MATERIAL	POROSITY, %	MATERIAL	POROSITY, %
1. VISKON 3406 cellulose & vinyon	73.4	25. WEBRIL EM 387 nylon & dynel	59.7
2. VISKON 25083-3 dynel	73.5	26. WEBRIL EM 414 nylon & dynel	69.3
3. PELLON T1800 (FT 2100) nylon	78.8	27. WEBRIL EM 444 vinyon & rayon	50.9
4. PELLON V20815 (FT 2100G) nylon	79.7	28. WEBRIL M 1401 dynel	47.8
5. PELLON FT 2100K nylon	83.8	29. PAPYLON FN 60 pva	68.3
6. PELLON FT 2101 nylon	79.8	30. PAPYLON FN 84 pva	72.1
7. PELLON FT 2101K nylon	57.5	31. PAPYLON FN 684 pva	42.4
8. PELLON FT 2101 K/U nylon	71.1	32. SYNPOR	56.5
9. PELLON FT 2110 dynel	83.4	33. AM. FELT EX 635 polypropylene	50.0
10. PELLON FT 2120 pvc	72.7	34. AM. FELT EX 636 polypropylene	46.8
11. PELLON FT 2121 pvc	71.1	35. AM FELT EX 661 polypropylene	53.0
12. PELLON N405A polypropylene	71.7	36. AM. FELT EX 662 polypropylene	52.0
13. PELLON N405B polypropylene	63.0	37. AM. FELT EX 709 polypropylene	47.4
14. PELLON 21342 nylon	76.5	38. POLYPOR PVA nylon base	61.5
15. PELLON 2505 nylon	78.6	39. POLYPOR WB nylon base	17.9
16. WEBRIL EM 230 dynel	62.3	40. POLYPOR ANGSTRA rayon base	72.2
17. WEBRIL EM 309 dynel	49.8	41. ROVYFASERPAPIER dynel	72.2
18. WEBRIL EM 403 dynel	59.0	42. PERLONGEWEBE nylon	66.3
19. WEBRIL EM 424 dynel	52.0	43. ONDULONGEWEBE nylon	83.8
20. WEBRIL EM 307 dynel	43.6	44. NATIONAL LEAD POLYETHYLENE	54.1
21. WEBRIL EM 341 dynel	43.3	45. RIEGEL dacron	88.9
22. WEBRIL EM 429 dynel	69.5	46. NYLON CLOTH	73.8
23. WEBRIL EM 430 dynel	45.2	47. 3-M acrylic	76.3
24. WEBRIL EM 312 nylon & dynel	69.9	48. EATON DIKEMAN 3042 dacron	41.9
		49. DORRON 37B	67.9

IV. OXYGEN PERMEABILITY

As is well known, the degree to which a separator material is permeable to gaseous oxygen is extremely important in sealed cells. The oxygen, as it is evolved from the positive plate during charge, must be allowed to diffuse through the separator to the negative plate at an adequate rate to avoid buildup of internal pressure to a dangerous level. This permeability is one of the parameters limiting the rate at which a cell can be charged or the amount that it can be overcharged.

The test setup for determining permeability involved two large bottles, connected by a tube across which the sample of the material was stretched. An oxygen pressure differential was established between the two bottles, and the time necessary for the diffusion of the oxygen through the sample to equalize the pressures of

the two bottles was observed. The volume of oxygen passed through the sample was then calculated from these pressure readings, and was in turn plotted against time.

The test equipment consisted of two 5 gal. bottles, a mercury manometer connected to each bottle, a vacuum pump which could be connected to either bottle, connecting tubing and valves, and the specimen holder. This holder was a fixture coupled into the tubing between the two bottles; it had an orifice .040" in diameter, across which the material sample was stretched, and through which the oxygen passed.

Details of the test procedure are as follows: Bottle No. 1 was evacuated, then filled with oxygen and brought to atmospheric pressure. Bottle No. 2 was evacuated to a pressure of 380 mm Hg. At the time when the valve was turned opening the connection between the two bottles, a stop watch was started. The pressure in Bottle No. 2 was read every 5 seconds as the oxygen flowed through the sample into the bottle; readings were taken for at least 1 minute, or longer if required to reach equilibrium. The volume of gas in this bottle was then calculated for each pressure reading, and these volumes were plotted against time. The rate of diffusion was then determined by taking the slope of this curve, and converting to cu.ft. per sec. per sq.ft. of sample. All slopes were read at the 603 cu.in. point on the curve, which with this experimental setup corresponds to 414 mm Hg; this was the single point at which all the materials, with their varying rates, could most easily be read.

Having established this procedure, the one remaining correction to be made was for the thickness of the material samples. The rate of diffusion is proportional to the thickness of the sample; sample thicknesses therefore had to be comparable if the results were to be valid. A thickness of .010" was arbitrarily chosen as the standard. If single or multiple layers of the specimen were .010" thick, the permeability was obtained directly by following the above procedure. If a dimension of .010" could not be obtained with any number of layers of the specimen, then experiments were run and pressures read with one layer, two layers, and three layers of the material in the fixture. These readings were plotted against specimen thickness, and from this curve a pressure figure equivalent to .010" could be obtained. The remainder of the calculations were then done as described above.

TABLE 6. AVERAGE OXYGEN PERMEABILITY

RESIN	O_2 FLOW (Cu. Ft./Sec./ Sq. Ft. Mat'l.)
Polypropylene (4 mat'ls)	28.40
Nylon (9)	32.96
Dynel (10)	22.24

TABLE 7. OXYGEN PERMEABILITY OF MATERIALS

MATERIAL	O_2 FLOW (Cu. Ft./Sec./ Sq. Ft. Mat'l.)	MATERIAL	O_2 FLOW (Cu. Ft./Sec./ Sq. Ft. Mat'l.)
1. VISKON 3406 cellulose & vinyon	21.75	10. PELLON FT 2121 pvc	53.0
2. PELLON T1800 (FT 2100) nylon	52.9	11. PELLON N405A polypropylene	8.6
3. PELLON V20815 (FT 2100G) nylon	47.7	12. PELLON N405B polypropylene	28.7
4. PELLON FT 2100K nylon	7.8	13. WEBRIL EM 230 dynel	9.3
5. PELLON FT 2101 nylon	43.1	14. WEBRIL EM 424 dynel	6.2
6. PELLON FT 2101K nylon	11.8	15. WEBRIL EM 307 dynel	3.25
7. PELLON FT 2101 K/U nylon	25.5	16. WEBRIL EM 341 dynel	5.3
8. PELLON FT 2110 dynel	57.6	17. WEBRIL EM 429 dynel	9.3
9. PELLON FT 2120 pvc	49.7	18. WEBRIL EM 430 dynel	3.1

TABLE 7. (Cont'd) OXYGEN PERMEABILITY OF MATERIALS

MATERIAL	O_2 FLOW (Cu. Ft./Sec./ Sq. Ft. Mat'l.)	MATERIAL	O_2 FLOW (Cu. Ft./Sec./ Sq. Ft. Mat'l.)
19. WEBRIL EM 312 nylon & dynel	13.2	29. POLYPOR WB nylon base	1.3
20. WEBRIL EM 387 nylon & dynel	1.2	30. POLYPOR ANGSTRA rayon base	9.3
21. WEBRIL EM 414 nylon & dynel	15.9	31. ROVYFASERPAPIER dynel	41.8
22. WEBRIL EM 444 nylon & dynel	3.6	32. PERLONGEWEBE nylon	15.3
23. WEBRIL M 1401 dynel	3.0	33. ONDULONGEWEBE nylon	61.0
24. PAPYLON FN 60 pva	41.8	34. RIEGEL dacron	25.2
25. PAPYLON FN 84 pva	25.2	35. 3-M nylon	31.5
26. PAPYLON FN 684 pva	37.8	36. 3-M polypropylene	31.8
27. AM. FELT EX 635 polypropylene	44.5	37. 3-M dynel	83.5
28. POLYPOR PVA nylon base	0.7		

V. ABSORBENCY

Since in the sealed cell all electrolyte must be absorbed either in the plates or in the separator, absorbency is one of the important material parameters. For the purposes of this experiment, absorbency is defined as the gain in weight of a specimen after being soaked in 25% KOH, divided by the dry material weight, or

$$\text{Absorbency} = \frac{W_w - W_d}{W_d}$$

where W_w = wet weight

W_d = dry weight

The absorbency was determined by soaking three weighed dry specimens of each material in 25% KOH for 45 min., draining the specimens for 3 min., and then reweighing them. The results from each group of three specimens were averaged, to obtain the absorbency values reported in Table 9.

The absorbency of a material is shown to be dependent on the physical characteristics of the material rather than on the chemical characteristics of the fiber. Surface smoothness, pore size, regularity of fiber, production procedures such as calendering and drying — all affect the absorption characteristics of the material.

As an illustration of the fact that absorbency is only one of the several more important material characteristics, several of the separators with the highest absorbency were cellulose, and would be wholly unsatisfactory in sealed cells because of their high reactivity with KOH. This group included Eaton Dikeman's 794 and 791, Polypor Angstra, and Webril EM 444. Since there are other materials with higher resistance to KOH, and absorbencies equal to any of these cellulose materials except the Eaton 794, it was not thought worthwhile in the electrical evaluation phase of the study to build test cells with the cellulose separators.

TABLE 8. AVERAGE ABSORBENCY BY RESIN

RESIN	ABSORBENCY
Polypropylene (7 mat'ls)	1.56
Nylon (10)	1.11
Dynel (12)	0.97

TABLE 9. MATERIAL ABSORBENCY

MATERIAL	ABSORBENCY
1. VISKON 3406 cellulose & vinyon	5.7
2. VISKON 25083-3 dynel	1.8
3. PELLON T1800 (FT 2100) nylon	6.3
4. PELLON V20815 (FT 2100G) nylon	6.7
5. PELLON FT 2100K nylon	3.5
6. PELLON FT 2101 nylon	6.4
7. PELLON FT 2101K nylon	1.4
8. PELLON FT 2101 K/U nylon	2.8
9. PELLON FT 2110 dynel	8.2
10. PELLON FT 2120 pvc	1.6
11. PELLON FT 2121 pvc	1.3
12. PELLON N405A polypropylene	1.9
13. PELLON N405B polypropylene	1.8
14. PELLON 21342 nylon	6.4
15. PELLON 2505 nylon	7.6
16. WEBRIL EM 230 dynel	0.9
17. WEBRIL EM 309 dynel	0.9
18. WEBRIL EM 403 dynel	0.7
19. WEBRIL EM 424 dynel	0.9
20. WEBRIL EM 307 dynel	0.9
21. WEBRIL EM 341 dynel	1.2
22. WEBRIL EM 429 dynel	3.0
23. WEBRIL EM 430 dynel	0.8
24. WEBRIL EM 312 nylon & dynel	3.7
25. WEBRIL EM 387 nylon & dynel	2.5
26. WEBRIL EM 414 nylon & dynel	5.0
27. WEBRIL EM 444 vinyon & rayon	7.1
28. WEBRIL M 1401 dynel	0.7
29. PAPYLON FN 60 pva	3.6
30. PAPYLON FN 84 pva	3.6
31. PAPLYON FN 684 pva	3. 2
32. PORON vinyl	0.3
33. SYNPOR	3.8
34. AM. FELT EX 635 polypropylene	0.8
35. AM. FELT EX 636 polypropylene	0.9
36. AM. FELT EX 661 polypropylene	1.7
37. AM. FELT EX 662 polypropylene	2.5
38. AM. FELT EX 709 polypropylene	1.3
39. POLYPOR PVA nylon base	1.9
40. POLYPOR WB nylon base	1.4
41. POLYPOR ANGSTRA rayon base	6.7
42. ROVYFASERPAPIER dynel	2.2
43. PERLONGEWEBE nylon	2.2
44. ONDULONGEWEBE nylon	7.5
45. NATIONAL LEAD POLYETHYLENE	4.5
46. RIEGEL dacron	6.3
47. NYLON CLOTH	1.4
48. 3-M acrylic, inner	3.9
49. 3-M acrylic, outer	3.3
50. 3-M nylon	2.9
51. 3-M polypropylene	3.0
52. 3-M dynel	3.8
53. EATON DIKEMAN 3042 dacron	0.9
54. EATON DIKEMAN 791 cellulose	7.6
55. EATON DIKEMAN 794 cellulose	9.3
56. EATON DIKEMAN 938 cellulose	4.2
57. EATON DIKEMAN 928 cellulose	4.2
58. DORRON 37B	1.8

VI. RATE OF ABSORPTION

The rate at which electrolyte is absorbed by the separator, as distinguished from the total amount of electrolyte which can be absorbed, is important in sealed cells. This is particularly true in space applications, where accelerative forces will drive the electrolyte to one side of the cell, and the cell must recover as quickly as possible following the release of these forces. As will be seen, absorbency and rate of absorption do not necessarily go hand-in-hand. Some materials have high rates of absorption but poor total absorbency — many of the Webrils and several of the Pellons, for example. On the other hand, Webril EM 312 is material with average absorbency and a rather poor rate of absorption.

The test procedure was as follows: A length of the sample material 1/4" in width was suspended in an air-tight chamber which contained a vessel of 25% KOH solution. Feeding into this vessel was a tube from the exterior of the test chamber, trapped so that additional KOH could be added to the vessel without admitting air to the test chamber. After the sample had been suspended over the vessel, the test chamber was closed and allowed to stand until equilibrium was reached between the KOH solution and vapor. Additional KOH was then added to the vessel, raising its level until it touched the bottom of the sample strip, at which point a stop watch was started. The time required for the elecrolyte to climb 0.5" up the specimen strip was observed. Three specimens of each material were evaluated, and the three readings were averaged and recorded.

TABLE 10. AVERAGE RATE OF ABSORPTION

RESIN	MINUTES PER ½" TRAVEL
Polypropylene (7 mat'ls)	5.28
Nylon (7)	1.128
Dynel (12)	1.096

TABLE 11. MATERIAL RATE OF ABSORPTION

MATERIAL	MINUTES PER ½" TRAVEL	MATERIAL	MINUTES PER ½" TRAVEL
1. VISKON 3406 cellulose & vinyon	0.1	14. WEBRIL EM 230 dynel	0.3
2. VISKON 25083-3 dynel	1.4	15. WEBRIL EM 309 dynel	0
3. PELLON T1800 (FT 2100) nylon	1.15	16. WEBRIL EM 403 dynel	0
4. PELLON V20815 (FT 2100G) nylon	0.50	17. WEBRIL EM 424 dynel	0.1
5. PELLON FT 2100K nylon	0.75	18. WEBRIL EM 307 dynel	0.1
6. PELLON FT 2101 nylon	1.3	19. WEBRIL EM 341 dynel	0.5
7. PELLON FT 2101 K/U nylon	1.3	20. WEBRIL EM 429 dynel	0.15
8. PELLON FT 2110 dynel	1.3	21. WEBRIL EM 430 dynel	0.1
9. PELLON FT 2120 pvc	2.7	22. WEBRIL EM 312 nylon & dynel	7.0
10. PELLON FT 2121 pvc	1.1	23. WEBRIL EM 387 nylon & dynel	4.0
11. PELLON N405A polypropylene	9.1	24. WEBRIL EM 414 nylon & dynel	1.5
12. PELLON N405B polypropylene	7.7	25. WEBRIL EM 444 vinyon & rayon	0.3
13. PELLON 21342 nylon	2.4	26. WEBRIL M 1401 dynel	2.8

TABLE 11. (Cont'd) MATERIAL RATE OF ABSORPTION

MATERIAL	MINUTES PER ½" TRAVEL	MATERIAL	MINUTES PER ½" TRAVEL
27. PAPYLON FN 60 pva	3.3	33. AM. FELT EX 662 polypropylene	6.2
28. PAPYLON FN 84 pva	2.4	34. AM. FELT EX 709 polypropylene	2.2
29. PAPYLON FN 684 pva	3.3	35. POLYPOR PVA nylon base	0
30. AM. FELT EX 635 polypropylene	1.1	36. ROVYFASERPAPIER dynel	6.4
31. AM. FELT EX 636 polypropylene	1.0	37. PERLONGEWEBE nylon	0.5
32. AM. FELT EX 661 polypropylene	9.7		

VII. REACTIVITY IN KOH

The degree to which a separator material reacts with the electrolyte is, of course, critical for any battery. Three aspects of reactivity were evaluated under this program:

A. The weight loss of the materials in KOH was determined.

B. The shrinkage or stretch of these materials was measured.

C. The amount of KOH that was lost through chemical reaction with the material was determined.

Samples weighing between 1.0 and 1.1 g. were rolled up and sealed with a measured quantity of electrolyte into "D" cell containers, so as to duplicate the conditions of the sealed cell as closely as could practicably be done. The seal was nylon-to-metal, with the standard production crimping and sizing operations used for commercial cells. Testing was done with 3 concentrations of KOH (20%, 30%, and 40%), 3 temperatures (24°, 54°, and 75°C), and 2 test durations (2 weeks and 12 weeks). The containers were opened at the end of the test period and the contents were titrated with HCl to determine the millequivalents of KOH reacted during the test. The samples were then washed thoroughly, and measured to determine the percentage of shrinkage or stretch. They were then dried and the weight loss was recorded.

It should be pointed out that the appearance of a value of 100% in the weight loss table does not necessarily mean that the material was 100% reacted, but rather that it was decomposed to the point that it could not be retrieved from the test cell and weighed. All of the materials submitted by 3-M were completely reacted in this manner; these values were therefore not included in any of the tables of average performance by resin type. Also included at the end of Section A, WEIGHT LOSS, are curves of percentage weight loss vs. KOH concentration for the materials tested (Figs. 1 through 6).

A. SAMPLE WEIGHT LOSS

TABLE 12. AVERAGE PERCENTAGE WEIGHT LOSS

* = no data available for these test conditions

MATERIAL	TEMP. °C	14 DAYS			84 DAYS		
		20% KOH	30% KOH	40% KOH	20% KOH	30% KOH	40% KOH
Polypropylene, (4 mat'ls)	24	.8	.9	.9	1.0	1.2	1.2
	54	1.2	1.0	1.3	1.3	1.2	1.6
	75	1.3	1.2	.9	1.4	1.5	1.0
Nylon (9)	24	2.1	2.7	2.3	2.1	2.0	2.0
	54	2.3	2.0	1.3	4.4	5.0	3.3
	75	4.3	3.8	2.7	91.0	91.0	78.5
Dynel (10)	24	*	*	*	.2	.2	.3
	54	*	*	*	.5	.4	.6
	75	*	*	*	80.7	51.8	41.2

TABLE 13. WEIGHT LOSS OF INDIVIDUAL SAMPLES

* = not evaluated under these conditions

MATERIAL	TEMP. °C	14 DAYS			84 DAYS		
		20% KOH	30% KOH	40% KOH	20% KOH	30% KOH	40% KOH
1. VISKON 3406 cellulose & vinyon	24	1.7	3.5	2.1	.4	2.3	0
	54	8.2	10.6	6.5	3.5	5.3	1.3
	75	9.9	11.2	5.5	4.9	6.9	2.5
2. PELLON T1800 (FT 2100) nylon	24	1.2	2.7	.8	.8	.5	.1
	54	2.1	3.0	.9	7.0	2.9	2.8
	75	5.5	2.9	4.1	100.0	100.0	100.0
3. PELLON V20815 (FT 2100G) nylon	24	2.7	4.9	3.1	1.4	1.6	2.7
	54	2.3	2.2	2.7	4.2	3.0	3.3
	75	2.1	4.4	2.0	100.0	100.0	100.0
4. PELLON FT 2100K nylon	24	3.7	3.2	2.9	4.5	4.3	4.0
	54	3.5	3.3	3.1	6.5	7.0	5.7
	75	5.1	4.9	4.4	100.0	100.0	100.0
5. PELLON FT 2101 nylon	24	2.3	2.6	2.5	3.6	3.7	2.7
	54	2.8	1.9	1.4	1.6	17.4	5.3
	75	7.9	5.8	3.3	100.0	100.0	100.0
6. PELLON FT 2101K nylon	24	1.4	1.5	2.2	2.2	.8	1.8
	54	4.6	2.2	0	6.2	5.2	5.8
	75	4.9	3.9	3.0	100.0	100.0	100.0
7. PELLON FT 2101K/U nylon	24	1.7	0.9	0.7	2.4	2.5	2.9
	54	1.7	1.1	1.0	5.5	3.5	3.5
	75	3.4	2.6	1.5	100.0	100.0	100.0
8. PELLON FT 2120 pvc	24	.5	1.4	1.2	3.3	1.5	2.3
	54	3.6	3.5	2.6	*	4.5	3.6
	75	2.8	3.5	1.5	5.0	5.4	1.8
9. PELLON FT 2121 pvc	24	0.6	0.7	1.0	1.1	1.4	1.5
	54	4.0	2.6	1.9	2.3	3.0	2.1
	75	2.5	2.5	1.7	1.9	2.8	1.9
10. PELLON N405A polypropylene	24	.1	.1	.3	.4	.3	.3
	54	.4	.4	.2	.4	.2	.2
	75	.4	.3	.2	.4	.1	.1
11. PELLON N405B polypropylene	24	.2	.5	.3	.3	.6	.7
	54	.4	.3	.6	.5	.8	.2
	75	.6	.6	.5	.6	.4	.1
12. WEBRIL EM 230 dynel	24	*	*	*	.6	.8	.9
	54	*	*	*	.9	.9	.8
	75	*	*	*	100.0	100.0	100.0
13. WEBRIL EM 309 dynel	24	*	*	*	0	.3	.3
	54	*	*	*	.4	.3	.7
	75	*	*	*	100.0	100.0	0
14. WEBRIL EM 403 dynel	24	*	*	*	0	0	.1
	54	*	*	*	.6	.4	.4
	75	*	*	*	100.0	0	0
15. WEBRIL EM 424 dynel	24	*	*	*	.2	0	.2
	54	*	*	*	.7	.3	.6
	75	*	*	*	100.0	100.0	100.0
16. WEBRIL EM 307 dynel	24	*	*	*	.1	.25	.3
	54	*	*	*	.3	.4	.4
	75	*	*	*	8.9	10.7	9.8
17. WEBRIL EM 341 dynel	24	*	*	*	.2	.3	.3
	54	*	*	*	.7	.4	.7
	75	*	*	*	100.0	7.6	100.0
18. WEBRIL EM 429 dynel	24	.2	.1	.4	.1	.2	.7
	54	.4	.3	.6	.1	0	.4
	75	0	.1	.5	100.0	100.0	1.0
19. WEBRIL EM 430 dynel	24	*	*	*	.2	.3	.2
	54	*	*	*	0	0	.5
	75	*	*	*	100.0	100.0	0
20. WEBRIL EM 312 nylon & dynel	24	0	0	0	.9	.6	.6
	54	.4	1.0	1.0	1.9	1.5	.6
	75	0	0	0	100.0	100.0	18.1
21. WEBRIL EM 387 nylon & dynel	24	.7	.5	.6	.1	0	.7
	54	.7	.4	.1	1.8	1.8	.7
	75	1.5	2.5	1.4	100.0	100.0	100.0

TABLE 13. (Cont'd) WEIGHT LOSS OF INDIVIDUAL SAMPLES

* = not evaluated under these conditions

MATERIAL	TEMP. °C	14 DAYS			84 DAYS		
		20% KOH	30% KOH	40% KOH	20% KOH	30% KOH	40% KOH
22. WEBRIL EM 414 nylon & dynel	24	10.4	10.8	9.0	10.0	12.5	9.3
	54	10.4	10.0	6.1	10.8	9.4	10.4
	75	9.8	14.6	13.9	100.0	100.0	26.4
23. WEBRIL EM 444 vinyon & rayon	24	.8	2.2	1.7	.7	3.7	2.0
	54	7.0	9.1	5.3	6.7	8.9	2.4
	75	9.0	10.9	4.8	9.9	12.5	6.6
24. WEBRIL M 1401 dynel	24	*	*	*	.1	.2	.2
	54	*	*	*	.7	.2	.5
	75	*	*	*	100.0	100.0	100.0
25. PAPYLON FN 60 pva	24	0	2.2	4.2	.6	3.1	5.1
	54	1.4	2.8	4.7	1.0	2.9	4.8
	75	1.1	10.3	1.9	4.8	5.3	8.8
26. PAPYLON FN 84 pva	24	0	16.7	3.2	.6	5.1	5.5
	54	1.4	2.5	4.2	1.6	3.4	5.1
	75	.5	8.9	1.7	4.4	4.6	4.8
27. PAPYLON FN 684 pva	24	.6	5.2	7.0	2.4	7.4	15.2
	54	1.4	2.4	4.6	2.4	4.0	5.8
	75	2.8	3.4	4.1	5.8	5.3	7.4
28. PORON	54	.2	.4	*	*	*	*
29. SYNPOR	54	24.7	24.2	24.8	*	*	*
30. AM. FELT EX 635 polypropylene	24	1.1	1.3	1.3	1.7	2.0	2.2
	54	2.1	2.3	2.3	2.5	2.6	2.6
	75	1.8	1.5	1.2	2.9	2.8	2.1
31. AM. FELT EX 636 polypropylene	24	1.7	1.7	1.8	1.6	1.7	1.9
	54	1.8	.9	1.9	1.6	2.4	2.3
	75	2.4	2.2	1.8	2.6	2.4	1.8
32. POLYPOR PVA nylon base	24	.8	1.1	1.6	1.3	1.9	1.2
	54	.9	1.4	.6	1.8	1.9	2.2
	75	.1	0	.3	100.0	100.0	5.3
33. POLYPOR WB nylon base	24	0	0	0	3.1	7.2	3.9
	54	1.6	1.0	.9	3.0	0	2.2
	75	0	0	0	100.0	100.0	1.0
34. POLYPOR ANGSTRA rayon base	24	8.5	10.1	9.9	10.3	11.8	10.1
	54	11.5	14.5	8.6	17.8	18.6	11.8
	75	19.0	20.7	13.3	23.2	24.4	16.1
35. ROVYFASERPAPIER dynel	24	0	0	0	.1	.5	.4
	54	.2	.6	.5	.5	.6	.5
	75	.8	.9	.9	.1	.6	1.0
36. PERLONGEWEBE nylon	24	.9	3.2	2.9	1.7	1.8	1.6
	54	1.0	.7	.3	3.3	2.0	1.2
	75	2.4	3.2	.6	100.0	100.0	100.0
37. ONDULONGEWEBE nylon	24	4.6	4.7	4.9	1.8	2.0	1.2
	54	1.9	2.3	2.2	3.4	2.7	1.2
	75	5.8	5.3	4.5	100.0	100.0	6.84
38. NATIONAL LEAD POLYETHYLENE	24	0	.1	0	.4	.3	0
	54	0	.1	0	.5	.6	0
	75	.1	.1	.4	.4	0	0
39. RIEGEL DACRON	54	*	100.0	*	*	*	*
40. 3-M nylon	24	100.0	100.0	100.0	100.0	100.0	100.0
	54	100.0	100.0	100.0	100.0	100.0	100.0
	75	100.0	100.0	100.0	100.0	100.0	100.0
41. 3-M polypropylene	24	100.0	100.0	100.0	100.0	100.0	100.0
	54	100.0	100.0	100.0	100.0	100.0	100.0
	75	100.0	100.0	100.0	100.0	100.0	100.0
42. 3-M dynel	24	100.0	100.0	100.0	100.0	100.0	100.0
	54	100.0	100.0	100.0	100.0	100.0	100.0
	75	100.0	100.0	100.0	100.0	100.0	100.0
43. NYLON CLOTH	24	.5	.7	.7	.3	.5	.7
	54	1.0	1.0	.5	1.9	1.4	1.1
	75	1.9	1.3	.9	21.0	21.0	*
44. EATON DIKEMAN 3042, dacron	54	*	100.0	*	*	*	*
45. DORRON 37B	24	*	*	*	1.8	1.4	1.1
	54	*	*	*	1.4	1.5	1.4
	75	*	*	*	5.2	4.5	1.5

FIG. 1. MATERIAL WEIGHT LOSS VS. KOH CONCENTRATION
TEST CONDITIONS: 14 DAY EXPOSURE, 24°C

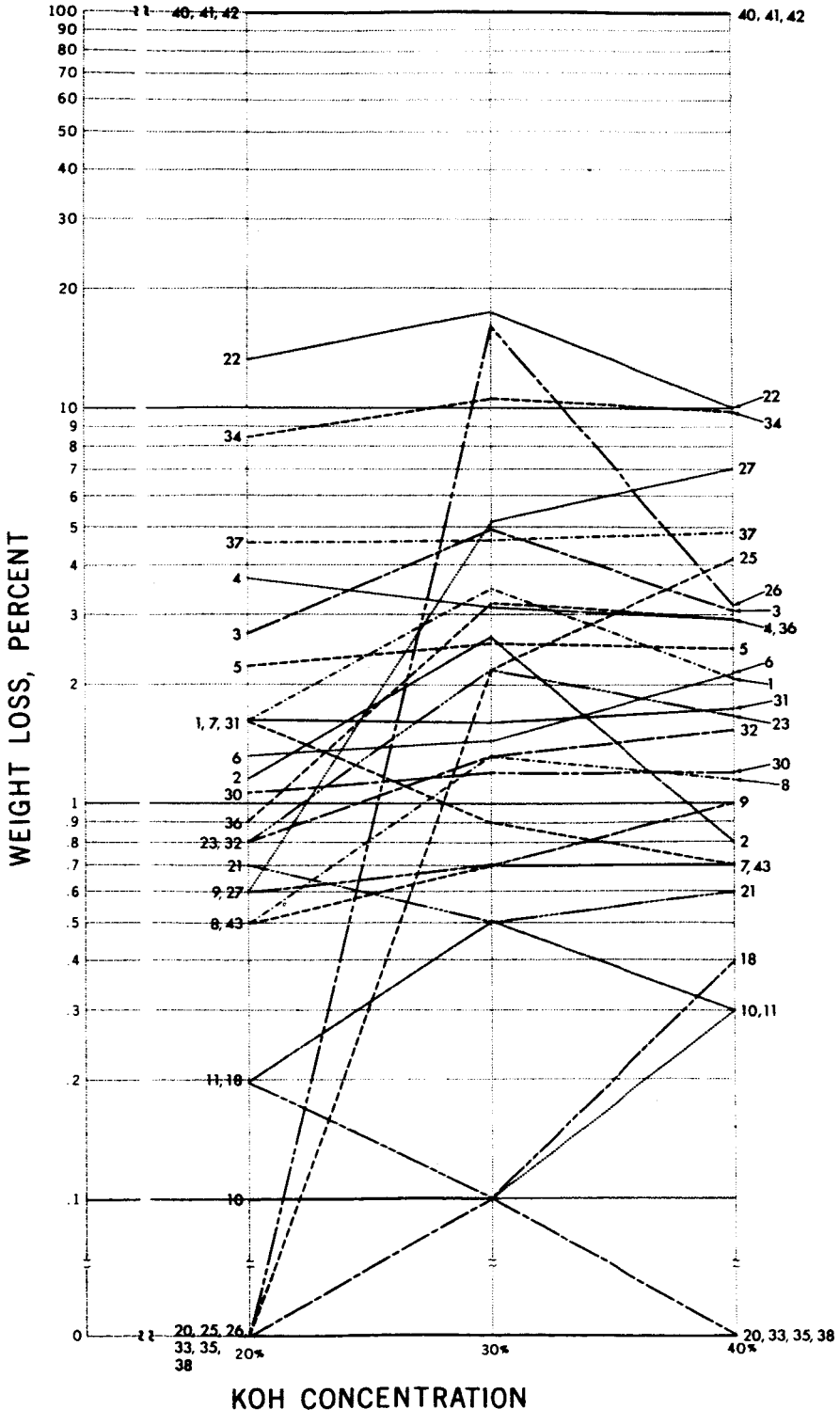

1. VISKON 3406
2. PELLON T1800
3. PELLON V20815
4. PELLON FT 2100K
5. PELLON FT 2101
6. PELLON FT 2101K
7. PELLON FT 2101 K/U
8. PELLON FT 2120
9. PELLON FT 2121
10. PELLON N405A
11. PELLON N405B
18. WEBRIL EM 429
20. WEBRIL EM 312
21. WEBRIL EM 387
22. WEBRIL EM 414
23. WEBRIL EM 444
25. PAPYLON FN 60
26. PAPYLON FN 84
27. PAPYLON FN 684
30. AM. FELT EX 635
31. AM. FELT EX 636
32. POLYPOR PVA
33. POLYPOR WB
34. POLYPOR ANGSTRA
35. ROVYFASERPAPIER
36. PERLONGEWEBE
37. ONDULONGEWEBE
38. NATIONAL LEAD POLYETHYLENE
40. 3-M nylon
41. 3-M polypropylene
42. 3-M dynel
43. NYLON CLOTH

FIG. 2. MATERIAL WEIGHT LOSS VS. KOH CONCENTRATION
TEST CONDITIONS: 14 DAY EXPOSURE, 54°C

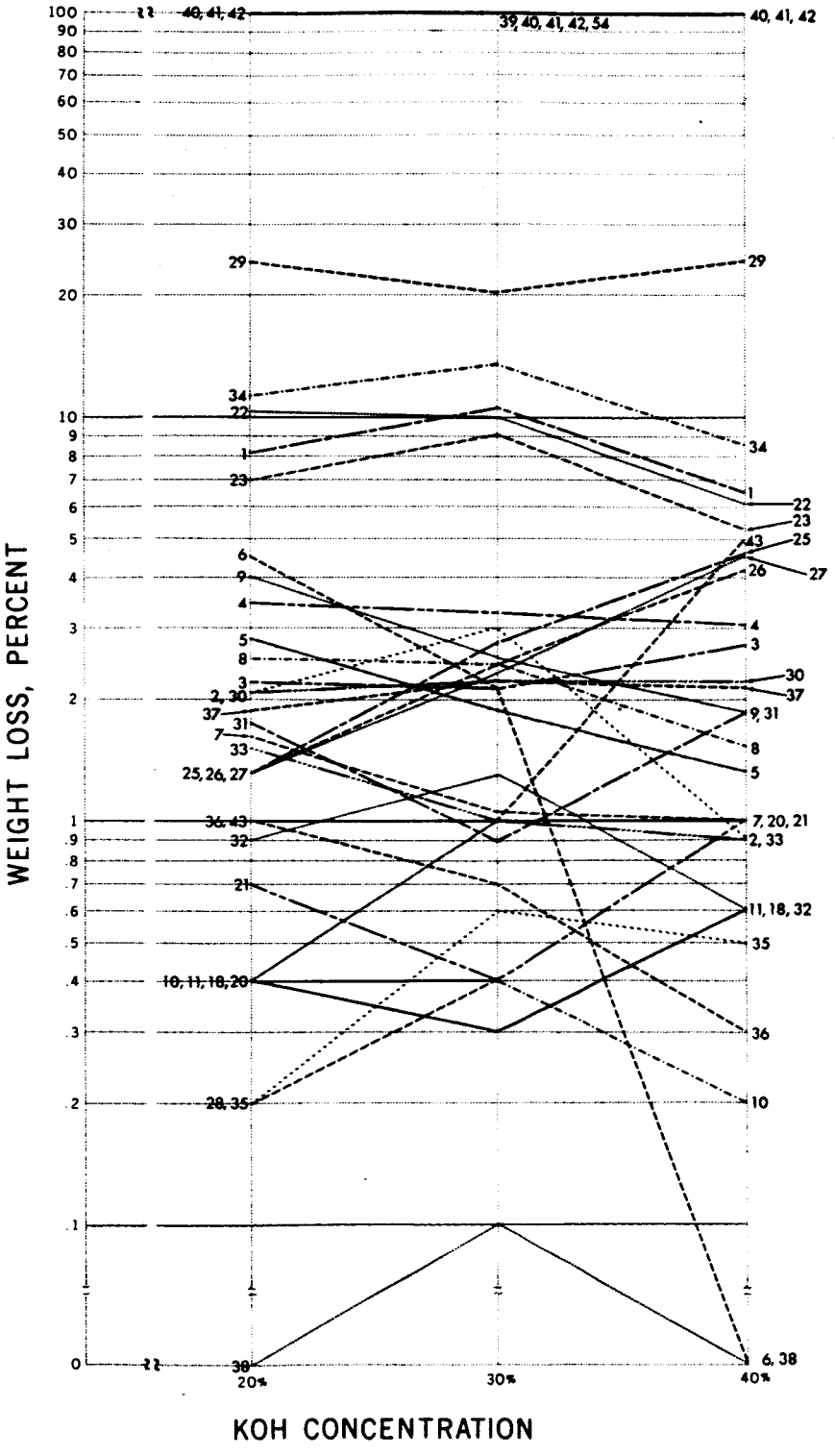

1. VISKON 3406
2. PELLON T1800
3. PELLON V20815
4. PELLON FT 2100K
5. PELLON FT 2101
6. PELLON FT 2101K
7. PELLON FT 2101 K/U
8. PELLON FT 2120
9. PELLON FT 2121
10. PELLON N405A
11. PELLON N405B
18. WEBRIL EM 429
20. WEBRIL EM 312
21. WEBRIL EM 387
22. WEBRIL EM 414
23. WEBRIL EM 444
25. PAPYLON FN 60
26. PAPYLON FN 84
27. PAPYLON FN 684
28. PORON
29. SYNPOR
30. AM. FELT EX 635
31. AM. FELT EX 636
32. POLYPOR PVA
33. POLYPOR WB
34. POLYPOR ANGSTRA
35. ROVYFASERPAPIER
36. PERLONGEWEBE
37. ONDULONGEWEBE
38. NATIONAL LEAD POLYETHYLENE
40. 3-M nylon
41. 3-M polypropylene
42. 3-M dynel
43. NYLON CLOTH

FIG. 3. MATERIAL WEIGHT LOSS VS. KOH CONCENTRATION
TEST CONDITIONS: 14 DAY EXPOSURE, 75°C

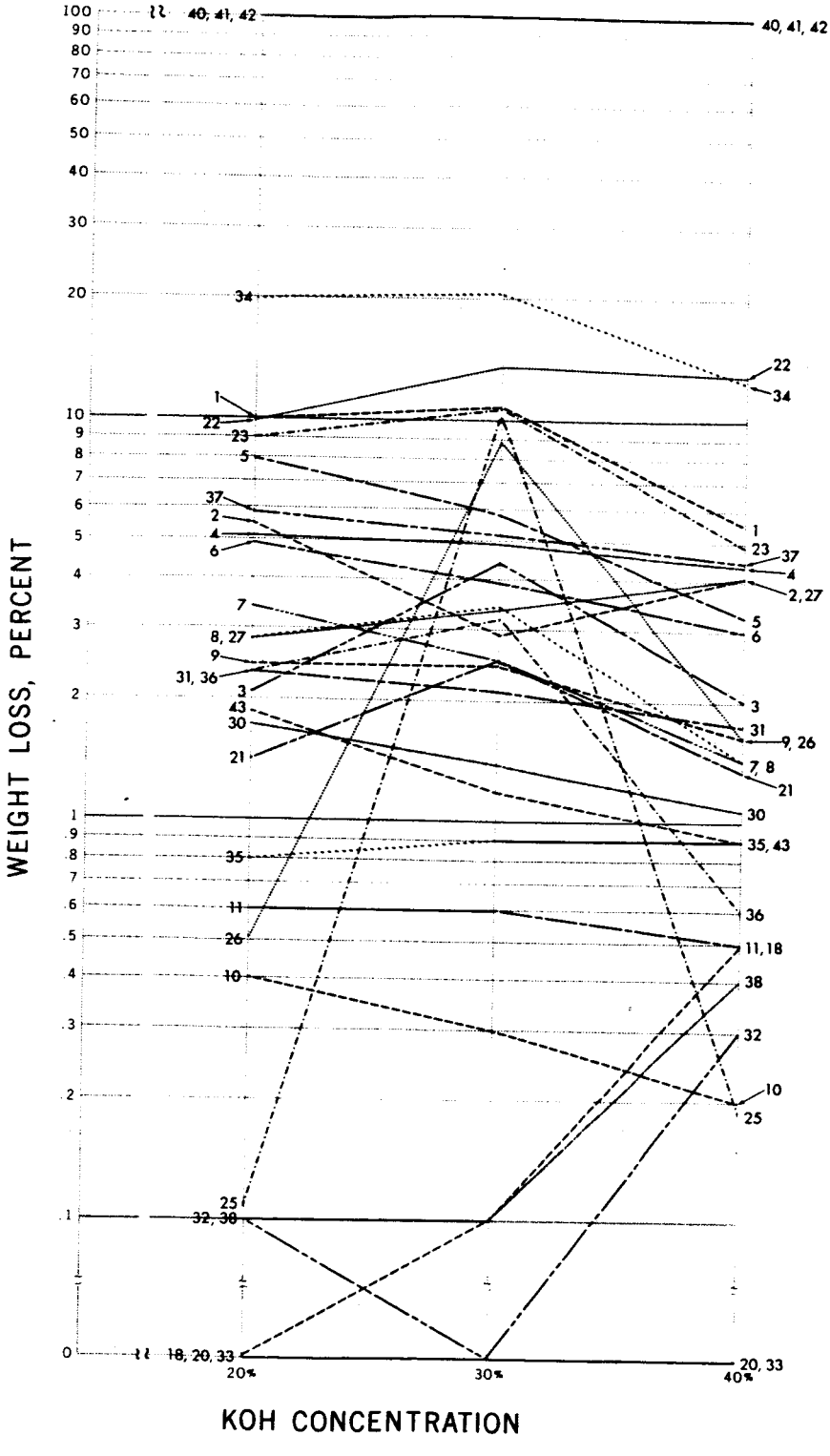

1. VISKON 3406
2. PELLON T1800
3. PELLON V20815
4. PELLON FT 2100K
5. PELLON FT 2101
6. PELLON FT 2101K
7. PELLON FT 2101 K/U
8. PELLON FT 2120
9. PELLON FT 2121
10. PELLON N405A
11. PELLON N405B
18. WEBRIL EM 429
20. WEBRIL EM 312
21. WEBRIL EM 387
22. WEBRIL EM 414
23. WEBRIL EM 444
25. PAPYLON FN 60
26. PAPYLON FN 84
27. PAPYLON FN 684
30. AM. FELT EX 635
31. AM. FELT EX 636
32. POLYPOR PVA
33. POLYPOR WB
34. POLYPOR ANGSTRA
35. ROVYFASERPAPIER
36. PERLONGEWEBE
37. ONDULONGEWEBE
38. NATIONAL LEAD POLYETHYLENE
40. 3-M nylon
41. 3-M polypropylene
42. 3-M dynel
43. NYLON CLOTH

FIG. 4. MATERIAL WEIGHT LOSS VS. KOH CONCENTRATION
TEST CONDITIONS: 84 DAY EXPOSURE, 24°C

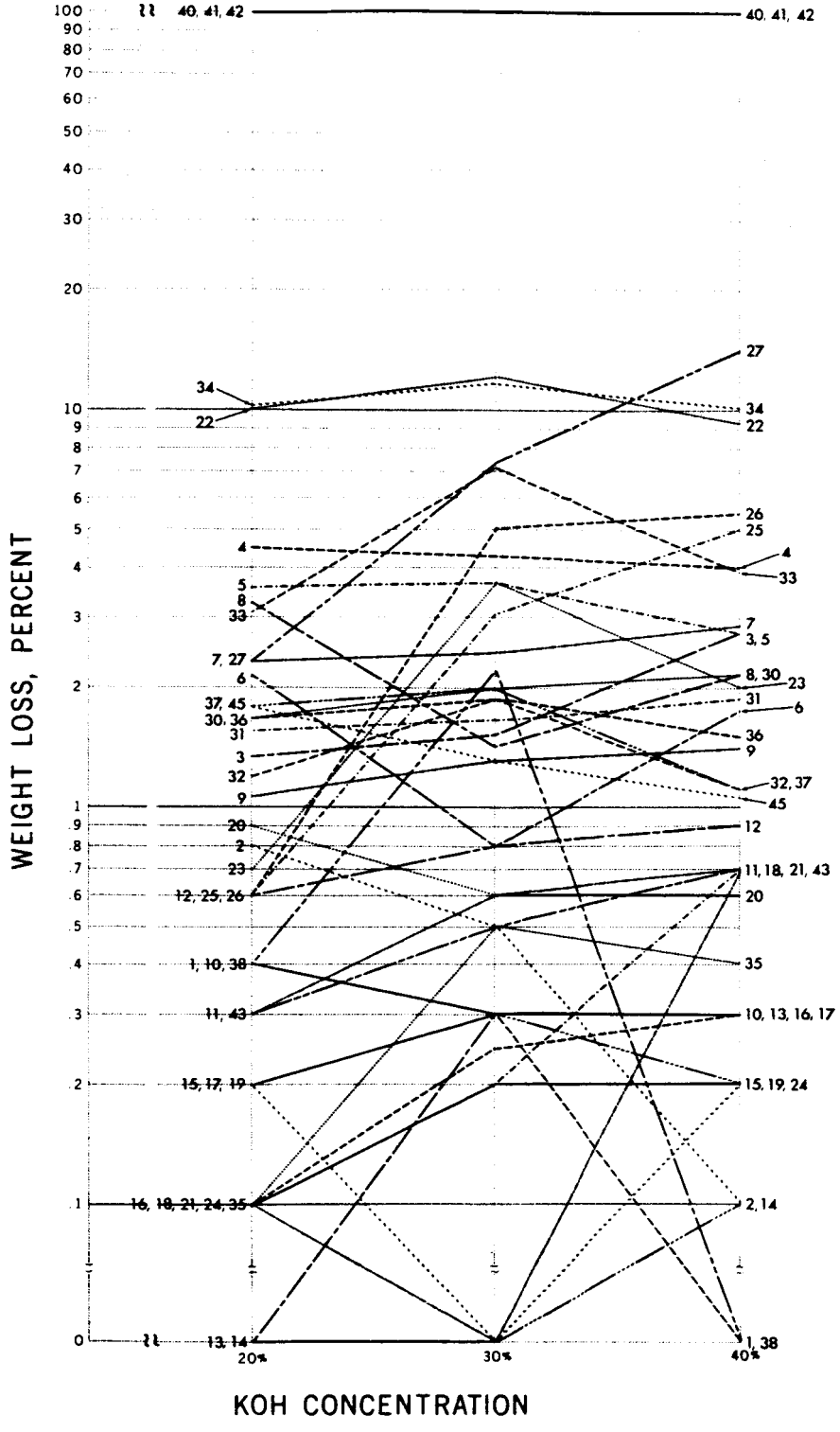

1. VISKON 3406
2. PELLON T1800
3. PELLON V20815
4. PELLON FT 2100K
5. PELLON FT 2101
6. PELLON FT 2101K
7. PELLON FT 2101 K/U
8. PELLON FT 2120
9. PELLON FT 2121
10. PELLON N405A
11. PELLON N405B
12. WEBRIL EM 230
13. WEBRIL EM 309
14. WEBRIL EM 403
15. WEBRIL EM 424
16. WEBRIL EM 307
17. WEBRIL EM 341
18. WEBRIL EM 429
19. WEBRIL EM 430
20. WEBRIL EM 312
21. WEBRIL EM 387
22. WEBRIL EM 414
23. WEBRIL EM 444
25. PAPYLON FN 60
26. PAPYLON FN 84
27. PAPYLON FN 684
30. AM. FELT EX 635
31. AM. FELT EX 636
32. POLYPOR PVA
33. POLYPOR WB
34. POLYPOR ANGSTRA
35. ROVYFASERPAPIER
36. PERLONGEWEBE
37. ONDULONGEWEBE
38. NATIONAL LEAD POLYETHYLENE
40. 3-M nylon
41. 3-M polypropylene
42. 3-M dynel
43. NYLON CLOTH

FIG. 5. MATERIAL WEIGHT LOSS VS. KOH CONCENTRATION
TEST CONDITIONS: 84 DAY EXPOSURE, 54°C

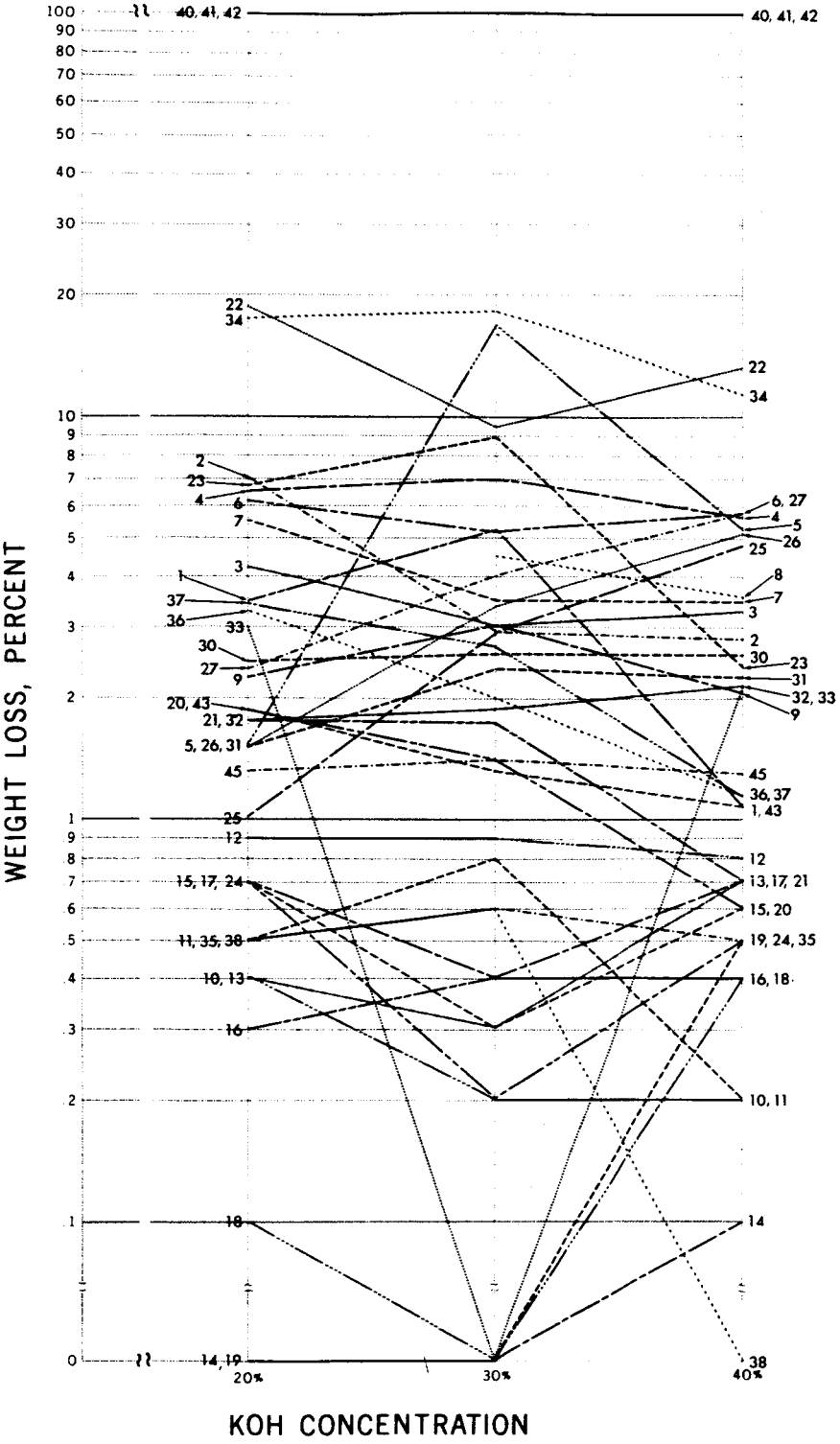

1. VISKON 3406
2. PELLON T1800
3. PELLON V20815
4. PELLON FT 2100K
5. PELLON FT 2101
6. PELLON FT 2101K
7. PELLON FT 2101 K/U
8. PELLON FT 2120
9. PELLON FT 2121
10. PELLON N405A
11. PELLON N405B
12. WEBRIL EM 230
13. WEBRIL EM 309
14. WEBRIL EM 403
15. WEBRIL EM 424
16. WEBRIL EM 307
17. WEBRIL EM 341
18. WEBRIL EM 429
19. WEBRIL EM 430
20. WEBRIL EM 312
21. WEBRIL EM 387
22. WEBRIL EM 414
23. WEBRIL EM 444
25. PAPYLON FN 60
26. PAPYLON FN 84
27. PAPYLON FN 684
30. AM. FELT EX 635
31. AM. FELT EX 636
32. POLYPOR PVA
33. POLYPOR WB
34. POLYPOR ANGSTRA
35. ROVYFASERPAPIER
36. PERLONGEWEBE
37. ONDULONGEWEBE
38. NATIONAL LEAD POLYETHYLENE
40. 3-M nylon
41. 3-M polypropylene
42. 3-M dynel
43. NYLON CLOTH
45. DORRON 37B

FIG. 6. MATERIAL WEIGHT LOSS VS. KOH CONCENTRATION
TEST CONDITIONS: 84 DAY EXPOSURE, 75°C

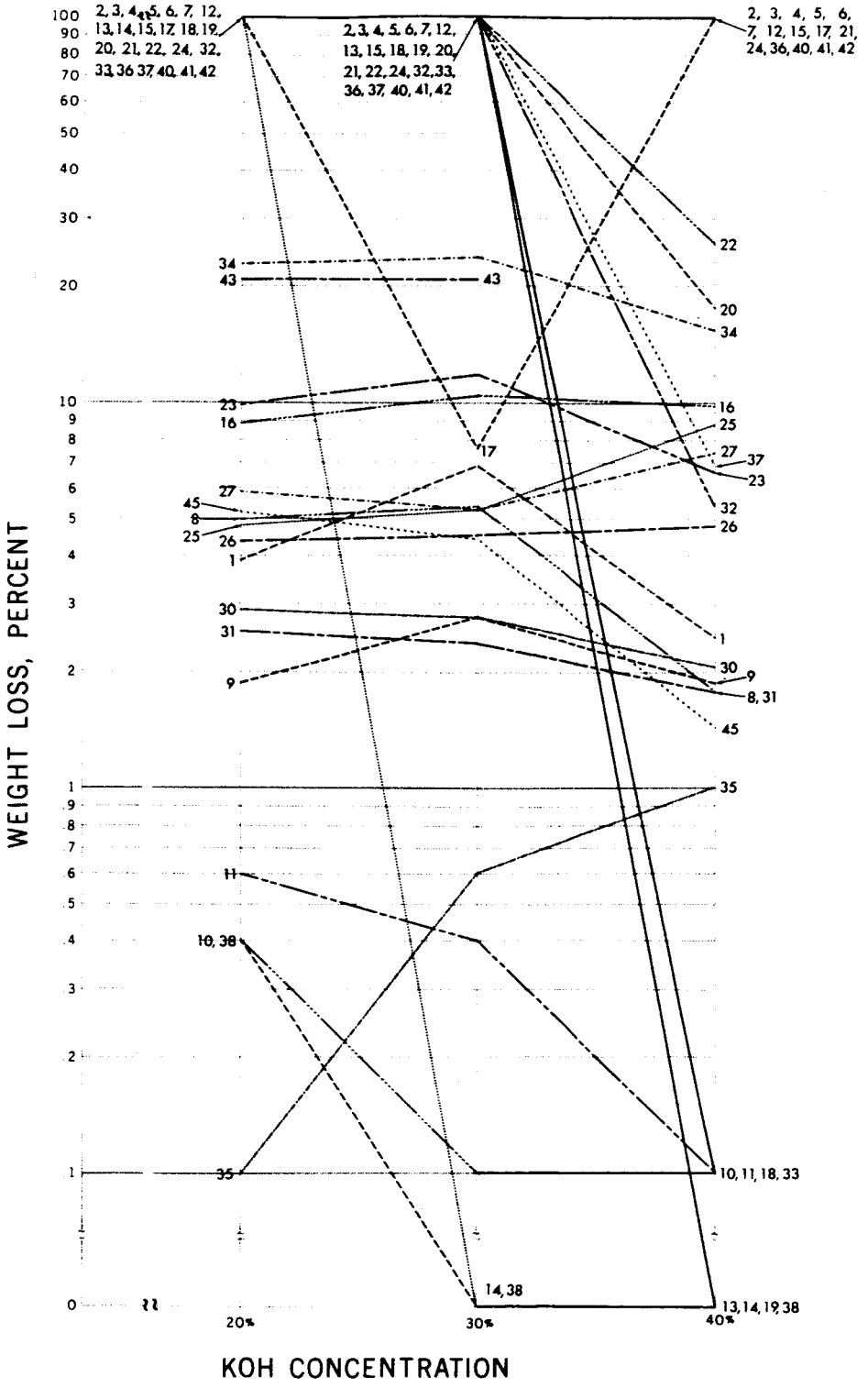

1. VISKON 3406
2. PELLON T1800
3. PELLON V20815
4. PELLON FT 2100K
5. PELLON FT 2101
6. PELLON FT 2101K
7. PELLON FT 2101 K/U
8. PELLON FT 2120
9. PELLON FT 2121
10. PELLON N405A
11. PELLON N405B
12. WEBRIL EM 230
13. WEBRIL EM 309
14. WEBRIL EM 403
15. WEBRIL EM 424
16. WEBRIL EM 307
17. WEBRIL EM 341
18. WEBRIL EM 429
19. WEBRIL EM 430
20. WEBRIL EM 312
21. WEBRIL EM 387
22. WEBRIL EM 414
23. WEBRIL EM 444
25. PAPYLON FN 60
26. PAPYLON FN 84
27. PAPYLON FN 684
30. AM. FELT EX 635
31. AM. FELT EX 636
32. POLYPOR PVA
33. POLYPOR WB
34. POLYPOR ANGSTRA
35. ROVYFASERPAPIER
36. PERLONGEWEBE
37. ONDULONGEWEBE
38. NATIONAL LEAD POLYETHYLENE
40. 3-M nylon
41. 3-M polypropylene
42. 3-M dynel
43. NYLON CLOTH
45. DORRON 37B

B. SHRINKAGE OR STRETCH

TABLE 14. PERCENTAGE OF SHRINKAGE OR STRETCH, AVERAGED BY RESIN TYPE

The subscript adjacent the value indicates number of samples averaged.
§ = Stretch value; otherwise, value is for shrinkage.
* = Not evaluated at these conditions.

MATERIAL	TEMP., °C	14 DAYS						84 DAYS					
		20% KOH		30% KOH		40% KOH		20% KOH		30% KOH		40% KOH	
		Length	Width	Length	Width	Length	Width	Length	Width	Length	Width	Length	Width
POLYPROPYLENE (4 mat'ls.)													
SHRINKAGE	24	0_4	0_4	0_4	0_4	0_4	0_4	0_4	0_4	$.22_4$	0_4	$.11_4$	0_4
	54	$.2_2$	0_2	$.33_2$	0_2	$.19_2$	0_2	$.3_1$	0_2	1.5_2	0_2	$.37_2$	0_2
	75	$.15_4$	0_4	$.38_4$	0_4	$.38_4$	0_4	$.44_4$	0_4	$.47_4$	0_4	$.45_4$	0_4
STRETCH	24												
	54							$.4_1$				$.32_1$	
	75												
NYLON (9)													
SHRINKAGE	24	0_1	0_1	2.9_1	0_1	2.9_1	3.0_1	$.78_2$	1.45_2	2.35_2	1.45_2	3.90_2	1.45_2
	54	3.30_2	0_2	2.80_2	1.40_2	5.00_2	1.40_2	$.78_2$	1.45_2	0_2	2.95_2	1.55_2	1.45_2
	75	2.9_1	3.0_1	2.9_1	6.0_1	2.9_1	6.0_1					10.3_1	1.2_1
STRETCH	24	1.93_6	2.98_6	1.58_6	2.75_6	1.27_6	2.75_6	2.50_7	5.24_7	2.68_7	5.12_7	2.33_7	5.03_7
	54	1.84_7	2.83_7	1.76_7	3.31_7	1.87_7	2.83_7	2.53_6	4.75_6	2.58_6	4.65_6	2.22_6	4.65_6
	75	3.04_6	2.20_6	1.65_6	2.75_6	1.73_6	2.75_6						
DYNEL (10)													
SHRINKAGE	24		0_2	$.28_2$	0_2		$.85_2$	0_9	0_9	0_9	0_9	0_9	0_9
	54	$.43_2$	0_2	2.25_2	0_2	$.5_2$	0_2	$.17_9$	0_9	$.07_9$	0_9	0_9	0_9
	75	2.3_1	0_1	1.15_1	0_1	$.91_1$	0_1	3.60_4	9.25_4	5.96_5	11.4_5	11.55_5	9.35_5
STRETCH	24	$.63_2$				$.28_2$							
	54												
	75												

TABLE 15. PERCENTAGE OF MATERIAL SHRINKAGE OR STRETCH

§ = Stretch value; otherwise, value is for shrinkage.
* = Not evaluated at these conditions.

MATERIAL	TEMP., °C	14 DAYS						84 DAYS					
		20% KOH		30% KOH		40% KOH		20% KOH		30% KOH		40% KOH	
		Length	Width	Length	Width	Length	Width	Length	Width	Length	Width	Length	Width
1. VISKON 3406 cellulose & vinyon	24	1.5	4.8	1.9	0.2	2.7	0.9	0	0	0	0	7.1	0
	54	2.7	3.3	3.4	3.3	4.0	3.3	1.1	0	1.1	0	3.3	0
	75	3.0	6.2	4.0	7.2	5.3	8.5	2.9	0	3.6	0	4.3	0
2. PELLON T1800 (FT 2100) nylon	24	§3.3	§1.3	§1.1	§3.3	§3.0	§3.3	§3.3	§6.7	§3.3	§6.7	§3.3	§6.7
	54	§1.7	§3.3	§1.7	§3.3	§2.2	§3.3	*	*	*	*	*	*
	75	§2.8	§3.3	§2.8	§3.3	§2.8	§3.3	*	*	*	*	*	*
3. PELLON V20815 (FT 2100G) nylon	24	§1.65	§3.3	§1.65	§3.3	0	§3.3	§2.2	§6.7	§2.2	§6.7	§2.2	§6.7
	54	§1.15	§3.3	§1.1	§3.3	§1.05	§3.3	§2.2	§6.7	§1.65	§6.7	§1.55	§6.7
	75	§1.65	§3.3	0	§3.3	§1.5	§3.3	*	*	*	*	*	*
4. PELLON FT 2100K nylon	24	*	*	*	*	*	*	§3.0	§6.7	§3.25	§6.7	§3.0	§6.7
	54	§2.75	§3.3	§2.75	§3.3	§3.0	§3.3	§3.5	§6.7	§3.5	§6.7	§3.5	§6.7
	75	*	*	*	*	*	*	*	*	*	*	*	*
5. PELLON FT 2101 nylon	24	§2.4	§6.7	§2.4	§3.3	§1.4	§3.3	§3.0	§6.7	§3.25	§6.7	§3.0	§6.7
	54	§2.1	§3.3	§2.1	§3.3	§2.1	§3.3	§3.5	§6.7	§3.5	§6.7	§3.5	§6.7
	75	§9.5	0	§2.4	§3.3	§1.9	§3.3	*	*	*	*	*	*
6. PELLON FT 2101K nylon	24	§1.9	§3.3	§1.9	§3.3	§1.9	§3.3	§2.05	§3.3	§2.14	§3.3	§1.9	§3.3
	54	§2.15	§3.3	§1.7	§6.7	§2.15	§3.3	§2.4	§3.3	§2.5	§3.3	§2.14	§3.3
	75	§1.9	§3.3	§1.9	§3.3	§1.9	§3.3	*	*	*	*	*	*
7. PELLON FT 2101 K/U nylon	24	§2.0	§3.3	§2.0	§3.3	§1.5	§3.3	§2.4	§4.65	§2.6	§4.0	§2.5	§3.3
	54	§2.6	§3.3	§2.6	§3.3	§2.6	§3.3	§2.6	§3.3	§2.5	§2.7	§2.4	§3.3
	75	§2.0	§3.3	§2.4	§3.3	§1.9	§3.3	*	*	*	*	*	*
8. PELLON FT 2120 pvc	24	.33	0	.62	0	0	0	0	§1.3	0	0	0	0
	54	1.5	0	1.2	0	1.5	0	*	*	1.5	0	1.45	2.0
	75	8.6	0	8.65	0	*	*	11.3	4.0	11.0	4.7	9.7	4.7
9. PELLON FT 2121 pvc	24	0	0	0	0	0	0	0	0	.6	0	.5	0
	54	1.65	0	2.0	0	1.65	0	.83	0	.83	0	.92	1.3
	75	8.3	0	9.2	0	9.2	0	10.0	1.3	10.5	2.7	10.0	3.3

TABLE 15. (Cont'd.) PERCENTAGE OF MATERIAL SHRINKAGE OR STRETCH

§ = Stretch value; otherwise, value is for shrinkage.
* = Not evaluated at these conditions.

MATERIAL	TEMP., °C	14 DAYS						84 DAYS					
		20% KOH		30% KOH		40% KOH		20% KOH		30% KOH		40% KOH	
		Length	Width	Length	Width	Length	Width	Length	Width	Length	Width	Length	Width
10. PELLON N405A polypropylene	24	0	0	0	0	0	0	0	0	.38	0	.39	0
	54	.4	0	.37	0	.37	0	§.4	0	0	0	§.32	0
	75	0	0	0	0	0	0	.75	0	.71	0	.36	0
11. PELLON N405B polypropylene	24	0	0	0	0	0	0	0	0	0	0	.3	0
	54	0	0	.29	0	0	0	.3	0	.3	0	.3	0
	75	.59	0	.59	0	.59	0	.6	0	.41	0	.47	0
12. WEBRIL EM 230 dynel	24	•	•	*	*	*	*	0	0	0	0	0	0
	54	*	*	*	*	*	*	.9	0	0	0	0	0
	75	•	*	*	*	*	•	*	*	*	*	2.4	6.7
13. WEBRIL EM 309 dynel	24	*	•	*	*	*	*	0	0	0	0	0	0
	54	•	*	*	*	*	*	0	0	0	0	0	0
	75	*	*	*	*	*	*	*	*	*	*	6.0	0
14. WEBRIL EM 403 dynel	24	*	*	*	*	•	*	0	0	0	0	0	0
	54	*	*	*	•	*	*	0	0	0	0	0	0
	75	•	*	*	*	*	*	*	*	25.0	16.7	•	*
15. WEBRIL EM 424 dynel	24	*	•	*	*	*	*	•	*	*	*	*	*
	54	•	*	•	*	*	*	*	*	*	•	*	•
	75	*	*	*	*	*	*	*	*	*	*	*	*
16. WEBRIL EM 307 dynel	24	*	•	•	*	*	*	0	0	0	0	0	0
	54	*	*	*	*	*	*	0	0	0	0	0	0
	75	•	•	*	*	*	*	12.3	27.0	21.5	27.0	24.0	20.0
17. WEBRIL EM 341 dynel	24	*	*	•	*	*	*	0	0	0	0	0	0
	54	*	•	•	*	•	•	0	0	0	0	0	0
	75	•	•	*	*	*	*	*	•	7.0	20.0	*	*
18. WEBRIL EM 429 dynel	24	§.7	0	0	0	0	0	0	0	0	0	0	0
	54	.85	0	.39	0	.4	0	0	0	0	0	0	0
	75	2.3	0	1.15	0	.91	0	*	*	*	*	*	*
19. WEBRIL EM 430 dynel	24	*	*	•	•	•	*	0	0	0	0	0	0
	54	•	*	•	•	*	*	.6	0	.6	0	0	0
	75	•	*	*	*	*	*	•	*	*	*	5.7	*
20. WEBRIL EM 312 nylon & dynel	24	0	0	0	0	0	0	0	0	0	0	0	0
	54	0	0	.76	0	1.7	0	0	0	0	0	0	0
	75	.37	0	.42	0	.91	0	*	*	*	*	18.2	13.3
21. WEBRIL EM 387 nylon & dynel	24	0	0	0	0	.59	0	§1.1	§3.3	§1.7	§3.3	§1.7	§3.3
	54	§.53	0	§.28	0	§.58	0	§.55	§3.3	§1.8	§3.3	§.59	§3.3
	75	§1.05	0	§1.84	0	§.57	0	•	*	*	*	*	•
22. WEBRIL EM 414 nylon & dynel	24	4.35	0	1.74	0	0	0	*	*	*	*	*	*
	54	0	0	0	0	0	0	0	0	0	0	0	0
	75	1.43	0	.95	0	1.43	0	*	*	*	*	17.4	§ .67
23. WEBRIL EM 444 vinyon & rayon	24	0	0	7.4	3.3	7.4	6.7	3.6	0	7.4	10.0	7.4	6.7
	54	5.8	6.7	5.6	3.3	9.7	6.7	5.2	6.7	7.4	3.3	8.1	3.3
	75	6.7	3.3	7.1	6.7	7.6	6.7	5.9	6.7	7.7	10.0	9.0	6.7
24. WEBRIL M 1401 dynel	24	•	•	*	*	*	•	0	0	0	0	0	0
	54	*	•	*	*	*	*	0	0	0	0	0	0
	75	*	*	*	*	•	*	0	0	0	0	24.5	13.3
25. PAPYLON FN 60 pva	24	0	0	1.56	20.0	3.1	6.3	0	0	§1.05	§3.3	0	0
	54	0	0	.56	*	5.15	*	§1.0	0	§.5	§3.3	1.0	3.3
	75	.31	0	2.2	13.3	6.9	6.7	§.51	0	§.51	0	12.8	10.0
26. PAPYLON FN 84 pva	24	0	0	•	*	4.2	3.3	§1.0	0	§.67	0	§.67	0
	54	.42	•	0	•	12.6	*	§1.33	0	§1.0	0	§.34	0
	75	.40	0	•	*	8.6	6.7	§1.1	0	§1.5	0	§.71	0
27. PAPYLON FN 684 pva	24	*	*	*	*	*	*	0	0	0	0	*	0
	54	0	0	0	0	3.1	6.7	0	0	0	0	3.1	3.3
	75	•	*	*	*	*	*	0	0	.38	0	1.9	6.7
28. SYNPOR	54	.50	0	0	0	0	0	•	*	*	*	•	*
29. AM. FELT EX 635 polypropylene	24	0	0	0	0	0	0	0	0	0	0	0	0
	54	0	0	0	0	0	0	0	0	0	0	0	0
	75	0	0	0	0	0	0	.42	0	.33	0	.42	0
30. AM. FELT EX 636 polypropylene	24	0	0	0	0	0	0	0	0	0	0	0	0
	54	0	0	0	0	0	0	0	0	0	0	.43	0
	75	0	0	.91	0	.91	0	0	0	.44	0	.43	0
31. POLYPOR PVA nylon base	24	§.82	§3.3	§.84	§3.3	§.83	§3.3	§1.25	0	§.83	0	§1.25	§3.3
	54	§.84	§3.3	§.84	§3.3	§.84	§3.3	§1.25	§3.3	§1.05	§3.3	§.83	§3.3
	75	0	§3.3	§.85	§6.7	§.83	§3.3	*	§3.3	*	§3.3	§1.25	§3.3
32. POLYPOR WB nylon base	24	§1.05	0	§1.08	0	§2.1	§3.3	§1.3	0	§1.36	0	§1.3	§3.3
	54	§1.6	§3.3	§1.5	§3.3	§1.25	§3.3	§1.42	§3.3	§2.25	§3.3	§1.25	§3.3
	75	§1.03	§3.3	§1.0	§3.3	§1.03	§3.3	*	*	*	*	§1.25	§6.7

TABLE 15. (Cont'd.) PERCENTAGE OF MATERIAL SHRINKAGE OR STRETCH

§ = Stretch value; otherwise, value is for shrinkage.
* = Not evaluated at these conditions.

MATERIAL	TEMP., °C	14 DAYS						84 DAYS					
		20% KOH		30% KOH		40% KOH		20% KOH		30% KOH		40% KOH	
		Length	Width	Length	Width	Length	Width	Length	Width	Length	Width	Length	Width
33. POLYPOR ANGSTRA rayon base	24	0	0	2.9	1.7	8.6	3.3	4.7	1.3	7.4	3.3	9.4	3.3
	54	6.2	3.1	5.8	3.3	10.3	6.7	4.9	0	7.0	3.3	9.8	4.7
	75	2.1	3.3	8.6	3.3	10.7	3.3	6.1	0	7.3	0	8.3	3.3
34. ROVYFASERPAPIER dynel	24	§.55	0	.55	0	§.55	1.7	0	0	0	0	0	0
	54	0	0	.6	0	.6	0	0	0	0	0	0	0
	75	*	*	*	*	*	*	2.1	10.0	1.3	10.0	1.2	6.7
35. PERLONGEWEBE nylon	24	*	*	*	*	*	*	0	0	0	0	0	0
	54	6.6	0	5.6	2.8	10.0	2.8	0	0	0	0	0	0
	75	*	*	*	*	*	*	*	*	*	*	*	*
36. ONDULONGEWEBE nylon	24	0	0	2.9	0	2.9	3.0	1.55	2.9	4.7	2.9	7.8	2.9
	54	0	0	0	0	0	0	1.05	2.9	0	5.9	3.1	2.9
	75	2.9	3.0	2.9	6.0	2.9	6.0	*	*	*	*	10.3	1.2
37. NATIONAL LEAD POLYETHYLENE	24	*	*	*	*	*	*	0	0	0	0	.6	0
	54	0	0	0	0	0	0	0	0	0	0	.51	0
	75	*	*	*	*	*	*	0	0	0	0	*	*
38. NYLON CLOTH	24	§.4	0	§.4	0	§.4	0	§1.6	§1.8	§2.0	§1.8	§.4	§1.8
	54	§.4	0	§.4	0	0	0	§1.0	§1.8	§1.8	§1.8	§.2	§1.2
	75	§.4	0	§.4	0	§.4	0	*	*	*	*	*	*
39. DORRON 37B	24	.39	0	0	0	.40	0	0	0	0	0	0	0
	54	3.8	0	3.1	0	1.5	0	4.0	0	4.0	0	0	0
	75	1.9	0	.91	0	.8	0	*	*	*	*	*	*

C. AMOUNT OF KOH REACTED

TABLE 16. MILLEQUIVALENTS KOH LOST, AVERAGED BY RESIN TYPE

* = Not evaluated under these conditions

MATERIAL	TEMP., °C.	14 DAYS			84 DAYS		
		20% KOH	30% KOH	40% KOH	20% KOH	30% KOH	40% KOH
Polypropylene (4 mat'ls)	24	.15 4	.42 4	.18 4	.38 4	.48 4	.80 4
	54	.10 4	.28 4	.28 4	.42 4	.52 4	.82 4
	75	.20 4	.32 4	.28 4	.51 4	.54 4	.71 4
Nylon (9)	24	.35 9	.35 9	.33 9	.33 9	.40 9	.64 9
	54	.23 9	.34 9	.08 9	.41 9	.47 9	1.12 9
	75	.41 9	.40 9	.54 9	.60 9	.63 9	.75 9
Dynel (10)	24	0 1	0 1	.1 1	.06 10	.1 10	.1 10
	54	.1 2	.15 2	.05 2	.29 10	.40 10	.29 10
	75	.1 2	.6 2	.6 2	9.81 10	9.76 10	5.43 10

TABLE 17. MILLEQUIVALENTS KOH LOST WITH INDIVIDUAL CELLS

* = Not evaluated under these conditions.
§ = Leaked.

MATERIAL	TEMP., °C	14 DAYS			84 DAYS		
		20% KOH	30% KOH	40% KOH	20% KOH	30% KOH	40% KOH
1. VISKON 3406 cellulose & vinyon	24	.3	.5	.7	.3	.4	.3
	54	.1	.7	0	.9	1.6	.6
	75	1.1	1.4	1.0	1.9	1.9	1.6
2. PELLON T1800 (FT 2100) nylon	24	.2	.3	0	.6	.7	.9
	54	.3	.5	0	.7	.7	1.2
	75	.3	.4	.4	.8	.7	1.1
3. PELLON V20815 (FT 2100G) nylon	24	.5	.7	.3	.3	.4	.1
	54	.3	.5	0	.4	.4	.4
	75	.6	.8	.8	.4	.5	.3
4. PELLON FT 2100K nylon	24	.4	.3	.3	.2	0	.3
	54	.3	0	0	.2	.4	.1
	75	.6	.3	.3	.4	.15	1.0

TABLE 17. (Cont'd.) MILLEQUIVALENTS KOH LOST WITH INDIVIDUAL CELLS

* = Not evaluated under these conditions.
§ = Leaked.

MATERIAL	TEMP., °C	14 DAYS			84 DAYS		
		20% KOH	30% KOH	40% KOH	20% KOH	30% KOH	40% KOH
5. PELLON FT 2101 nylon	24	.5	.4	.4	.3	.3	.3
	54	.3	.5	.3	.3	.5	.5
	75	.9	.2	.3	.7	.7	.8
6. PELLON FT 2101K nylon	24	.6	.2	0	.2	.4	.5
	54	.1	.4	0	.3	.4	.9
	75	.5	.5	.3	.6	.7	1.0
7. PELLON FT 2101 K/U nylon	24	.7	1.2	1.9	.1	.2	.1
	54	.2	.4	.2	.3	.2	.8
	75	1.1	1.5	2.1	.7	.5	.8
8. PELLON FT 2120 pvc	24	.9	1.4	1.9	.1	.4	1.2
	54	.6	.9	.8	*	.9	1.9
	75	.5	2.1	3.1	1.2	1.1	2.1
9. PELLON FT 2121 pvc	24	.1	.9	.8	.4	.5	1.6
	54	.5	.8	1.1	1.0	1.0	.6
	75	.3	1.3	1.6	.7	1.2	2.1
10. PELLON N405A polypropylene	24	.2	.6	.5	.4	.8	1.4
	54	.2	.3	.3	.4	.6	1.2
	75	.2	.5	.5	.45	.5	.8
11. PELLON N405B polypropylene	24	.1	.6	.2	.4	.5	1.0
	54	.1	.4	.5	.4	.6	1.1
	75	.2	.4	.5	.5	.6	.9
12. WEBRIL EM 230 dynel	24	*	*	*	0	0	0
	54	*	*	*	.4	.5	.2
	75	*	*	*	9.5	10.7	16.7
13. WEBRIL EM 309 dynel	24	*	*	*	0	0	0
	54	*	*	*	.1	.6	.4
	75	*	*	*	12.0	12.4	4.3
14. WEBRIL EM 403 dynel	24	*	*	*	0	.5	.6
	54	*	*	*	.3	.7	.2
	75	*	*	*	11.9	11.7	3.9
15. WEBRIL EM 424 dynel	24	*	*	*	0	0	0
	54	*	*	*	.3	.3	.3
	75	*	*	*	10.1	9.5	8.5
16. WEBRIL EM 307 dynel	24	*	*	*	.1	.1	0
	54	*	*	*	.4	.1	.3
	75	*	*	*	11.0	10.5	10.5
17. WEBRIL EM 341 dynel	24	*	*	*	0	0	0
	54	*	*	*	0	.3	.6
	75	*	*	*	12.4	11.4	*
18. WEBRIL EM 429 dynel	24	0	0	0	0	0	0
	54	.2	.3	.1	.3	.3	.2
	75	.1	1.1	1.1	9.9	9.7	7.5
19. WEBRIL EM 430 dynel	24	*	*	*	0	0	0
	54	*	*	*	.3	.4	.3
	75	*	*	*	10.9	10.8	3.1
20. WEBRIL EM 312 nylon & dynel	24	.1	.1	.3	0	.1	.2
	54	.1	.2	0	.3	.2	0
	75	0	.4	.4	2.5	3.0	2.5
21. WEBRIL EM 387 nylon & dynel	24	.1	.2	.3	.2	0	0
	54	.1	.1	0	.4	.2	.2
	75	.6	.7	.9	2.8	2.4	*
22. WEBRIL EM 414 nylon & dynel	24	.9	1.3	.6	1.0	1.1	.5
	54	1.1	1.1	.3	1.2	.5	.2
	75	1.3	2.0	1.9	2.3	3.7	3.3
23. WEBRIL EM 444 vinyon and rayon	24	0	0	0	.2	.3	.1
	54	.4	.8	.3	.9	.8	.4
	75	1.8	.9	.6	1.4	1.3	.5
24. WEBRIL M 1401 dynel	24	*	*	*	0	0	0
	54	*	*	*	.4	.3	.1
	75	*	*	*	9.6	10.3	9.1
25. PAPYLON FN 60 pva	24	.1	0	.3	0	.1	.1
	54	.1	.2	0	.2	.1	.1
	75	3	.3	.4	.7	.5	.8
26. PAPYLON FN 84 pva	24	.1	.2	.1	.1	0	0
	54	.1	.1	0	.2	0	0
	75	.2	.5	.4	.3	.3	.5

TABLE 17. (Cont'd.) MILLEQUIVALENTS KOH LOST WITH INDIVIDUAL CELLS

* = Not evaluated under these conditions.
§ = Leaked

MATERIAL	TEMP., °C	14 DAYS			84 DAYS		
		20% KOH	30% KOH	40% KOH	20% KOH	30% KOH	40% KOH
27. PAPYLON FN 684 pva	24	.1	.5	.9	.3	.1	.2
	54	.1	.1	0	.5	.9	.5
	75	.3	.4	.1	.9	.7	1.1
28. PORON vinyl	54	.5	.9	•	•	•	*
29. SYNPOR	54	.5	2.0	.8	•	*	•
30. AM. FELT EX 635 polypropylene	24	0	.1	0	.4	.4	.5
	54	.1	.2	.3	.4	.4	.5
	75	.2	.3	0	.6	.5	.5
31. AM. FELT EX 636 polypropylene	24	.3	.4	0	.3	.2	.3
	54	0	.2	0	.5	.5	.5
	75	.2	.1	.1	.5	.55	.65
32. POLYPOR PVA nylon base	24	0	0	0	0	.6	1.0
	54	.4	.4	0	.4	1.3	1.0
	75	.6	1.5	2.2	.9	2.1	2.0
33. POLYPOR WB nylon base	24	0	0	0	.7	1.0	.5
	54	.7	.9	.3	.7	1.7	1.5
	75	.7	1.6	1.4	2.2	2.5	2.5
34. POLYPOR ANGSTRA rayon base	24	.4	.6	.8	.7	1.0	.8
	54	.5	1.2	.5	.7	2.0	1.4
	75	2.2	2.2	2.5	2.4	2.6	1.7
35. ROVYFASERPAPIER dynel	24	0	0	.1	.5	.4	.4
	54	0	0	0	.35	.5	.3
	75	.1	.1	.1	.8	.6	.7
36. PERLONGEWEBE nylon	24	0	0	0	.4	.5	.3
	54	.1	.2	0	.5	.4	.5
	75	.1	.1	.1	.5	.6	.5
37. ONDULONGEWEBE nylon	24	.2	0	0	.4	.4	.2
	54	.2	.2	0	.4	.4	.5
	75	.3	.2	0	.5	.4	.5
38. NATIONAL LEAD POLYETHYLENE	24	.4	.5	0	.1	.4	.5
	54	.1	.5	0	.3	.4	.5
	75	.4	.3	.3	.5	.5	.5
39. RIEGEL DACRON	54	•	3.3	•	*	*	*
40. NYLON CLOTH	24	.1	.1	.1	.5	.7	§3.1
	54	.3	.6	.2	.6	.8	§5.2
	75	.3	.6	•	.8	1.4	•
41. 3-M acrylic inner	24	1.7	3.8	2.8	•	*	*
	54	5.2	6.3	4.4	*	*	*
	75	.7	.8	4.8	*	•	*
42. 3-M acrylic outer	24	4.3	4.9	4.5	*	*	•
	54	6.9	6.4	6.6	*	•	*
	75	6.5	6.7	7.1	*	•	*
43. 3-M nylon	24	4.9	4.6	5.5	5.4	5.43	6.1
	54	5.3	5.2	4.9	5.84	3.0	6.3
	75	4.9	5.4	4.9	6.6	6.0	6.6
44. 3-M polypropylene	24	5.2	5.8	5.1	5.3	5.7	6.8
	54	5.8	4.8	5.0	6.2	5.7	7.5
	75	5.9	5.6	6.2	6.1	6.6	7.7
45. 3-M dynel	24	5.2	5.8	5.1	5.9	5.64	6.5
	54	5.8	4.8	5.0	6.5	9.3	10.0
	75	5.9	5.6	6.2	9.9	10.4	11.2
46. EATON DIKEMAN 3042	24	•	*	•	*	*	•
	54	*	10.7	*	*	*	*
47. DORRON 37B	24	.1	.2	0	.5	.8	1.3
	54	.2	.5	.4	.9	1.1	1.6
	75	.7	.9	.6	10.7	12.4	12.0

VIII. REACTIVITY WITH KOH IN THE PRESENCE OF OXYGEN

In the sealed cell, the problem of the reactivity of the separator material with the electrolyte is particularly acute since large quantities of oxygen are also present in the cell during charge. The importance of this factor led to the construction of a special experiment, in which material samples were subjected to KOH plus oxygen at an elevated temperature for 48 hours.

Five weighed samples of each material were used; each individual sample was folded and placed in a test tube containing a measured amount of 30% KOH. Sample sizes and amounts of KOH used are as follows:

Sample No.	Size, in.	ml. of KOH
1	3.5 × 1.5	1.6
2	3.5 × 1.5	1.6
3	3.5 × 1.5	0
4	3.5 × 1.5	1.6
5	7 × 1.5	3.5

In each case Sample No. 3, exposed to oxygen without KOH, served as a control. The test tubes were placed in a pressure reaction vessel and oxygen was introduced through an inlet in the cover of the vessel at a pressure of 45 lbs./sq. in. The vessel was maintained between 52° and 60°C, thus paralleling the 54° condition used for the determination of reactivity in sealed containers (described in the previous section). The material samples were then washed, dried, and the weight loss was recorded.

The weight loss values of all the materials except the 3-M materials were grouped and averaged by resin type and are listed below. As would be expected from the results of the previous experiment, the polypropylene, nylon, and dynel materials again evinced good resistance to attack by the KOH, and would be expected to perform better as cell separators than the other materials tested under this program.

It is expected that the reactivity of these materials would be somewhat higher in an operating sealed cell than in this experiment, since they would be exposed to oxygen in the nascent state as well as gaseous oxygen, and since cell temperature will at times be higher than in this experiment. However, regardless of whether the values recorded in the following table are correct in an absolute sense, this experiment should give a valid idea of the relative performance of the various separator materials tested.

TABLE 18. AVERAGE RESIN REACTIVITIES WITH KOH & O_2

RESIN	WT. LOSS (%)	RESIN	WT. LOSS (%)
Polypropylene (7 mat'ls.)	1.4	PVC (2)	8.6
Nylon (10)	2.3	PVA (3)	63.7
Dynel (12)	3.3	Viskon (1)	61.6
Dynel-Nylon (3)	12.6	Dacron (1)	100.0

TABLE 19. MATERIAL REACTIVITY WITH KOH & O_2

In per cent weight loss
+ Value indicates gain in sample weight

MATERIAL	SAMPLE NO.				AVERAGE OF 1, 2, 4, 5	SPECIMEN 3, O_2 ALONE
	1	2	4	5		
1. VISKON 3406 cellulose & vinyon	63.0	58.4	64.7	60.4	61.6	0.1
2. VISKON 25083-3 dynel	5.7	6.3	5.4	3.6	5.3	0.35
3. PELLON T1800 (FT 2100) nylon	2.5	2.8	2.0	2.7	2.5	0.7
4. PELLON V20815 (FT 2100G) nylon	4.4	5.3	5.7	8.8	6.1	+2.4
5. PELLON FT 2100K nylon	2.9	3.6	3.7	3.8	3.5	0.14
6. PELLON FT 2101 nylon	0.3	0.33	*	.23	0.3	0.28
7. PELLON FT 2101 K/U nylon	1.1	1.4	7.5	1.1	2.8	0.08
8. PELLON FT 2110 dynel	1.7	1.7	2.5	2.7	2.2	0.20
9. PELLON FT 2120 pvc	11.0	9.9	11.3	4.8	9.3	+0.14

TABLE 19. (Cont'd). MATERIAL REACTIVITY WITH KOH & O_2

In per cent weight loss
+ Value indicates gain in sample weight

MATERIAL	SAMPLE NO.				AVERAGE OF 1, 2, 4, 5	SPECIMEN 3, O_2 ALONE
	1	2	4	5		
10. PELLON FT 2121 pvc	7.8	7.7	7.0	6.9	7.9	0.1
11. PELLON N405A polypropylene	0.4	0.25	0	0.06	0.18	0
12. PELLON N405B polypropylene	0	0	0.6	0.2	0.2	0
13. PELLON 21342 nylon	2.9	3.1	3.1	3.0	3.0	0.43
14. PELLON 2505 nylon	0.17	1.7	2.0	3.8	2.0	+0.25
15. WEBRIL EM 230 dynel	7.4	9.6	5.4	3.4	6.5	0.13
16. WEBRIL EM 309 dynel	3.8	0.9	4.36	1.8	2.7	0.25
17. WEBRIL EM 403 dynel	6.4	7.3	8.2	6.5	7.1	0.07
18. WEBRIL EM 424 dynel	2.0	2.9	2.4	0.7	2.0	+0.1
19. WEBRIL EM 307 dynel	2.0	3.6	1.7	1.1	2.1	+0.1
20. WEBRIL EM 341 dynel	0	•	0.6	0.5	0.4	0
21. WEBRIL EM 429 dynel	1.7	3.7	1.8	1.2	2.1	+0.42
22. WEBRIL EM 430 dynel	2.0	1.3	3.0	1.6	2.0	0.05
23. WEBRIL EM 312 nylon & dynel	6.2	1.8	1.6	0.9	2.6	1.1
24. WEBRIL EM 387 nylon & dynel	2.9	0.7	0.7	0.7	1.3	0.11
25. WEBRIL EM 414 nylon & dynel	10.8	11.8	9.9	9.2	7.9	+0.2
26. WEBRIL EM 444 nylon & dynel	45.1	44.8	46.0	18.9	38.7	0.7
27. WEBRIL M 1401 dynel	3.3	2.1	2.8	3.4	2.9	+0.32
28. PAPYLON FN 60 pva	61.3	58.2	54.7	26.2	50.1	0.24
29. PAPYLON FN 84 pva	100.0	100.0	100.0	100.0	100.0	+0.7
30. PAPYLON FN 684 pva	43.3	39.7	58.7	14.5	39.1	0
31. AM. FELT EX 635 polypropylene	1.8	2.0	2.1	2.5	2.4	0.1
32. AM. FELT EX 636 polypropylene	1.5	1.9	1.5	2.0	1.7	0.24
33. AM. FELT EX 661 polypropylene	1.6	1.7	1.7	1.7	1.7	0.07
34. AM. FELT EX 662 polypropylene	1.6	1.6	1.6	1.7	1.6	+0.08
35. AM. FELT EX 709 polypropylene	2.1	2.1	1.5	1.8	1.9	0.09
36. POLYPOR PVA nylon base	3.7	2.9	6.3	5.0	4.5	0
37. ROVYFASERPAPIER dynel	3.3	1.8	2.4	2.3	2.5	+0.1
38. PERLONGEWEBE nylon	0.8	1.0	0.7	1.0	0.9	1.2
39. ONDULONGEWEBE nylon	1.9	2.0	1.8	1.5	1.8	2.8
40. NYLON CLOTH	0.6	0.2	0.1	0	0.2	0.1
41. 3-M nylon	100.0	100.0	100.0	100.0	100.0	0.5
42. 3-M polypropylene	100.0	100.0	100.0	100.0	100.0	0.2
43. 3-M dynel	100.0	100.0	100.0	100.0	100.0	0.1
44. NATIONAL LEAD POLYETHYLENE	0.6	0.4	0.9	1.6	0.9	0.3
45. 3-M acrylic, outer	100.0	100.0	100.0	100.0	100.0	0
46. RIEGEL DACRON	100.0	100.0	100.0	100.0	100.0	+0.05

IX. ELECTRICAL PERFORMANCE IN SEALED CELL

There is no known series of laboratory conditions that will duplicate the conditions existing in operating sealed cells — the only known way to determine accurately how well a material will perform as a separator material is to build cells with the materials in question and test them under the desired operating conditions. This phase of the study therefore involved building groups of test cells containing 35 of the more promising materials. These cells were evaluated for performance at various charge and discharge rates, internal resistance in the charged and discharged state, continuous overcharge, and internal shorting.

Specimens of the materials were cut to the size of the separators used in our production "D" cell design, and were built into "D" cans with lab-processed plates having capacities of approximately 4.0 AH when used in our present production cells. 25% KOH was added, in an amount calculated for each material to be equal to roughly 30% of the material's absorbent capacity, which is the factor presently used in our production cells.

The following test schedule was performed:

CYCLES 1 THROUGH 3:
- — Charge at the 10 hr. rate (.4 amp) for 16 hrs.
- — Discharge at the 5 hr. rate (.8 amp).
- — On the third cycle, record the internal resistance for the charged and the discharged state.

CYCLE 4:
- — Charge at 10 hr. rate (.4 amps) for 16 hrs.
- — Discharge at 1 hr. rate (4 amps).

CYCLE 5:
- — Charge at 10 hr. rate (.4 amp) for 16 hrs., recording charge voltage.
- — Discharge at 5 hr. rate (.8 amp).

CYCLE 6:
- — Charge at 8 hr. rate (.5 amp) for 13 hrs.
- — Discharge at 5 hr. rate (.8 amp).

CYCLE 7:
- — Charge at 6 hr. rate (.667 amp) for 10 hrs.
- — Discharge at 5 hr. rate (.8 amp).

CYCLE 8:
- — Charge at 5 hr. rate (.8 amp) for 8 hrs.
- — Discharge at 5 hr. rate (.8 amp).

CYCLE 9:
- — Continuously charge at 10 hr. rate (.4 amp) for three days.
- — Leave cells on open circuit for two weeks, recording their potential each day.

A. CAPACITY AND INTERNAL RESISTANCE

It has been our experience that the third cycle of a fresh cell is generally the most representative of the initial cell characteristics. It is usually not the peak capacity cycle (the peak generally occurs on the second cycle), but it does give a good idea of what the optimum capacity will be throughout the following several cycles of the cell's life. Therefore, the following initial capacity values (Table 22) were taken on Cycle No. 3, as were the measurements of cell internal resistance in the charged and discharged state. As before, the materials have first been grouped by resin type and the average values given for each resin (Table 20). Table 23 is the complete tabulation of the average capacities obtained from each material test cell group, for discharges 1 through 8; the "Total Capacity" values as averaged for each resin group given in Table 20 were derived from this table. Following the tables is a chart of the discharge curves of these cell groups (Fig. 7). In preparing this chart, the readings from each group of cells were averaged to give a composite curve for that material; in some cases, the curve of the best cell is given in addition, in order to give an idea of the range of the data.

As would be expected, a general correlation can be seen between capacity and internal resistance. Study of the complete tabulation of data in Tables 22 and 23 reveals, however, that this correlation is by no means perfect. For instance, the separator with the highest initial capacity (Pellon FT 2101K) had a charged internal resistance high enough to place it in the middle third of the performance range; the separator with the lowest resistance (both charged and discharged — Pellon 2505) had capacity at the bottom end of the upper third of the performance range. At the bottom of the capacity range, on the other hand, the correlation between capacity and internal resistance is rather close: The separator with the lowest capacity (Webril EM 230) had

close to the highest resistance, both charged and discharged — and the separators with the highest resistance of all (Webrils M 1401 for the charged state and EM 424 for the discharged) had the third and the second lowest capacities, respectively.

It is interesting to note that the material which yielded the highest initial capacity, Pellon FT 2101K, has rather poor absorbency — only half again as great as the material which yielded the poorest capacity, Webril EM 230. As to the other parameters that would be expected to have an influence on capacity, it might be pointed out that the FT 2101K has slightly lower porosity and slightly higher oxygen permeability than EM 230, but has less than half the charged internal resistance of the EM 230 (one-fifth the discharged internal resistance). One might conjecture that the material with the highest internal resistance would be that with the lowest absorbency — and this proved to be true. Webril M 1401 had the highest charged internal resistance and the lowest absorbency of all materials tested; the absorbency of Webril EM 424, the material which had the highest discharged resistance, was only slightly higher.

Another aspect that should be given special attention is the spread of the performance values obtained from each group of cells made with the same material type. The spread of the initial capacity and the internal resistance readings for each cell group was recorded, and these spreads were in turn grouped and averaged for resin type and are presented in Table 21. It will be seen that polyproplyene yielded the widest spread in initial capacities, by a considerable margin over the next highest group, the dynels. American Felt EX 635, a material which produced one of the lowest initial capacities, had the broadest spread of any material tested. Interestingly, though the spread of initial capacities with the dynel materials is only 60% of the polyproylene capacity spread, the dynels produced a spread of internal resistances almost fully as wide as the polypropylenes.

TABLE 20. AVERAGE CAPACITIES & INTERNAL RESISTANCES

RESIN	INITIAL CAPACITY (AH)	TOTAL CAPACITY (AH)	INTERNAL RESISTANCE, CHARGED (m Ω)	INTERNAL RESISTANCE, DISCHARGED (m Ω)
Nylon (9 mat'ls)	4.0	3.88	7.5	11.9
Viskon (1)	3.9	3.72	8.0	13.4
Dynel-Nylon (3)	3.8	3.65	8.7	16.1
Polypropylene (7)	3.6	3.71	11.3	21.7
PVA (3)	3.3	3.43	10.1	17.5
Dynel (10)	3.0	2.92	14.6	35.6
PVC (2)	2.9	2.66	10.9	31.8

TABLE 21. AVERAGE PERFORMANCE SPREAD

(Maximum minus minimum values)

RESIN	INITIAL CAPACITY (CYCLE # 3) (AH)	INTERNAL RESISTANCE, CHARGED (m Ω)	INTERNAL RESISTANCE, DISCHARGED (m Ω)
Polypropylene (7 mat'ls)	.9	6.125	17.011
Dynel (10)	.522	4.877	16.022
Viskon (1)	.5	2.0	4.2
PVC (2)	.45	3.7	21.3
Nylon (9)	.433	1.211	3.233
Nylon-Dynel (3)	.366	1.2	3.114
PVA (3)	.233	1.866	4.633

TABLE 22. INITIAL PERFORMANCE BY INDIVIDUAL CELL

All values taken on Cycle No. 3

MATERIAL	CELL NO.	CAPACITY (AH)		INTERNAL RESISTANCE, CHARGED (m Ω)		INTERNAL RESISTANCE, DISCHARGED (m Ω)	
		Per Cell	Average	Per Cell	Average	Per Cell	Average
1. VISKON 3406 cellulose & vinyon	101	4.1		7.5		13.0	
	102	3.6		9.2		15.7	
	103	4.0		7.2		11.5	
			3.9		7.97		13.4

TABLE 22. (Cont'd.) INITIAL PERFORMANCE BY INDIVIDUAL CELL

All values taken on Cycle No. 3

MATERIAL	CELL NO.	CAPACITY (AH)		INTERNAL RESISTANCE, CHARGED (mΩ)		INTERNAL RESISTANCE, DISCHARGED (mΩ)	
		Per Cell	Average	Per Cell	Average	Per Cell	Average
2. VISKON 25083-3 dynel	101	3.2		18.5		27.0	
	102	2.8		21.5		53.5	
	103	3.5		15.5		34.0	
	104	3.3		16.5		34.5	
			3.2		18.00		37.25
3. PELLON T1800 (FT 2100) nylon	101	4.1		6.8		9.9	
	102	4.1		7.8		9.5	
	103	4.1		7.25		9.8	
	104	3.6		7.3		10.5	
	105	4.1		7.0		10.6	
			4.0		7.23		10.06
4. PELLON V20815 (FT 2100G) nylon	101	3.9		7.0		9.5	
	102	4.2		6.0		9.6	
	103	4.1		6.5		9.7	
	104	4.3		6.5		10.0	
	105	3.9		7.0		10.0	
			4.08		6.6		9.76
5. PELLON FT 2100K nylon	101	4.2		7.5		15.0	
	102	4.2		7.5		13.5	
	103	4.1		7.5		15.0	
	104	3.9		9.0		15.8	
	105	3.9		7.7		13.0	
			4.06		7.84		14.46
6. PELLON FT 2101 nylon	101	3.8		7.0		11.2	
	102	3.8		6.8		9.2	
	103	4.1		6.5		9.8	
	104	4.2		7.4		11.4	
	105	3.8		7.5		11.1	
			3.94		7.04		10.54
7. PELLON FT 2101K nylon	101	4.3		7.5		8.8	
	102	4.4		8.6		11.5	
	103	4.0		8.1		10.5	
			4.23		8.07		10.27
8. PELLON FT 2101 K/U nylon	101	3.6		9.4		17.9	
	102	3.6		9.5		22.0	
	103	3.6		8.2		16.0	
	104	3.6		8.0		18.2	
			3.6		8.78		18.53
9. PELLON FT 2110 dynel	101	3.9		8.0		12.4	
	102	3.9		8.0		12.5	
	103	3.6		9.8		17.4	
	104	3.9		7.4		11.6	
			3.82		8.3		13.48
10. PELLON FT 2120 pvc	101	2.8		10.9		38.0	
	102	2.8		10.6		34.0	
	103	2.5		12.4		50.0	
	104	3.0		9.3		25.7	
	105	2.5		10.5		20.4	
			2.72		10.74		33.62
11. PELLON FT 2121 pvc	101	3.2		10.5		24.0	
	102	3.2		8.7		27.5	
	103	2.8		12.2		29.5	
	104	3.2		13.0		37.0	
			3.1		11.1		29.5
12. PELLON N405A polypropylene	101	4.3		10.5		28.0	
	102	3.8		11.2		18.6	
	103	3.4		11.5		14.6	
	104	4.1		11.5		14.5	
			3.9		11.18		18.93
13. PELLON N405B polypropylene	101	3.2		10.0		20.8	
	102	3.9		9.0		16.5	
	103	3.4		11.0		18.6	
	104	3.0		11.5		20.1	
	105	3.2		12.4		27.3	
			3.34		10.78		20.66
14. PELLON 21342 nylon	101	3.7		7.2		10.0	
	102	4.1		6.6		9.1	
	103	4.2		6.7		9.2	
	104	4.1		8.0		9.4	
	105	3.9		7.0		9.5	
	106	3.9		7.4		9.5	
	107	3.6		7.4		21.0	
			3.93		7.19		11.1

TABLE 22. (Cont'd.) INITIAL PERFORMANCE BY INDIVIDUAL CELL

All values taken on Cycle No. 3

MATERIAL	CELL NO.	CAPACITY (AH)		INTERNAL RESISTANCE, CHARGED (mΩ)		INTERNAL RESISTANCE, DISCHARGED (mΩ)	
		Per Cell	Average	Per Cell	Average	Per Cell	Average
15. PELLON 2505 nylon	101	4.1		6.2		9.5	
	102	3.7		6.3		9.0	
	103	4.4		6.1		9.3	
	104	3.7		6.3		9.4	
			3.99		6.23		9.3
16. WEBRIL EM 230 dynel	101	1.6		22.0		67.0	
	102	2.4		19.5		50.0	
	103	2.4		15.3		37.0	
	104	2.2		18.5		48.0	
			2.15		18.83		50.5
17. WEBRIL EM 424 dynel	101	2.4		25.0		50.0	
	102	1.5		24.0		75.0	
	103	2.4		17.0		58.0	
	104	2.4		15.5		57.0	
			2.18		20.38		60.0
18. WEBRIL EM 307 dynel	101	3.2		16.5		23.6	
	102	3.5		17.4		30.5	
	103	3.0		15.5		20.0	
	104	3.2		16.5		28.5	
	105	3.2		15.5		26.5	
			3.22		16.28		25.82
19. WEBRIL EM 341 dynel	101	3.2		7.8		19.1	
	102	3.3		7.4		12.5	
	103	3.2		7.9		27.0	
	104	3.3		7.6		13.0	
			3.25		7.68		17.9
20. WEBRIL EM 429 dynel	101	4.1		9.2		12.0	
	102	4.1		8.0		12.1	
			4.1		8.6		12.05
21. WEBRIL EM 430 dynel	101	2.8		14.5		25.5	
	102	2.5		21.5		70.0	
	103	2.5		24.5		78.0	
	104	3.3		13.0		21.9	
	105	2.8		17.0		46.0	
			2.78		18.1		48.18
22. WEBRIL EM 312 nylon & dynel	101	3.2		7.8		19.1	
	102	3.3		7.4		12.5	
	103	3.2		7.9		27.0	
	104	3.3		7.6		13.0	
			3.25		7.68		17.9
23. WEBRIL EM 387 nylon & dynel	101	4.1		9.5		18.5	
	102	4.3		10.5		23.0	
	103	4.1		9.5		17.5	
	104	3.9		11.0		22.5	
			4.1		10.13		20.38
24. WEBRIL EM 414 nylon & dynel	101	4.1		9.2		9.6	
	102	4.1		8.2		9.7	
	103	4.4		7.8		9.2	
	104	3.8		7.6		11.0	
			4.1		8.2		9.88
25. WEBRIL M 1401 dynel	101	2.4		20.0		44.0	
	102	2.0		22.0		54.0	
	103	2.5		25.0		74.0	
	104	2.5		20.5		58.0	
	105	2.0		24.7		45.0	
			2.28		22.44		55.0
26. PAPYLON FN 60 pva	101	3.5		11.0		23.1	
	102	3.2		9.6		16.5	
	103	3.2		10.5		18.6	
	104	3.2		12.0		24.0	
	105	3.2		11.0		20.6	
			3.26		10.82		20.56
27. PAPYLON FN 84 pva	101	3.7		9.3		14.5	
	102	4.1		10.0		16.5	
	103	4.1		9.5		14.9	
			3.97		9.6		15.3
28. PAPYLON FN 684 pva	101	3.7		10.0		18.0	
	102	3.7		9.0		14.6	
	103	3.7		11.5		16.0	
	104	3.7		9.0		15.0	
	105	3.7		9.9		19.0	
			3.7		9.88		16.52

TABLE 22. (Cont'd.) INITIAL PERFORMANCE BY INDIVIDUAL CELL

All values taken on Cycle No. 3

MATERIAL	CELL NO.	CAPACITY (AH)		INTERNAL RESISTANCE, CHARGED (mΩ)		INTERNAL RESISTANCE, DISCHARGED (mΩ)	
		Per Cell	Average	Per Cell	Average	Per Cell	Average
29. AM. FELT EX 635 polypropylene	101	4.7		6.4		9.5	
	102	2.4		28.0		67.0	
	103	3.2		15.0		34.0	
	104	2.4		21.5		46.0	
			3.18		17.73		39.13
30. AM. FELT EX 636 polypropylene	101	3.2		16.0		33.0	
	102	2.4		22.0		44.0	
	103	3.2		17.0		28.0	
	104	4.1		7.4		8.5	
	105	2.4		17.5		38.0	
			3.06		15.98		30.3
31. AM. FELT EX 661 polypropylene	101	4.3		8.5		10.0	
	102	4.0		9.3		16.1	
	103	4.4		12.1		15.7	
	104	3.8		10.0		16.6	
	105	3.8		9.6		15.6	
			4.05		9.9		14.8
32. AM. FELT EX 662 polypropylene	101	3.7		7.2		11.2	
	102	3.9		9.4		13.2	
	103	3.9		6.9		11.2	
	104	3.9		7.8		11.3	
			3.85		7.28		11.73
33. AM. FELT EX 709 polypropylene	101	3.6		12.1		22.0	
	102	3.6		11.9		20.0	
	103	3.6		13.3		27.5	
	104	3.6		12.5		21.0	
			3.6		12.45		22.63
34. ROVYFASERPAPIER dynel	101	3.7		6.8		13.5	
	102	3.5		6.5		11.0	
	103	4.1		6.4		13.0	
	104	3.7		7.2		13.6	
	105	3.7		7.0		13.7	
			3.74		6.78		12.96
35. PERLONGEWEBE nylon	101	4.3		8.6		13.3	
	102	3.7		7.3		12.0	
	103	4.3		7.6		12.8	
	104	4.1		10.5		13.5	
			4.1		8.5		12.9

FIG. 7. DISCHARGE CURVES OF SEPARATOR MATERIALS

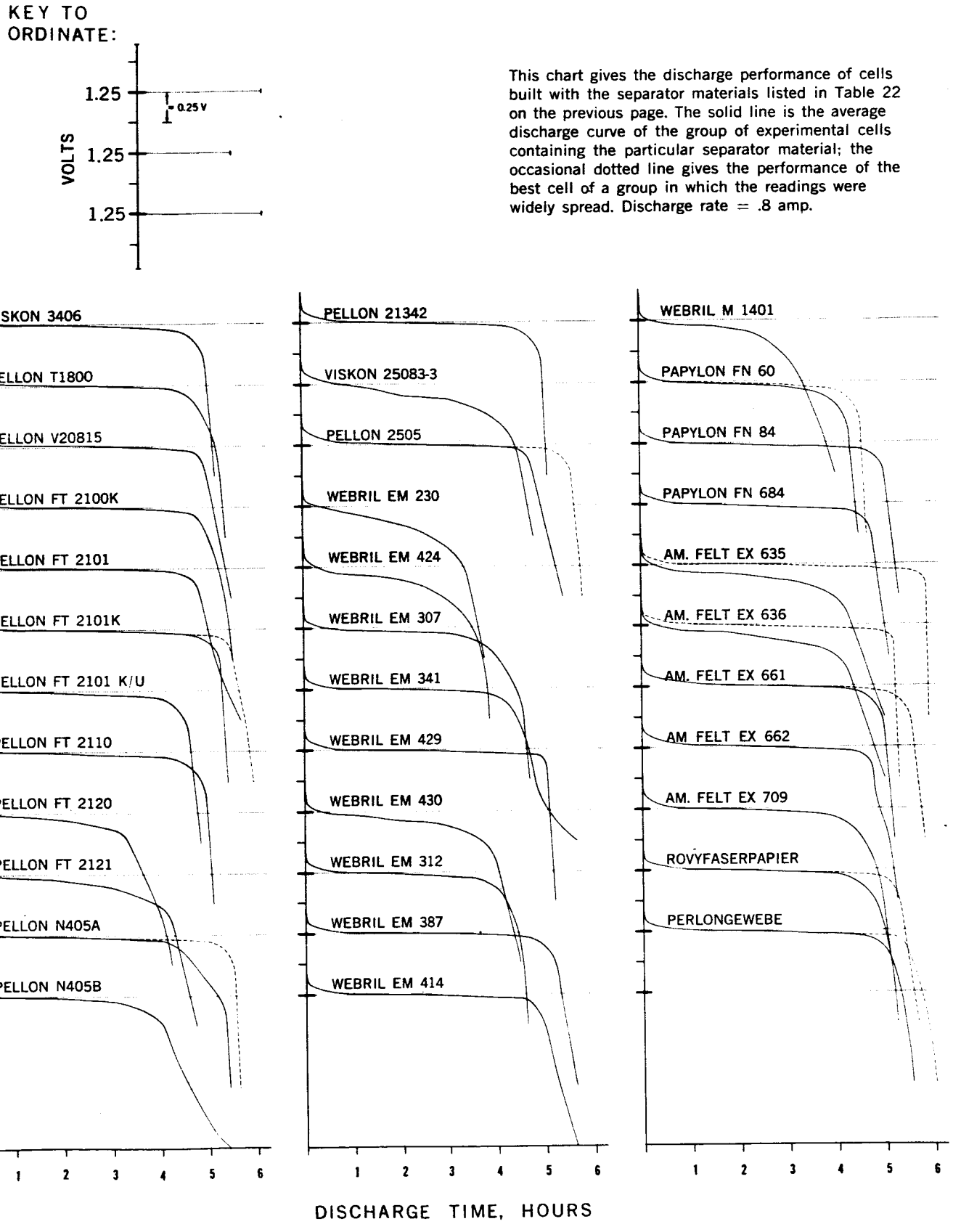

This chart gives the discharge performance of cells built with the separator materials listed in Table 22 on the previous page. The solid line is the average discharge curve of the group of experimental cells containing the particular separator material; the occasional dotted line gives the performance of the best cell of a group in which the readings were widely spread. Discharge rate = .8 amp.

TABLE 23. CAPACITIES FOR EACH DISCHARGE

Values are average readings for each cell group, and are in amp-hours.

MATERIAL	CAPACITY, DISCHARGE NO.								AVERAGE CAPACITY, 1 THRU 8
	1	2	3	4	5	6	7	8	
1. VISKON 3406 cellulose & vinyon	4.1	4.1	3.9	2.5	3.8	3.8	3.8	3.8	3.73
2. VISKON 25083-3 dynel	3.0	3.3	3.2	2.0	3.4	2.7	2.2	2.9	2.84
3. PELLON T1800 (FT 2100) nylon	4.1	4.2	4.0	3.3	4.1	3.9	3.9	3.9	3.93
4. PELLON V20815 (FT 2100G) nylon	4.1	4.2	4.1	3.5	4.2	4.0	4.1	4.0	4.03
5. PELLON FT 2100K nylon	4.2	4.3	4.1	3.3	4.0	4.0	3.9	3.8	3.95
6. PELLON FT 2101 nylon	4.1	4.2	4.0	3.2	4.2	4.0	4.0	4.0	3.96
7. PELLON FT 2101K nylon	4.3	4.3	4.1	3.3	4.0	4.0	4.0	4.0	4.00
8. PELLON FT 2101 K/U nylon	3.6	3.7	3.6	2.3	3.4	3.5	3.5	3.4	3.38
9. PELLON FT 2110 dynel	3.9	3.8	3.8	2.3	3.7	3.6	3.6	3.7	3.55
10. PELLON FT 2120 pvc	2.7	2.7	2.7	1.2	2.6	2.6	2.6	2.5	2.45
11. PELLON FT 2121 pvc	3.1	3.2	3.1	1.9	2.9	2.9	2.9	2.9	2.86
12. PELLON N405A polypropylene	3.8	4.0	3.9	2.3	3.9	3.8	3.8	3.9	3.68
13. PELLON N405B polypropylene	3.4	3.6	3.3	2.1	3.4	3.2	3.0	3.0	3.13
14. PELLON 21342 nylon	3.9	4.0	3.9	3.2	3.8	3.8	3.8	3.9	3.79
15. PELLON 2505 nylon	4.0	4.1	4.0	3.6	3.8	4.1	4.1	4.3	4.00
16. WEBRIL EM 230 dynel	2.2	2.4	2.2	0.70	2.3	2.2	2.3	2.3	2.08
17. WEBRIL EM 424 dynel	2.5	2.5	2.2	0.50	2.5	2.4	2.3	2.4	2.16
18. WEBRIL EM 307 dynel	3.5	3.6	3.1	2.5	3.1	3.0	3.0	3.0	3.10
19. WEBRIL EM 341 dynel	3.9	3.9	3.6	2.4	3.6	3.2	3.2	3.1	3.36
20. WEBRIL EM 429 dynel	4.2	4.2	4.1	2.7	3.7	3.8	3.6	3.7	3.75
21. WEBRIL EM 430 dynel	2.7	3.0	2.8	1.5	2.9	2.8	2.6	2.6	2.55
22. WEBRIL EM 312 nylon & dynel	3.5	3.5	3.3	2.0	3.3	3.3	3.2	3.2	3.16
32. WEBRIL EM 387 nylon & dynel	4.1	4.1	4.1	2.3	4.1	3.9	3.9	3.9	3.80
24. WEBRIL EM 414 nylon & dynel	4.1	4.2	4.1	3.4	4.2	4.0	4.0	4.0	4.00
25. WEBRIL M 1401 dynel	2.4	3.0	2.3	1.3	2.5	2.4	2.2	2.2	2.29
26. PAPYLON FN 60 pva	3.4	3.4	3.3	2.4	3.1	3.1	3.1	3.1	3.13
27. PAPYLON FN 84 pva	4.1	4.1	4.0	2.4	3.8	3.7	3.8	3.7	3.70
28. PAPYLON FN 684 pva	3.8	3.8	3.7	2.6	3.5	3.5	3.5	3.4	3.49
29. AM. FELT EX 635 polypropylene	3.1	3.3	3.2	2.0	3.1	3.2	3.0	2.9	2.98
30. AM. FELT EX 636 polypropylene	3.2	3.3	3.1	1.9	3.1	3.1	3.0	2.9	2.95
31. AM. FELT EX 661 polypropylene	3.8	4.0	4.0	3.0	3.6	3.6	3.2	3.6	3.60
32. AM. FELT EX 662 polypropylene	3.8	3.9	3.8	3.3	3.6	3.9	4.0	4.0	3.83
33. AM. FELT EX 709 polypropylene	3.5	3.8	3.6	2.3	3.3	3.2	2.8	3.4	3.61
34. ROVYFASERPAPIER dynel	3.9	4.0	3.8	2.7	3.5	3.5	3.5	3.4	3.54
35. PERLONGEWEBE nylon	4.4	4.3	4.1	3.0	3.9	3.9	3.9	3.9	3.93

B. HIGH RATE DISCHARGE PERFORMANCE

Since the ability to withstand high rates of discharge is important in many sealed cell applications, the test cells were discharged at the 1 hr. rate in the fourth cycle, and the percentage of the Cycle No. 3 capacity thus obtained was recorded. As might be expected, the separator with the lowest internal resistance (Pellon 2505) suffered the least under this high rate; incidentally, the initial capacity of this material was not nearly the best — it fell toward the bottom of the upper third of the range of capacities. Conversely, the material with the highest discharged internal resistance (Webril EM 424) had the lowest percentage capacity output at this high rate.

TABLE 24. HIGH RATE DISCHARGE, AVERAGED FOR RESIN TYPE

Values given are percentage of 5 hr. rate capacity which was obtained at the 1 hr. discharge rate.

RESIN	% CAPACITY OBTAINED
Nylon (9 mat'ls)	79.9
PVA (3)	68.3
Dynel-Nylon (3)	66.9
Viskon (1)	61.5
Polypropylene (7)	67.4
Dynel (10)	56.8
PVC (2)	51.7

TABLE 25. HIGH RATE DISCHARGE PERFORMANCE

Values given are percentage of 5 hr. rate capacity which was obtained at the 1 hr. discharge rate.

MATERIAL	% CAPACITY OBTAINED
1. VISKON 3406 cellulose & vinyon	61.5
2. VISKON 25083-3 dynel	62.1
3. PELLON T1800 (FT 2100) nylon	82.8
4. PELLON V20815 (FT 2100G) nylon	85.4
5. PELLON FT 2100K nylon	81.6
6. PELLON FT 2101 nylon	81.1
7. PELLON FT 2101K nylon	77.8
8. PELLON FT 2101 K/U nylon	64.8
9. PELLON FT 2110 dynel	59.2
10. PELLON FT 2120 pvc	43.2
11. PELLON FT 2121 pvc	60.2
12. PELLON N405A polypropylene	60.0
13. PELLON N405B polypropylene	62.2
14. PELLON 21342 nylon	81.4
15. PELLON 2505 nylon	91.6
16. WEBRIL EM 230 dynel	32.5
17. WEBRIL EM 424 dynel	21.7
18. WEBRIL EM 307 dynel	79.0
19. WEBRIL EM 341 dynel	66.5
20. WEBRIL EM 429 dynel	65.1
21. WEBRIL EM 430 dynel	52.7
22. WEBRIL EM 312 nylon & dynel	61.4
23. WEBRIL EM 387 nylon & dynel	56.1
24. WEBRIL EM 414 nylon & dynel	83.4
25. WEBRIL M 1401 dynel	58.6
26. PAPYLON FN 60 pva	73.9
27. PAPYLON FN 84 pva	61.2
28. PAPYLON FN 684 pva	69.8
29. AM. FELT EX 635 polypropylene	62.8
30. AM. FELT EX 636 polypropylene	62.6
31. AM. FELT EX 661 polypropylene	73.1
32. AM. FELT EX 662 polypropylene	85.1
33. AM. FELT EX 709 polypropylene	65.8
34. ROVYFASERPAPIER dynel	71.0
35. PERLONGEWEBE nylon	73.0

C. CORRELATION BETWEEN ABSORBENCY AND CAPACITY

It appears that cell capacity is to some extent correlated with the absorbency of the separator material. In general, materials with higher absorbency yield cells with higher capacities, and vice versa, although there are many exceptions to this. As an example, several of the Pellon materials have good absorbency and resulted in high cell capacities; on the other hand, Pellon FT 2101K which has rather poor absorbency, resulted in the highest capacity of any of the materials tested. Another example: Webril materials are generally very low in absorbency; however, EM 429 and EM 387 (which had the lowest absorbency of all materials), had capacities which were second only to the FT 2101K.

As an attempt to clarify this situation, the average capacities of Cycle No. 3 were plotted against absorbency. When plotted on logarithmic paper, a high correlation is evident in those materials with absorbencies above 2.0 (particularly when considering the many other variables influencing capacity which were not controlled in this group of cells). The points for materials with absorbencies below 2.0 are increasingly spread from the curve. Tables of absorbency compared with the third cycle capacity of individual materials, and of materials grouped and averaged by resin type, are presented following, as is the plot of capacity vs. absorbency.

TABLE 26. AVERAGE ABSORBENCIES VS. CAPACITY

RESIN	ABSORBENCY	CAPACITY
Nylon (9 mat'ls)	4.8	4.0
Viskon (1)	5.7	3.9
Dynel-Nylon (3)	3.8	3.8
Polypropylene (7)	1.6	3.6
PVA (3)	3.5	3.3
Dynel (10)	2.1	3.1
PVC (2)	1.4	2.9

TABLE 27. MATERIAL ABSORBENCY VS. CAPACITY

MATERIAL	ABSORBENCY	CAPACITY (AH)	MATERIAL	ABSORBENCY	CAPACITY (AH)
1. VISKON 3406 cellulose & vinyon	5.7	3.9	19. WEBRIL EM 341 dynel	1.2	3.6
2. VISKON 25083-3 dynel	1.8	3.2	20. WEBRIL EM 429 dynel	3.0	4.1
3. PELLON T1800 (FT 2100) nylon	6.3	4.0	21. WEBRIL EM 430 dynel	0.8	2.8
4. PELLON V20815 (FT 2100G) nylon	6.7	4.1	22. WEBRIL EM 312 nylon & dynel	3.7	3.3
5. PELLON FT 2100K nylon	3.5	4.1	23. WEBRIL EM 387 nylon & dynel	2.5	4.1
6. PELLON FT 2101 nylon	6.4	4.0	24. WEBRIL EM 414 nylon & dynel	5.0	4.1
7. PELLON FT 2101K nylon	1.4	4.1	25. WEBRIL M 1401 dynel	0.7	2.3
8. PELLON FT 2101 K/U nylon	2.8	3.6	26. PAPYLON FN 60 pva	3.6	3.3
9. PELLON FT 2110 dynel	8.2	3.8	27. PAPYLON FN 84 pva	3.6	4.0
10. PELLON FT 2120 pvc	1.6	2.7	28. PAPYLON FN 684 pva	3.2	3.7
11. PELLON FT 2121 pvc	1.3	3.1	29. AM. FELT EX 635 polypropylene	0.8	3.2
12. PELLON N405A polypropylene	1.9	3.9	30. AM. FELT EX 636 polypropylene	0.9	3.1
13. PELLON N405B polypropylene	1.8	3.3	31. AM. FELT EX 661 polypropylene	1.7	4.0
14. PELLON 21342 nylon	6.4	3.9	32. AM. FELT EX 662 polypropylene	2.5	3.8
15. PELLON 2505 nylon	7.6	4.0	33. AM. FELT EX 709 polypropylene	1.3	3.6
16. WEBRIL EM 230 dynel	0.9	2.2	34. ROVYFASERPAPIER dynel	2.2	3.8
17. WEBRIL EM 424 dynel	0.9	2.2	35. PERLONGEWEBE nylon	2.2	4.1
18. WEBRIL EM 307 dynel	0.9	3.1			

FIG. 8. MATERIAL ABSORBENCY VS. CAPACITY

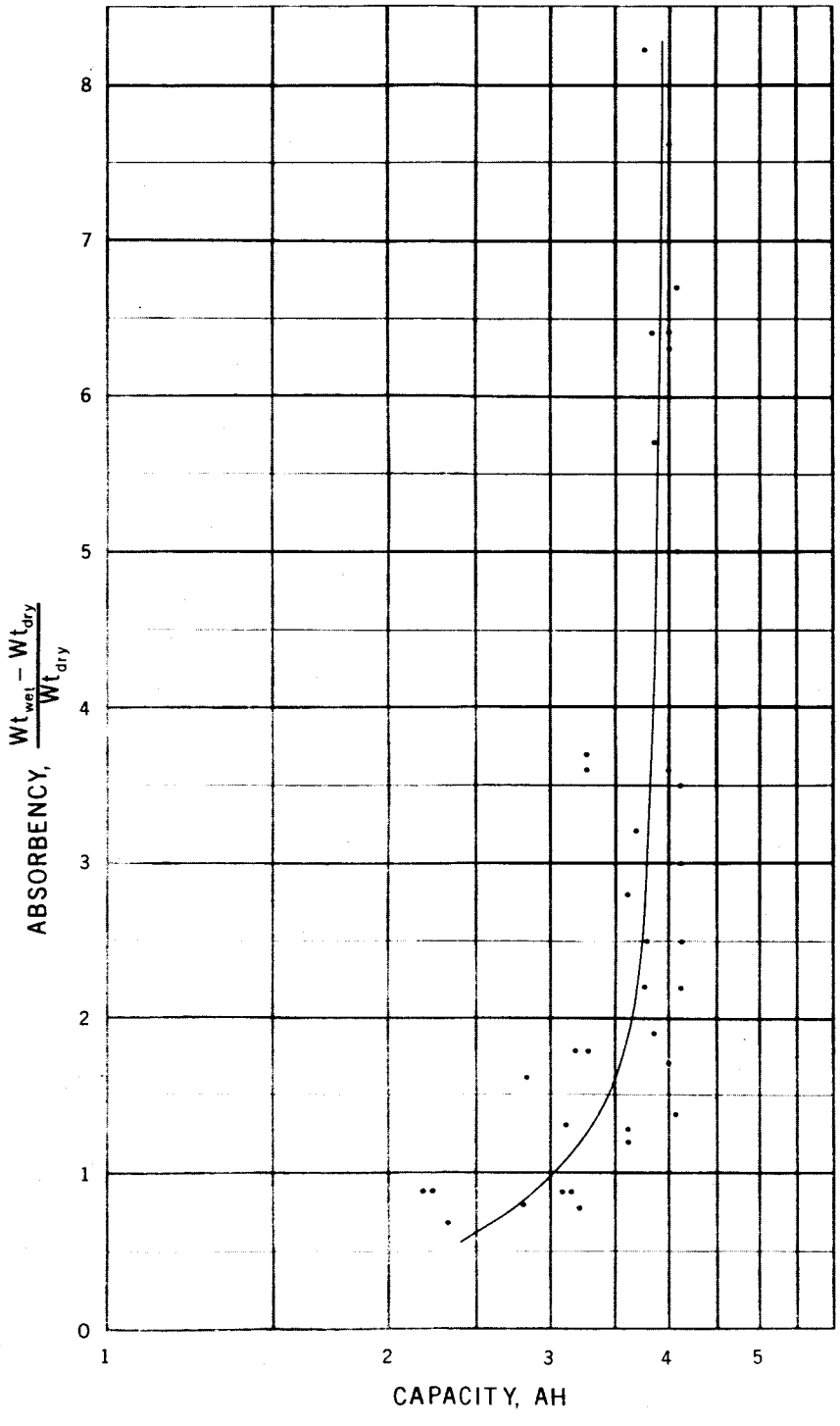

D. INTERNAL SHORTING

In order to determine whether any of the materials had allowed shorts to develop within the test cells, the entire lot of fully charged cells, after having been put through all other electrical testing, was placed on stand for 2 weeks, and their potentials recorded each day. By the end of this period, the potential of each cell had dropped 3 to 5% below its original value, except for 2 cells which had previously given evidence of having internal shorts. It therefore seems that within the limitations of the test conditions used in this program, none of the materials has a pronounced tendency to develop shorts. Similarly, there was no discernible relationship between separator material and the amount of self discharge; among the materials tested, it appears doubtful that the type of material has any effect on the retention of charge.

X. SPECIAL CELL INVESTIGATION OF POLYPROPYLENE

Polypropylene evinced better resistance to attack by KOH than any other resin type tested under this program, and it showed significant promise with respect to several of the other parameters evaluated. However, its electrical performance in the sealed cells was rather poor.

For these reasons, as the program progressed, it was decided to study this material more intensively. American Felt EX 635 was chosen as the research vehicle, since among the polypropylenes which were more completely tested, this was the one with the best general performance. A series of cells was constructed using EX 635 and varying volumes of 25% KOH. In the construction of the polypropylene cells for the original electrical evaluation, 6.7 ml of KOH had been used, since this corresponded roughly to 30% of the material's absorbent capacity. The new test series was built using volumes of 6.3, 7.0, 7.3, 7.7, and 8.0 ml, thus providing an even coverage of this range. It was not thought advisable to use volumes above 8.0 ml since such high volumes would have a deleterious effect on charge characteristics, and therefore would be unsatisfactory for production designs regardless of their effect on capacity.

The cells were subjected to the same test sequence as was used for the original electrical evaluation; the results of this testing are given following. It will be seen that the capacity of these cells increased with increasing electrolyte volume as far as 7.7 ml; at this point, the capacity reached a plateau. The ability to withstand the high discharge rate also increased with the increasing electrolyte volume, and tapered off at the same point. The discharge voltage curves of these cells had the typical configuration: The plateau voltage of each cell except those in the first volume group (6.3 ml) was almost exactly at 1.25 V; the major difference between groups was the shifting of the knee of the curve to the right as capacity increased with increasing electrolyte volume. Since the absorbency of polypropylene is next to the lowest of all materials tested, it is understandable that increasing the volume of electrolyte in these cells had this pronounced effect on their performance. It must be noted that despite the great improvement in performance seen in this experiment, the capacity of the best cell still did not nearly equal the capacity of the Viskon cells or the average capacity of the nylon cells; furthermore, increasing the amount of electrolyte in the Viskon and nylon cells would similarly increase their capacities above values recorded. The percentage of capacity obtained from these cells at the high rate, on the other hand, equaled the nylon and exceeded the Viskon.

TABLE 28. SPECIAL POLYPROPYLENE INVESTIGATION AMERICAN FELT EX 635

KOH VOL. (ml)	CAPACITY, BY CYCLE (AH) 1	2	3	4	5	6	7	8	AVG. CAP. (AH)	CHARGED RESISTANCE (mΩ)	DISCHARGED RESISTANCE (mΩ)	HIGH§ RATE PERFORMANCE (%)
6.3	3.2	3.1	3.1	2.0	3.0	3.3	3.2	3.0	3.0	14.8	43.0	63.6
7.0	3.2	3.3	3.5	2.4	3.3	3.5	3.6	3.4	3.27	10.0	17.2	68.7
7.3	3.5	3.5	3.6	2.5	3.3	3.4	3.6	3.5	3.36	9.6	16.8	69.5
7.7	3.7	3.8	3.8	3.0	3.4	3.7	3.7	3.8	3.63	8.5	13.8	79.0
8.0	3.6	3.7	3.7	3.0	3.4	3.7	3.8	3.8	3.60	8.0	12.7	81.2

§ Percentage of 5 hr. capacity (Cycle No. 3) obtained at the 1 hr. discharge rate (Cycle No. 4).

XI. CELL INTERNAL PRESSURE ON OVERCHARGE

As a sealed cell is charged, the oxygen evolved from the positive plate increases the internal pressure until an equilibrium is reached between this evolution and the recombination of the oxygen at the negative plate.

The value of the equilibrium pressure was expected to depend, among other things, on the resistance offered by the separator to the diffusion of oxygen to the negative plate.

An attempt was made to establish a relationship between the permeability of a separator material and the level of the equilibrium pressure. Eight cells of good capacity were selected, 2 each containing separators of nylon, dynel, polypropylene, and Viskon, as follows:

PELLON T1800 nylon	cells no. 111 & 112
PELLON FT 2110 dynel	cells no. 114 & 115
AM. FELT EX 635 polypropylene	cells no. 101 & 103
VISKON 3406 cellulose & vinyon	cells no. 111 & 114

The bottom of each cell can was punctured, and the cells were clamped into a fixture which established a sealed path between the puncture and a pressure gauge. The cells were then placed on continuous overcharge and the pressure was recorded roughly every hour.

As will be seen in Table 29, the readings were quite erratic, and the correlation between permeability and internal pressure was not nearly as close as had been expected. We have found in other research programs that it is quite difficult to measure cell internal pressure reliably, and we have reason to suspect that in this experiment also, the erratic nature of the readings may be due to deficiencies in the experimental procedure. This is a problem area that should be pursued further; a method of reading internal pressure should be developed which would be more reliable, and which would make practicable the testing of much larger numbers of cells.

It was observed that the pressure in each cell rose to a certain maximum, then began oscillating between this maximum and a lower value. This pressure oscillation has been noticed in the cell performance information released by other sources in the industry. The amplitude of this oscillation was generally between 1 and 3 lbs./in^2; the oscillation amplitudes evinced no apparent relation to material type. The period of this oscillation varied between 20 and 35 hours, seeming to be shortest for the EX 635 and longest for the FT 2110, with the other 2 materials falling between.

TABLE 29. INTERNAL PRESSURE VS. OXYGEN PERMEABILITY

MATERIAL	O_2 PERMEABILITY (Ft^3/Sec./Ft^2)	CELL NO.	INITIAL MAXIMUM PRESSURE (Lbs./In^2) Per Cell	Average
PELLON FT 2110 dynel	57.6	114	26	28
		115	30	
PELLON T1800 nylon	52.9	111	26	28.25
		112	30.5	
AM. FELT EX 635 polypropylene	44.5	101	37.5	29
		103	20.5	
VISKON 3406 cellulose & vinyon	21.75	111	38.5	32.87
		114	27.25	

XII. PERFORMANCE IN CELL UNDER ACCELERATION

The discharge performance under acceleration of cells containing four of the more promising separator materials was recorded, since this is a particularly important performance parameter in cells intended for space use. The materials and cells used are as follows:

Pellon FT 2101 nylon	Cell 104
Webril EM 429 dynel	Cell 101
Pellon N405A polypropylene	Cell 101
Viskon 3406 cellulose and vinyon	Cell 101

The cells were fully charged and run in the centrifuge at 25 g's. While under acceleration, the cells were discharged to 0.0 V, at which point the centrifuge was stopped.

The discharge was continued as the acceleration ceased, and it was observed that in each case, the voltage of the test cell rose to a certain height before returning again to zero. This premature depression of the discharge voltage was assumed to be due to the draining of the electrolyte from the separator and the plates to the bottom of the cell; the electrolyte would be re-absorbed after the acceleration ceased, resulting in the rise in voltage that was observed before exhaustion of the cell. The discharge curves for these four test cells are shown in Fig. 9 which follows.

FIG. 9. EFFECT OF ACCELERATION ON DISCHARGE PERFORMANCE

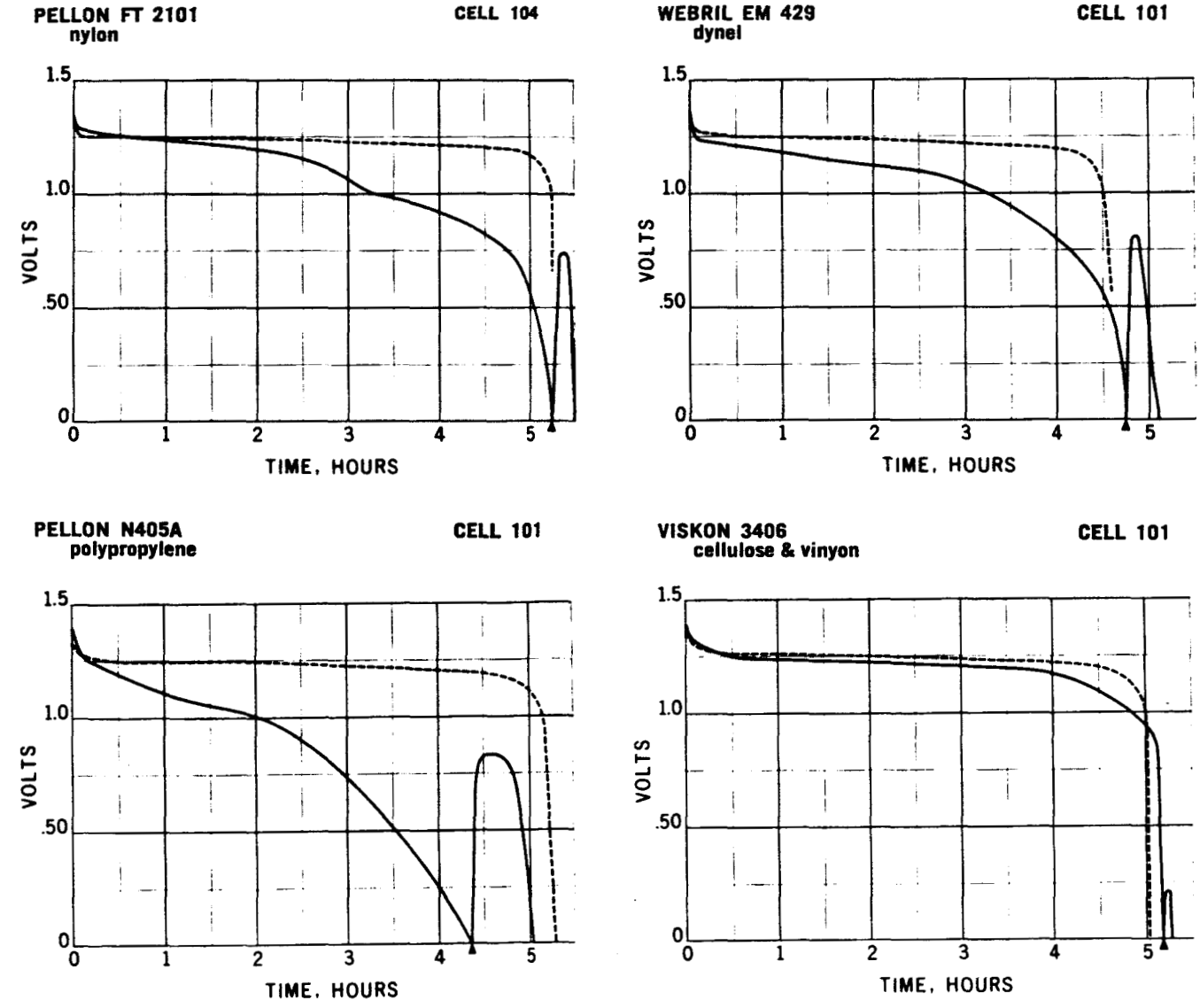

The deleterious effect of the acceleration was most noticeable with the Pellon N405A. This might be expected, since both the absorbency and rate of absorption of this material were rather poor. The Webril EM 429 has fair absorbency and excellent rate of absorption, and the Pellon FT 2101 is considerably above average in both respects; the effect of the acceleration on these two materials was much less than with the N405A, but was still quite significant. The Viskon, with its good absorbency and top rate of absorption, was

only slightly affected by acceleration. This may be at least partially explained by the fact that it is partially composed of 100% cellulose; the electrolyte would actually be absorbed into the cellular structure of this material, whereas with the other materials, it probably would be only adsorbed onto the surface of the fiber, and therefore retained less effectively.

There is good cause to believe that cells which are cycled during acceleration, or after the acceleration but before the electrolyte has been reabsorbed into the separator and the plates, will be thrown out of balance electrochemically. The internal resistance of cells with the electrolyte partially drained from the element would be quite high; if the charge voltage is limited, these cells would not be fully recharged, and might therefore become unbalanced on subsequent cycles. This is a factor that should be kept in mind when establishing the position relative to the accelerative forces, and designing the operational time pattern, of cells in any space vehicle.

XIII. CONCLUSIONS — AREAS FOR FUTURE STUDY

Of the three general categories of tests — physical fiber characteristics (strength, porosity, absorbency, etc.), chemical reactivity, and electrical performance — the reactivity experiments produced by far the most uncertain results. Most of the materials behaved fairly consistently — whether good, average, or bad — in the fiber characteristic and electrical performance tests. Results from the reactivity tests, though, were generally quite erratic. With the preponderant majority of the materials, performance was spread from the lowest third of the overall performance range under one test condition, to the highest third under another. The only resin that behaved with any consistency was polypropylene; these materials ranged over no more than two-thirds of the overall performance range.

One of the most puzzling instances of this erratic reactivity behavior occurred for several of the dynel and nylon materials. Under the 84 day test condition, the materials showed rather low weight loss under all KOH concentrations at 24°C and 54°C; then, at 75°C, the materials were 100% reacted in the 20% and 30% KOH, but in 40% KOH still showed a relatively low reactivity. This pattern occurred for Webrils EM 309, 429, and 430 (which are dynel), for EM 312 and 414 (nylon-dynel), for Ondulongewebe (nylon), and for Polypor PVA (which has a nylon base). Determining the cause for this and the other erratic aspects of reactivity performance would be one likely area for future investigation in separator materials.

Generally speaking, nylon, dynel, and polypropylene performed better than any of the other resin types tested. The nylon materials (most of which were Pellons) had the best general electrical performance of any resin. Nylon materials had the highest capacities of all materials tested; this was true both of initial capacities, and of the average capacities over 8 cycles. The percentage of capacity recovered at the high discharge rate was considerably better for nylon than for the other resins. Pellon V 20815 had the top average capacity of all the materials tested. This material had fiber characteristics and resistance to reactivity that were as good or better than the other nylons; it would be one of the two or three materials studied, none of which emerges from this program as being unqualifiedly the best, but which perform well in most respects, and which merit consideration as optimum types. The resistance to reactivity of the nylon materials was generally average to good, except at high temperature; they frequently were 100% reacted under the 84 day test condition at 75°C. The fiber characteristics of the nylon materials were average to good, except for absorbency, which with several of them was poor. The materials had good body, and would handle well in the production situation. Perlongewebe, a nylon material, had very high electrical performance (except for its high rate discharge performance, which was merely average; furthermore, its resistance to KOH was good (standing in the upper third of the overall performance range under most of the test conditions), and its fiber characteristics were average or good except for rather low strain performance. This material is another of the few materials that would be considered as an optimum type.

The dynel materials, with a few exceptions, were Webril materials. This resin generally had good rate of absorption but average or poor performance in the other fiber characteristics, average resistance to KOH (being roughly equal to nylon in this respect), and electrical performance ranging from low to high. Materials that were a mixture of dynel and nylon were slightly superior to pure dynel in fiber characteristics and electrical performance, although they did not match nylon in these respects, and their resistance to KOH was no better than that of pure nylon. Many of these materials were very thin, requiring two or three layers in the experimental cells; this layering may have affected their performance. The only Pellon material composed of dynel, FT 2110, performed better than average electrically, and was notably superior to the Webril materials in fiber characteristics; it had the top absorbency of all materials tested. Development of a dynel sheet of sufficient thickness, having the good fiber characteristics of FT 2110 and the high electrical performance qualities of, for example, Webril EM 429, would be one promising area of future work.

Polypropylene consistently had the best resistance to KOH of any of the more common resins tested. It was the only important resin that did not exhibit a wide range of performance under the various reactivity test conditions, and that did not exhibit increased reactivity at high temperature. This contrasts with the electrical performance of the polypropylene materials; they exhibited a much wider spread of performance values than the other materials. This fiber has a waxy surface which does not wet quickly; it is expected that this is a contributing factor to its low rate of absorption. The polypropylene materials generally had average strength and average to low absorbency and porosity. There was considerable variation in the weights and porosities of the samples tested; the technology of producing this material has not yet developed to the point where the uniformity of the product matches that obtainable with nylon or dynel.

National Lead Polyethylene had probably the best performance of any material tested throughout all of the reactivity test conditions. This was the only material tested that was the top performer in more than one of these test conditions. However, the material has poor strength and porosity, and would not therefore be considered as one of the optimum separator types.

The area of future work that should be most strongly pursued is search for, or developmental effort in cooperation with the fiber manufacturers toward, a material that would have the fiber characteristics and electrical performance of nylon, combined with polypropylene's resistance to KOH.

Other problem areas that should be studied further include causes for the variation from material to material of the oscillation of cell internal pressure on overcharge; more precise establishment of the relative importance of absorbency, rate of absorption, internal resistance, and other parameters, in determining cell capacity; alteration of fiber characteristics so as to reduce to a minimum the influence of accelerative forces; further attempts to isolate material parameters having a bearing on cell performance, in addition to those studied under this program.

Fig. 10 which follows is a graphic summary of the performance of all the separator materials under each test condition to which they were subjected. In preparing this chart, the analysis of the data for each test condition began with the plotting on one axis of the performance of all materials tested under that condition. The over-all performance range was then split into thirds, each third containing roughly the same number of materials; in establishing the breaking-points between these thirds, natural breaks in the groupings of material data were sought, rather than the points embracing precisely one-third of the materials tested. The particular third — upper, middle, or lower — in which the performance of each material fell, was then recorded on the chart. Also, the top performer and the bottom performer in each third of the performance range is indicated.

A note of caution must be expressed regarding the use of this chart. It should be looked on as a general aid, which will provide a broad idea of the performance of each material. It must not be relied on, to the exclusion of the complete tables of data, to provide the final answer as to the performance of a material under any specific condition. As an example, Polypor WB is indicated as being in the bottom third of the materials with respect to tensile strain; it exhibited an increase in length during tensile test that was several times that of the average material. However, this material was by far the strongest material tested, so it is by no means certain that the "poor" tensile strain rating would argue against the use of this material in sealed cells.

KEY:

● ● ● } indicates performance in { upper third / middle third / lower third } of over-all performance range

■ at top of third indicated
□ at bottom of third indicated

Fig. 10 SEPARATOR MATERIAL SUMMARY

	FIBER CHARACTERISTICS						REACTIVITY WITH KOH									ELECTRICAL PERFORMANCE				
	MECHANICAL STRENGTH		POROSITY	O_2 PERMEABILITY	ABSORBENCY	RATE OF ABSORPTION	WEIGHT LOSS		SHRINKAGE OR STRETCH				KOH REACTED		WEIGHT LOSS IN PRESENCE OF O_2	INITIAL CAPACITY	INTERNAL RESISTANCE		AVERAGE CAPACITY 8 CYCLES	HIGH RATE DISCHARGE
									14 DAY		84 DAY									
	Stress	Strain					14 Day	84 Day	Lgth.	Width	Lgth.	Width	14 Day	84 Day			Charged	Disch'gd.		
1. VISKON 3406, cellulose & vinyon	●	●	●	●	□	■	●	●	●	●	●	●	●	●	●	●	●	●	●	●
2. VISKON 25083-3, dynel			●		●	●									●	●	●	●	●	●
3. PELLON T1800 (FT2100), nylon	●	●	●	●	●	●	●	●	●	●	●	●	●	□	●	●	●	●	●	●
4. PELLON V20815 (FT 2100G), nylon	●	●	●	●	●	●	●	●	●	■	●	●	●	●	●	●	●	●	■	●
5. PELLON FT 2100K, nylon			■	●	●	□	●	●	●	●	●	●	●	●	●	●	●	■	●	●
6. PELLON FT 2101, nylon			●	●	●	●	●	□	●	●	●	●	●	●	●	■	●	●	●	●
7. PELLON FT 2101K, nylon			●	□	□		●	●	■	●	■	●	●			■	●	●	●	□
8. PELLON FT 2101 K/U, nylon			●	●	●	●	●	●	●	■	●	●	■		●	●	●	●	●	●
9. PELLON FT 2110, dynel			●	●	■	●									●	●	●	□	●	●
10. PELLON FT 2120, pvc			●	●	□	□	●	●	●	●	●	●	●	■	■	□	●	●	●	●
11. PELLON FT 2121, pvc			●	●	●	●	●	●	●	●	●	●	●	●	●	●	●	●	●	■
12. PELLON N405A, polypropylene			■	●	●	■	●	●	●	●	□	●	●	●	■	●	●	●	□	●
13. PELLON N405B, polypropylene			●	●	●	●	●	●	□	●	□	●	●	●	●	●	●	●	●	●
14. PELLON 2134-2, nylon			●		●	□									●	●	●	●	●	●
15. PELLON 2505, nylon			●		●										●	●	■	■	●	■
16. WEBRIL EM 230, dynel			●			●			●	●	●	□			●					
17. WEBRIL EM 309, dynel			●	□	●			●	●	●	●	●	●	●			●	●	□	●
18. WEBRIL EM 403, dynel			●		●			●					●							
19. WEBRIL EM 424, dynel			●			■			●	●	●	●								
20. WEBRIL EM 307, dynel			●	●	●	■		●	●	●			●	●	□	●	●	□	●	□
											●	□		●		■	●	●	□	●

KEY:

● ● ● } indicates performance in { upper third / middle third / lower third } of over-all performance range

■ at top of third indicated
□ at bottom of third indicated

Fig. 10 SEPARATOR MATERIAL SUMMARY (CONT'D)

	FIBER CHARACTERISTICS						REACTIVITY WITH KOH								ELECTRICAL PERFORMANCE				
	MECHANICAL STRENGTH		POROSITY	O_2 PERMEABILITY	ABSORBENCY	RATE OF ABSORPTION	WEIGHT LOSS		SHRINKAGE OR STRETCH				KOH REACTED		WEIGHT LOSS IN PRESENCE OF O_2	INITIAL CAPACITY	INTERNAL RESISTANCE		AVERAGE CAPACITY 8 CYCLES	HIGH RATE DISCHARGE
									14 DAY		84 DAY									
	Stress	Strain					14 Day	84 Day	Lgth.	Width	Lgth.	Width	14 Day	84 Day			Charged	Disch'gd.		
21. WEBRIL EM 341, dynel	■	●	●	□	●	□	●	□	□	□	●	●								●
22. WEBRIL EM 429, dynel	●	■	●	●	●	●	●	●	■	■	■	●	■	●	■	●	●	●	●	●
23. WEBRIL EM 430, dynel	●	●	●	●	●	●	●	●	●	●	●	●	●	●	●	●	●	●	●	
24. WEBRIL EM 312, nylon & dynel	□	■	●	●	●		■	●	□	●	●	●	●	●	□					●
25. WEBRIL EM 387, *nylon & dynel*	●	●	□		●		■	■	●	●	●	●	●	●	●					●
26. WEBRIL EM 414, nylon & dynel	●	●	■	●	●		●						●							●
27. WEBRIL EM 444, vinyon & rayon			●		□		●	■	●	●	●	●	■	●	●					
28. WEBRIL M 1401, dynel			●		■								●							●
29. PAPYLON FN 60, pva			●		■								●		□					■
30. PAPYLON FN 84, pva				●	□								●	●	□					□
31. PAPYLON FN 684, pva				■	●								●	●	□					●
32. PORON, vinyl				■	●								●	■	□					
33. SYNPOR																				
34. AM. FELT EX 635, polypropylene	●	●	●		●		●						●							●
35. AM. FELT EX 636, polypropylene					●															●
36. AM. FELT EX 661, polypropylene					■															●
37. AM. FELT EX 662, polypropylene					□															●
38. AM. FELT EX 709, polypropylene					□															●
39. POLYPOR PVA, nylon base			●		●			●	●	●	●	●	●	●						
40. POLYPOR WB, nylon base																				

KEY:

● ● ● } indicates performance in { upper third / middle third / lower third } of over-all performance range

■ at top of third indicated
□ at bottom of third indicated

Fig. 10 SEPARATOR MATERIAL SUMMARY (CONT'D)

	FIBER CHARACTERISTICS						REACTIVITY WITH KOH								ELECTRICAL PERFORMANCE				
	MECHANICAL STRENGTH		POROSITY	O_2 PERMEABILITY	ABSORBENCY	RATE OF ABSORPTION	WEIGHT LOSS		SHRINKAGE OR STRETCH				KOH REACTED		WEIGHT LOSS IN PRESENCE OF O_2	INITIAL CAPACITY	INTERNAL RESISTANCE		AVERAGE CAPACITY 8 CYCLES	HIGH RATE DISCHARGE
									14 DAY		84 DAY									
	Stress	Strain					14 Day	84 Day	Lgth.	Width	Lgth.	Width	14 Day	84 Day			Charged	Disch'gd.		
41. POLYPOR ANGSTRA, rayon base	■	●	●	□	●	□	●	□	□	□	●	●								
42. ROVYFASERPAPIER, dynel	●	■	●	●	●	●	●	●	■	■	■	●	■	●	■	●	●	●	●	●
43. PERLONGEWEBE, nylon	●	●	●	●	●	●	●	●	●	●	●	●	●	●	●	●	●	●	●	●
44. ONDULONGEWEBE, nylon	□	■	●	●	●		■	●	□	●	●	●	●	●	□					
45. NATIONAL LEAD POLYETHYLENE	●	●	□		●		■	■	●	●	●	●	●	●	●					
46. RIEGEL DACRON	●	●	■	●	●		●						●							
47. NYLON CLOTH			●		□		●	■	●	●	●	●	■	●	●					
48. 3-M, acrylic inner			●		■								●							
49. 3-M, acrylic outer			●		■								●		□					
50. 3-M, nylon				●	□								●	●	□					
51. 3-M, polypropylene				■	●								●	●	□					
52. 3-M, dynel				■	●								●	■	□					
53. ALDINE ALDEX 514, cellulose																				
54. EATON DIKEMAN 3042, dacron	●	●	●		●		●						●							
55. EATON DIKEMAN 791, cellulose					●															
56. EATON DIKEMAN 794, cellulose					■															
57. EATON DIKEMAN 938, cellulose					□															
58. EATON DIKEMAN 928, cellulose					□															
59. DORRON 37B			●		●			●	●	●	●	●	●	■						

CELL CLOSURE

I. INTRODUCTION

One of the major problems in the development of a satisfactory glass-to-metal seal has been the corrosion of the glass by the electrolyte. Much effort throughout the industry has been expended on this problem, but the problem has not yet been satisfactorily resolved. Attempts have been made to develop a glass with superior resistance to KOH which would have resistance to stress and shock equal or superior to the stronger glasses presently available. Up to the present, however, the glasses with good caustic resistance are entirely too susceptible to thermal and physical shock. Use of ceramics resolves the problem of caustic resistance, but brings in a new set of problems revolving around the difficult fusion of the material to metal.

Given the great amount of effort that a wide variety of organizations have thus far expended on this glass problem, with results that are only partly satisfactory, we felt that an alternative approach should be tried. Since it's difficult to develop a glass with satisfactory resistance to the electrolyte, we felt that a more fruitful approach might be to isolate the glass from the electrolyte. Two approaches were proposed to achieve this — first, an investigation of caustic-resistant coatings to be applied to the inner surfaces of the cover assembly, and second, development of a nylon seal between the glass seal and the cell interior. The results of this work are described in the following section.

The second major problem area in cell closure, standing apart from the problems involving the glass or ceramic seal itself, is the welding of the cover assembly to the can. Based on our experience and on what we know of the experience of others, this is an area in which there is much room for improvement. Two avenues of investigation were proposed, one revolving around projection welding techniques, and the other involving heli-arc welding. We feel that the work done under this program has resulted in a better and more reliable technic of cell weld closure.

All of the work described in this section was done on cells of "D" configuration, having a capacity of roughly 4.0 AH. Work done in the following problem areas will be discussed:

Glass Corrosion

- — Coating inner surface of glass and cover with epoxy resins
- — Development of a nylon inner seal assembly to isolate the glass

Projection Welding

- — Proper configuration and location of the projection
- — Cleansing of the weld components
- — Shielding weld components following purge and during welding with inert gas
- — Strike-plating weld components with silver and mercury
- — Gold-plating weld components
- — Design and material of welding electrodes
- — Fabrication of weld components
- — Welding currents and pressures
- — Welding impulse characteristics: heat times, cool times, number of impulses
- — Effects of upslope and downslope conditions
- — Drawing up of projection welded area from horizontal to vertical position preparatory to heli-arc secondary weld

Heli-Arc Welding

- — Material and fabrication of weld components
- — Positioning of weld components prior to and during weld
- — Seam welding of cover to can prior to heli-arc
- — Block temperatures, use of heat sinks
- — Weld speed and currents
- — Composition and feeding of inert gas
- — Composition and dimensions of welding tip
- — Design and cooling of torch

II. PREVENTION OF CORROSION OF THE GLASS

A. EPOXY COATINGS

Prior to the NASA program, our center had done an intensive survey of the epoxy resins available on the market, with particular attention directed toward stability in KOH. This work was done in the course of developing a superior nickel-cadmium storage battery for aircraft use. One resin was found—Cook's 836-R-9 epoxy — which resisted attack by KOH very well, and provided a superior exterior coating for alkaline cells.

This material was therefore chosen for evaluation as a caustic-resistant coating for the inner surface of the glass seal area. The material was brushed onto the underside of the cover assembly, covering the inside portion of the positive post, the glass, and the majority of the metal of the cover, out to the perimeter. The preparation and application of this material was done in strict accordance with the manufacturer's directions. It adhered very well both to the metal and to the glass, as had previously been our experience. The treated cover assemblies were then built into cells and the cells were placed on stand for one month. The cells were opened at the end of the month, and in every case the coating had been completely stripped from the surface to which it was applied, and had dropped down into the cell. This behavior coincided with reports we have received from other organizations interested in the same problem, that the continued application even of a relatively low electromotive force across such a coating will reduce its life to the barest fraction of normal. Such an electromotive force (the open circuit voltage of the cell) does of course exist across the surface of a coated cover, between the negative cell can and the positive post and positive plate lug.

Following the unsatisfactory outcome of this test, further inquiry was made of persons familiar with resins and protective coatings, in an attempt to locate additional materials that had not been previously evaluated by us. A ceramics specialist recommended that we try a new series of epoxies known to form a superior bond with ceramic materials. In addition, samples of Armstrong A-1, A-2, and A-21 were secured. The complete series of materials evaluated is as follows:

Rubber & Asbestos Corp. M-620
Synthetical Labs S-16, S-34
PVC with MEK filler
Ciba 506 + phenolic + filler with Hypol "C" hardener
Ciba 506 + 85 parts coal tar with triethylenetetramine as hardener
Genepoxy 177 + Versamide 140 (70:30)
3-M Scotch Cast No. 3
Armstrong A-1, A-2, and A-21

A preliminary evaluation was done on these materials; they were applied to the under surface of metal cover blanks and immersed in KOH. Application usually was by brushing them onto the surface, though some of the more viscous ones were smeared on. The ceramic-based epoxies, for the most part, were stripped from the surface of the nickel very quickly. Sand blasting of the surface of the nickel did not seem to improve the bond. The adherence of the Armstrong A-21 was somewhat better, though not much. The least unsatisfactory of these materials were applied to complete cover assemblies, including the glass. They adhered reasonably well to the glass, but again were stripped off fairly quickly when immersed in KOH. Since coverage of the glass would be ineffectual without coverage of the adjoining metal, and since it is known that in a cell, with the voltage of the cell applied across them, their performance would be far inferior even to these preliminary tests, investigation of these materials was dropped.

It appears that the Cook 836-R-9 chosen as a result of our initial evaluation program is still one of the best coatings on the market with respect to KOH resistance. The geometry of sealed cells, either cylindrical or rectangular, would make it difficult if not impossible to provide an epoxy coating which would not be subjected to the cell Emf. And it is felt that, even with a fairly broad coverage of the epoxy, any defect in the coating large enough to admit an electrolyte ion would provide a site for the beginning of the stripping action. In view of these difficulties, this approach was dropped.

B. NYLON INNER SEAL

The alternative method of preventing the corrosion of the glass seal by KOH which was proposed for this program is the development of a nylon seal around the positive post, between the glass and the electrolyte. It was expected during the planning of this program that this would be the most successful approach, and this proved to be true. This sealing element is a nylon gasket with an ID considerably smaller than the diameter of the positive pin. The gasket is forced over the positive pin, and is supported by a metal diaphragm which is in turn welded to the underside of the cover, thus providing a complete barrier between the glass sealing material and the cell interior. The general configuration of this assembly is shown in Fig. 11. A photograph of this assembly is given as View B of Fig. 24 on p. 66.

FIG. 11. COVER AND INNER SEAL CONFIGURATION

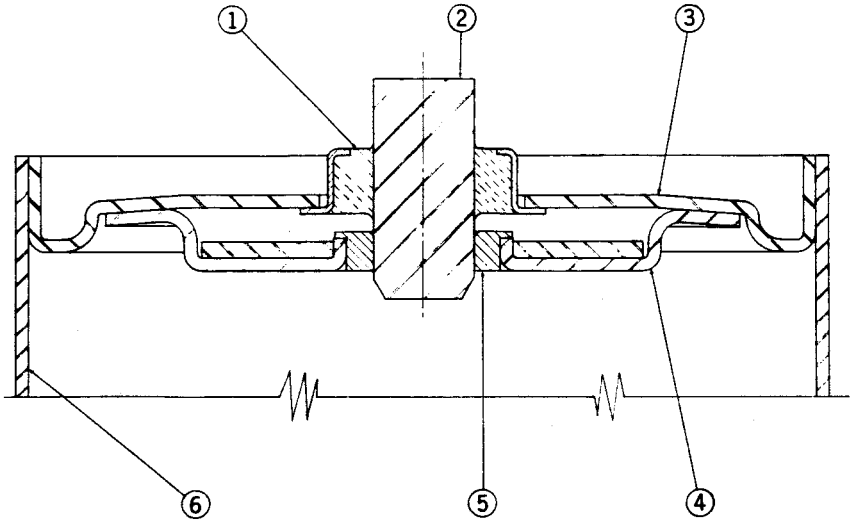

1. glass
2. positive post
3. cover
4. supporting diaphragm
5. nylon gasket
6. can wall

One problem which had to be resolved was the location of the weld joint between the supporting metal diaphragm and the underside of the cover. One alternative that was tried was bringing the perimeter of the diaphragm out into the area where the welding between the can edge and the cover was to be done. The seal would then be formed during the weld closure of the cell. Provided that the diaphragm could be held in proper position during closure, this method would offer the advantage of eliminating one step during cell assembly (the separate welding of the diaphram to the cover). It was found that the 3 components — cover, can, and supporting diaphram — could be satisfactorily heliarced together simultaneously. Fig. 12 is a photograph of a cross section of such a weld area, enlarged 10 times.

FIG. 12. CROSS SECTION OF EXPERIMENTAL INNER SEAL / CELL CLOSURE WELD (10 X)

One disadvantage of this method, however, is that the span of the diaphram between the weld and the nylon gasket is so great that the nylon gasket is not positioned as securely against the positive post as it should be for optimum seal. Also, the support offered by this assembly to the positive pin is minimal; it was felt from the beginning of the program that full advantage should be taken of the support that might be offered by the inner seal assembly. Furthermore, this weld requires considerably more heat than does the welding of the cover only to the can; there is therefore danger of doing damage either to the cell interior or to the glass seal.

These factors, plus the fact that our resistance welding was becoming more satisfactory later in the program, led us to design a diaphragm of smaller diameter, which was projection welded to the cover prior to cell assembly. The final diaphragm design, together with the design of the dies used in the fabrication of these diaphragms, are given as Figs. 13 and 14, which follow. The problems involved in developing this design were primarily welding problems, and were worked out hand-in-hand with the work done on the projection welding of the cover to the can; these problems are therefore discussed in the following section.

In the program proposal, the use of annular rings around the positive post in the glass area was discussed as a means of improving the physical support given to the post. It developed that these rings retain gas, which causes bubbling as the glass is fused into the seal area and results in defective seals. This feature was therefore dropped.

FIG. 13. INNER SEAL DIAPHRAGM

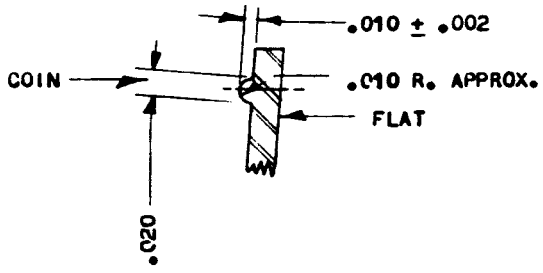

DETAIL "B"

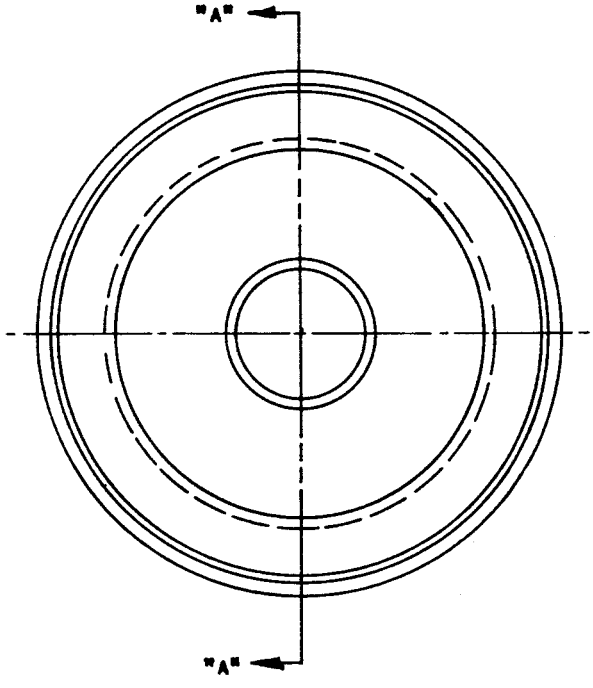

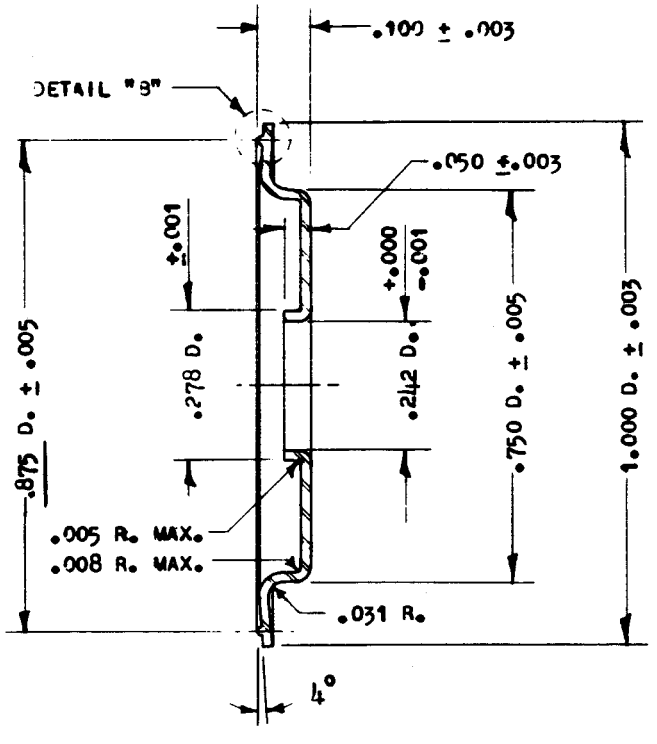

SECTION "A-A"

MATERIAL: ELECTRONIC "A" NICKEL. .018 TO .023 THICK.

NOTE: THE 1.000, .937, .750, .278 AND .242 DIAS. MUST BE CONCENTRIC WITHIN .005 T.I.R..

ISSUE	DATE	REVISION	TITLE	GOULD-NATIONAL BATTERIES, INC.
A	2-1-62	.875 D. WAS .937 D.	INNER DIAPHRAGM GLASS TO METAL SEAL - NASA	DR. EMB CH. DATE 4-3-61 PART NO.
			ORDER NO.	B/M NO.

DRAWING NO. MHA 101747

FIG. 14-A. DIES FOR INNER SEAL DIAPHRAGM

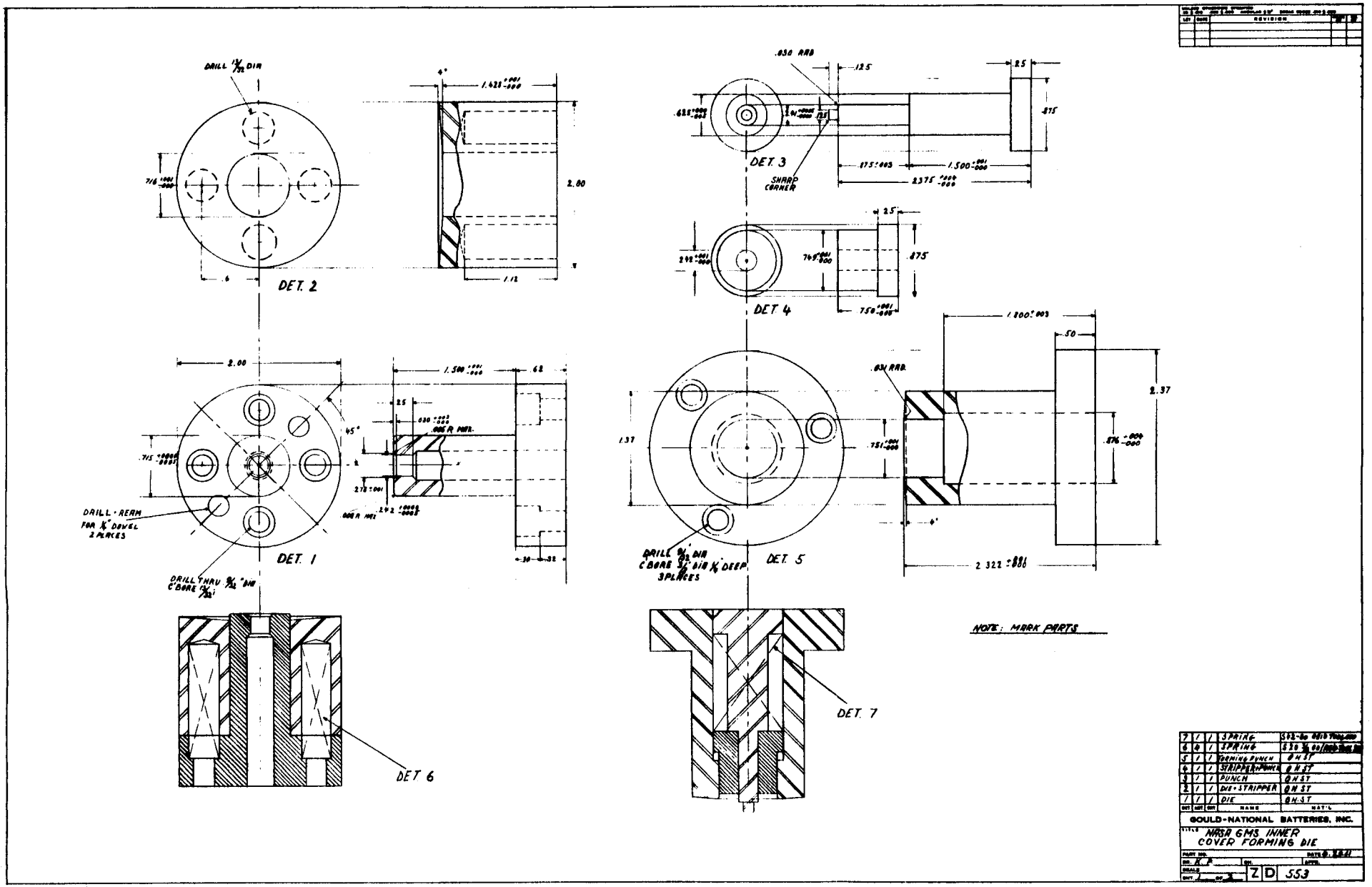

FIG. 14-B. DIES FOR INNER SEAL DIAPHRAGM (Cont.)

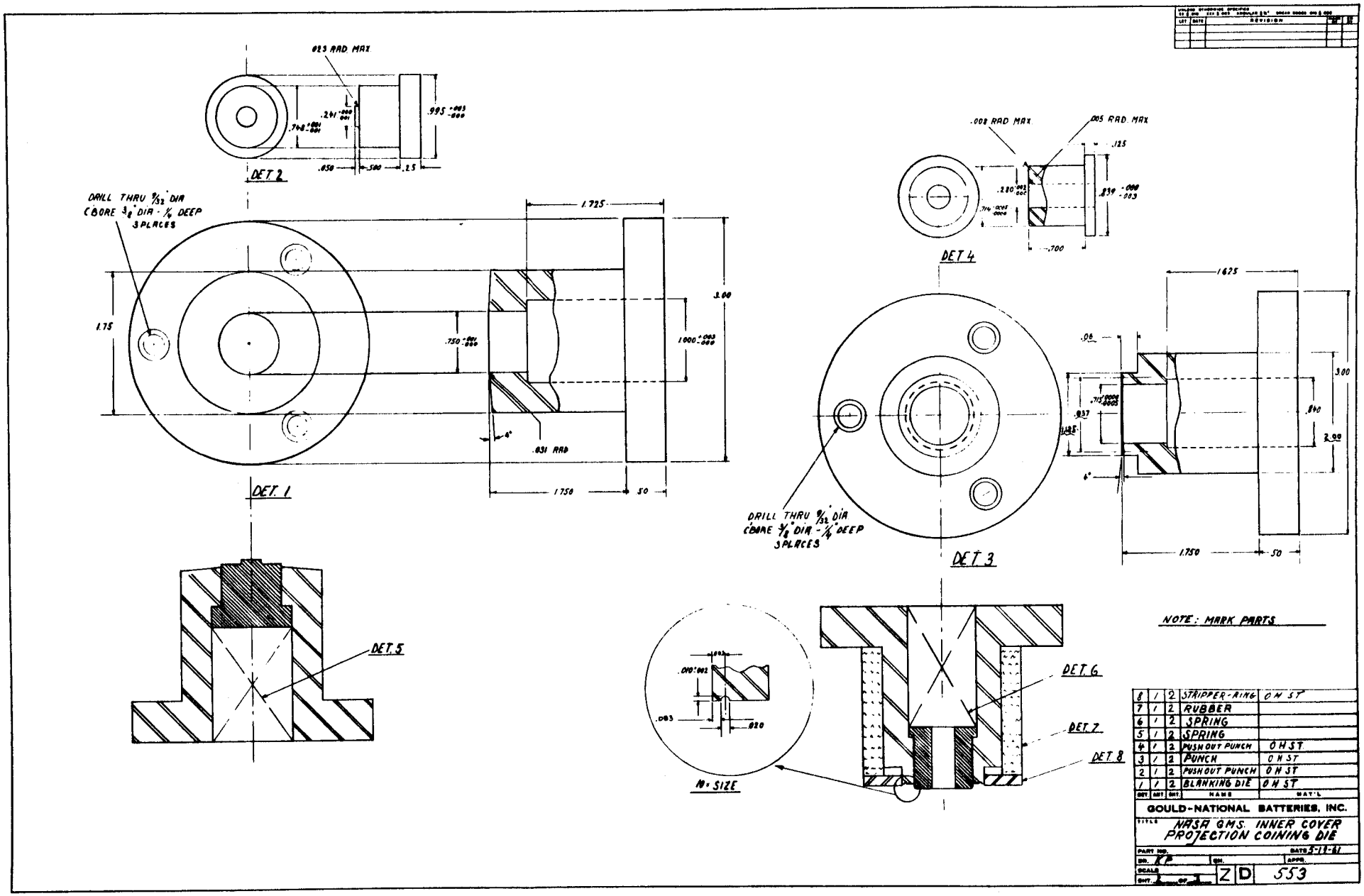

FIG. 14-C. DIES FOR INNER SEAL DIAPHRAGM (Cont.)

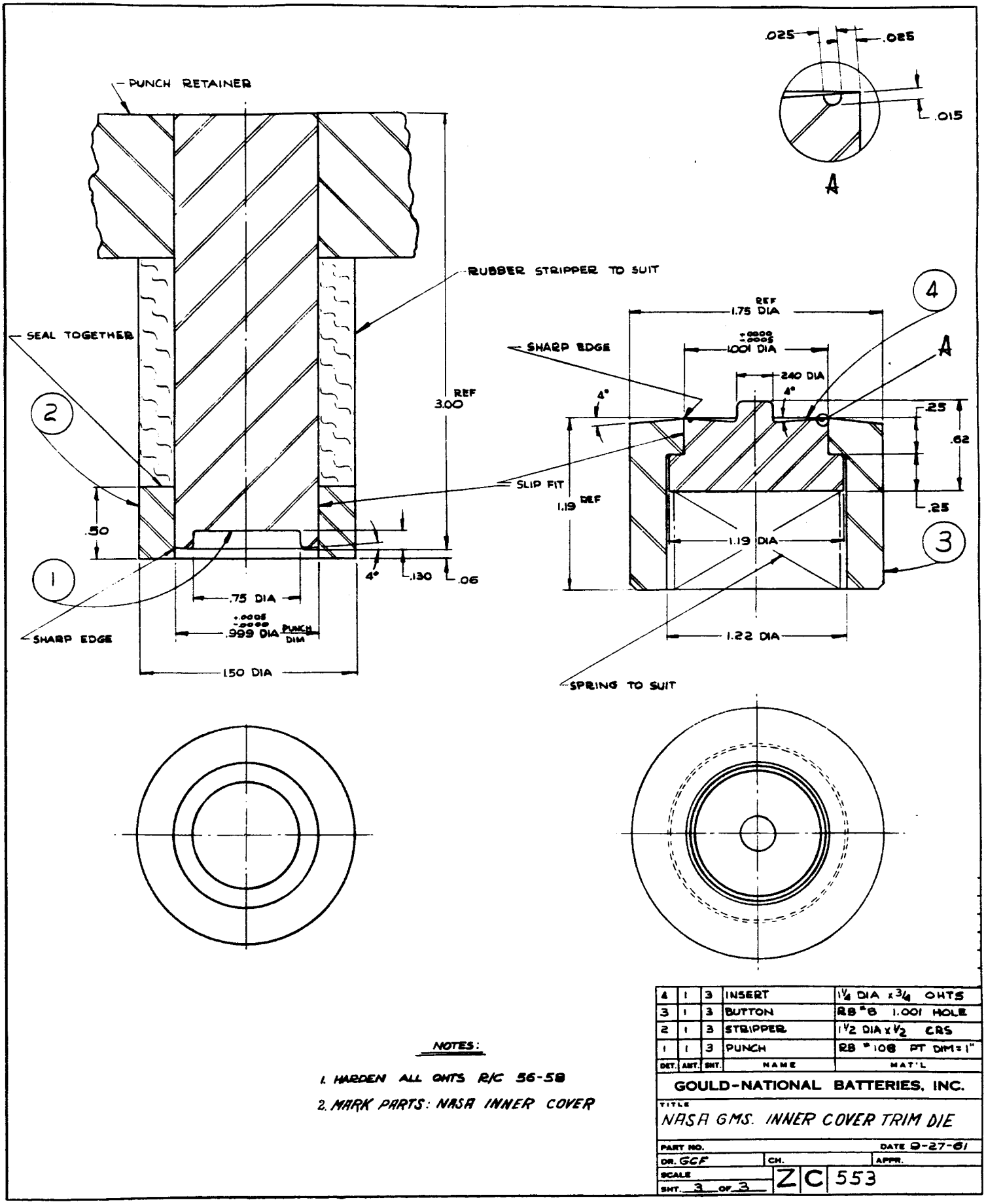

4	1	3	INSERT	1¼ DIA x ¾ OHTS
3	1	3	BUTTON	RB "B 1.001 HOLE
2	1	3	STRIPPER	1½ DIA x ½ CRS
1	1	3	PUNCH	RB "108 PT DIM = 1"
DET.	ASST.	SHT.	NAME	MAT'L

GOULD-NATIONAL BATTERIES, INC.

TITLE: NASA GMS. INNER COVER TRIM DIE

PART NO. | DATE 9-27-61

DR. GCF | CH. | APPR.

SCALE | SHT. 3 OF 3 | ZC 553

NOTES:

1. HARDEN ALL OHTS R/C 56-58
2. MARK PARTS: NASA INNER COVER

III. PROJECTION WELD

In our initial proposal to NASA, and in the plan for the program released April 12, 1961, we discussed the importance of improving the welding of the cell cover assembly to the can. It was pointed out that when this closure is done by heli-arc welding only, there are two grave problems, standing above and beyond the normal problems of selection of the proper metals to be welded, welding head configuration, welding speeds and currents, maintenance of proper inert environment around the weld area, and so on. These two problems are: (1) Our present cell design and seal test method involves conventional assembly, and filling of the cell with electrolyte prior to sealing. In previous investigation done before the beginning of this program, it seemed that it was not possible to complete the heli-arc welding of the cell quickly enough after filling with electrolyte to avoid having the electrolyte rise up the inner cell wall by capillary action, and evaporate during the welding, thus leaving pin holes in the weld. (2) There will inevitably be a certain amount of thermal expansion of the metal ahead of the welding head. The normal configuration of seal parts intended for heli-arc weld closure involves a small flange drawn vertically at the perimeter of the cover; the cover is fitted within the cell can, with this flange abutting the edge of the can. (This arrangement can be seen in Fig. 24. p. 66.) Therefore, as the metal expands ahead of the welding head, it will move in the only direction possible — the can rim will move outward and the flange of the cover will move inward so that it is impossible to maintain the close contact between these components that an optimum weld requires.

We therefore planned to develop a seal design in which the primary weld would be a resistance (projection) weld. This weld could be performed immediately after filling the cell with electrolyte, before the electrolyte had had a chance to climb the cell wall. A cross section of the cover and can configuration to be used can be seen in Fig. 20, p. 60 (see also Fig. 21); it was felt that performing a projection weld with components of any other than this horizontal configuration would be difficult, if not impossible. Following the projection weld, the intent was that the welded flange area would be drawn upright into the vertical position, resulting in the normal sealed cell configuration. Then, as the secondary weld, the rim of the cell would be heli-arced.

During the early weeks of the program, it became evident that it was not going to be easy to achieve a satisfactory projection weld. It was therefore decided that, simultaneous with the projection weld effort, work should be continued on cell closure by heli-arc welding only.

In the program proposal, it was said that we would investigate other alloys, Fernico in particular, as well as pure nickel, for both the projection and the heli-arc weld components. It was learned that although the characteristics of Fernico are matched well with the glass used in the seal, they are not matched with the brazing alloys used in the joining of the glass to the metal. This problem is not encountered when using pure nickel. Because of the difficulty there would be in finding an alloy that is properly balanced both with the glass and the brazing alloy, plus the fact that we were making significant progress with pure nickel, we looked no further into the use of other alloys.

A. DEVELOPMENTAL WORK

The design of the cover to be used for the projection weld technic has been perfected; such a cover for a cell with "D" diameter is shown in Fig. 21, p. 61. This design incorporates a flexible area between the weld area and the glass seal, which serves to evenly distribute the stresses caused by the welding, and prevent fracturing of the glass. Glass is fused between a positive pin and a ring insert, both of which are of Kovar; the insert is projection welded to this cover. The supporting diaphragm for the inner seal (cf. Fig. 13, p. 50) is easily fabricated from .020" sheet nickel, and is projection welded to the underside of the cover. The sealing element of this inner seal is 6/6 nylon, which is forced between the supporting diaphragm and the positive pin.

The principal problems in forming the projection weld were: (1) establishment of the proper geometry of the projection, (2) finding an easy, effective method of purging the weld area of contaminants and oxides, and keeping it clean until the weld is performed, and (3) establishment of proper welding values and cycle characteristics. These problem areas are discussed following.

(1) **Geometry of Projection.** Our first step in this area was fabrication of cover blanks with a typical projection as recommended in the industry. Dies were cut to give a projection generally semi-circular in cross section, with a base width between .025" and .030" and a height of .010". Covers were swedged with these dies in our laboratory at pressures of 18 tons. The attempts to weld these covers were totally unsatisfactory. Samples of the covers were then cross sectioned and examined on a shadowgraph at a moderate magnification. It was found that the top of the projection was not round, as was intended, but had been left flattened,

FIG. 15. DEVELOPMENTAL (ABOVE) AND FINAL (BELOW) COVER PROJECTIONS (20 X)

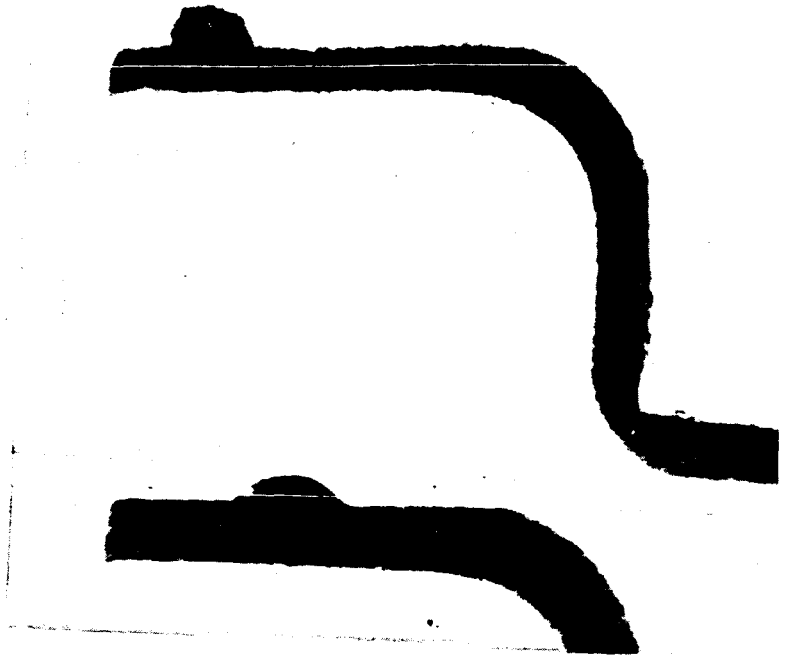

and the projection was not as high as was desired. It was assumed that this was due to inadequate swedging pressure.

As the next step, the dies were jobbed out to a commercial metalworking shop and covers were swedged at much higher pressures (roughly 150 to 175 tons). This produced a well-formed projection; a magnified photograph of the cross section of such a projection (enlarged 20 times) is given as the upper view of Fig. 15. However, the welds done with these covers were still totally unsatisfactory. This confirmed our suspicions that the projection geometry recommended for use with steel is not satisfactory for nickel.

The third step in this effort was to cut new dies, giving a projection with roughly the same base width, but with steeper slopes, thus appearing more triangular than hemispherical in cross-section, and having less mass. Again the swedging was done outside our laboratory, at pressures of 150 to 175 tons, resulting in the configuration shown in the lower view of Fig. 15. The diameter of this projection is 1.370". These covers, once the other welding parameters had been satisfactorily established, gave what appeared to be very satisfactory welds.

The supporting diaphragm of the inner seal, as was mentioned previously, is projection welded to the underside of the cover. In the first trial, the bead had been placed too close to the perimeter of the diaphgram, and it deformed prematurely, resulting in defective welds. This was a standard bead, with a base width of .024" and a height of .011". For the second trial, the bead was moved in to a distance of .030" from the rim of the diaphragm. This was still a standard bead, and did not produce a satisfactory weld. The projection used for the final trial was broader than standard (.030" by .006") and had a higher base-to-height ratio; the diameter of the bead is 895". This configuration (see Fig. 16) produced good welds.

FIG. 16. DEVELOPMENTAL (ABOVE) AND FINAL (BELOW) INNER DIAPHRAGM PROJECTIONS (20 X)

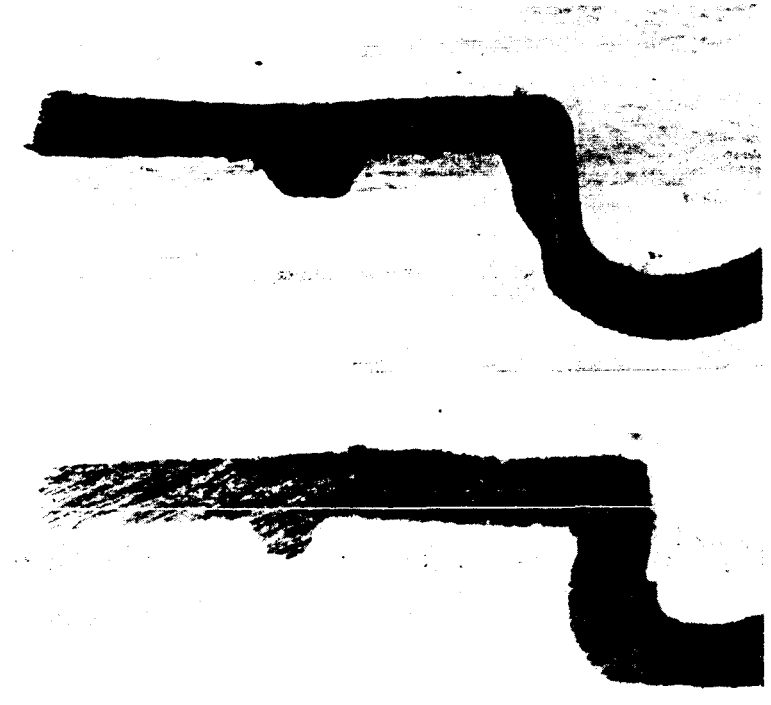

(2) **Decontamination of Weld Area.** In the earliest stages of the work, when attempting to establish causes for the difficulty in performing the projection weld, it was obvious that the presence of oxides and other contaminants on the surface of the weld components was one factor that had to be considered. Working with the weld components only, not with completed cells, various methods of rinsing and purging were tried. Components were immersed in various organic solvents, and maintained in an argon stream to keep them clean as they were transferred to the welder and the welds performed. We also dipped covers and

cans in nitric acid, followed by a rinse dip in alcohol; these components were then dried in a nitrogen stream, and maintained in the nitrogen until they were welded. This method produced very satisfactory welds in a few cases. However, the results did not seem to be completely reproducible; moreover, purging by immersion would not be possible during cell assembly. An attempt was made, using cans filled with elements, to perform this type of purge by swabbing the acid and the alcohol onto the weld surfaces. This did not produce satisfactory welds, perhaps partly because of impurities left on the surfaces by the swab. In view of the fact that this type of purging, even if it could be made effective and reproducible in the laboratory situation, would at best be cumbersome to incorporate into a production situation, this approach was abandoned.

As an alternative, plating of the covers and the cans with gold was tried. The technic used was electroless plating from potassium gold cyanide in a buffered tartaric acid solution*. The plating seemed to make it possible to reduce the welding current necessary to bring the weldment to a cherry-red heat; leak-free welds were not, however, obtained with these parts. Striking the parts with silver and with mercury was then tried, also with poor results. The silver striking was done with silver cyanide and potassium cyanide in an aqueous solution; the mercury was precipitated from a mercurous chloride solution. We suspected inadequacies in our plating technique, and approached a commercial plating establishment as our next step. Gold was acid-plated onto the covers, and these welded very well. As an additional experiment, we cyanide-plated several can rims with gold; this made no apparent difference in the welding.

(3) **Establishment of Operating Characteristics.** The multiple-impulse synchronous welding unit acquired under this program offers rather sophisticated control of welding cycle and pulse characteristics. We feel that with the flexibility thus afforded us by this unit, the investigation of projection welding done under this program was thorough and quite representative of the better state of welding art. Fig. 17 is a diagrammatic representation of the various welding operations that the unit will perform, as they might be arranged in a typical welding sequence; it also lists the parameters that can be varied for each operational component, and gives the terminology for these components that will be used throughout this report.

FIG. 17. WELDING OPERATIONS AND VARIABLES

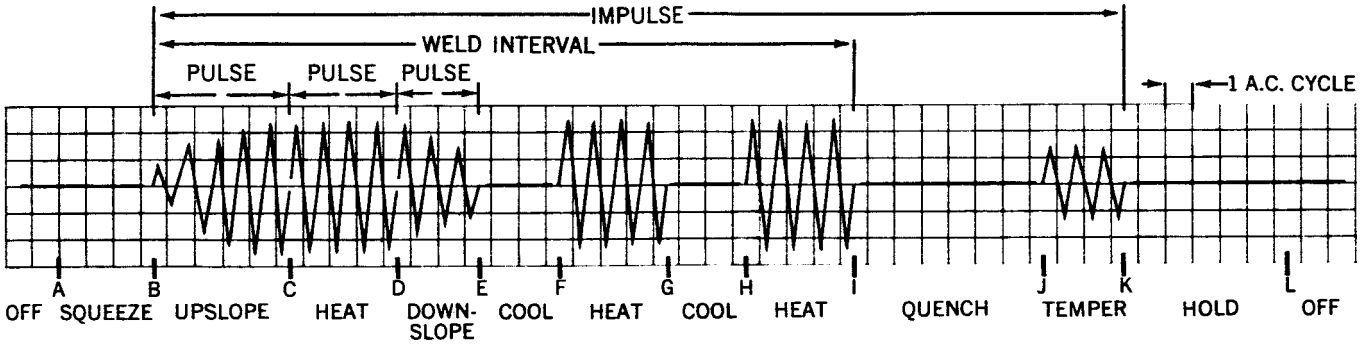

OPERATIONAL COMPONENT	VARIABLE PARAMETERS
Squeeze	Duration (no. of cycles); welding head pressure.
Upslope	Duration (no. of cycles); % of weld heat applied on initial cycle; repetition (can be used on first pulse only, or on all pulses).
Heat	Duration (no. of cycles); amount of current (% of welding transformer output) applied; repetition (no. of pulses applied per weld interval).
Downslope	Duration (no. of cycles); % of weld heat applied on final cycle; will be applied on any pulse having upslope, or can be omitted completely.
Cool	Duration (no. of cycles).
Quench	Duration (no. of cycles).
Temper	Duration (no. of cycles); amount of heat (% of weld heat) applied.
Total Impulse	Repetition (no. of impulses applied).
Hold	Duration (no. of cycles).

* "Electroless Deposition of Gold from Aqueous Solution on Base Metals of Nickel and Iron-Nickel-Cobalt Alloys," Robert F. Walton; Vol. 108, No. 8, Journal of the Electrochemical Society, p. 767.

In the program proposal, we discussed a controlled-delay device which was intended to hold the moving electrode in a fixed position for a few micro-seconds until optimum melt was reached, and then would release and allow the operating pressure to be applied to the work. Observation of prototype equipment incorporating this feature done early in the program indicated that it was not performing satisfactorily and, at least at the present stage of design of the equipment, is of limited value. This feature was therefore not acquired.

The parameters that were explored more thoroughly under this phase of work are:

— Electrode material and configuration
— Pressure: amount and timing
— Welding current and voltage
— Number and timing of cycles of welding current to be used per weld duration
— Duration of cool time to be used between weld pulses
— Upslope and downslope: duration, degree, and repetition

In the early stages the electrodes were fabricated from RWMA Group A, Class 2 copper. As the work progressed however, a change was made to an alloy of copper and tungsten (RWMA Group B, Class 11 & 12). Welding with these electrodes is a little trickier than with Group A copper, but they offer better high temperature characteristics. The configuration of the final electrodes used for the welding of the cover to the can and the supporting diaphragm to the cover is given in Fig. 23 on p. 63.

The first of the projection welds to be discussed will be that between the cover and the can, since (as would be expected, considering the diameter) it was the most difficult. Most of the welding currents used in this investigation were between 58,000 and 136,000 amps, with the final welds being done with 100,000 amps. (The transformer used throughout this work has an output of 13,650 amps per volt.)

The length of the squeeze time used, as might be anticipated with a weld of this type, turned out to be unimportant. In the experimental work, it was generally left at the maximum (360 cycles) as a safety factor — to give the operator time to check the alignment of the weldment, and hit the emergency stop if necessary.

We received recommendations from an outside authority that we first attempt the can/cover weld using approximately 12 cool cycles following each pulse of weld current; the number of weld cycles to be used per pulse would, of course, be empirically determined for each weldment. This proved unsatisfactory; the number of cool cycles was then increased from 12 to 25. This produced no better results, regardless of the number of weld cycles used per pulse, or the total number of pulses applied. In fact, working with 12 to 15 cool cycles and 6 to 10 weld cycles per pulse, the weldment remained so cool even when working at currents of 136,000 amps that the welding pressure had to be decreased to roughly 200 psi (1/2 of our usual working value) in order to increase resistance and bring the weldment heat up to a minimally acceptable level. The cool time was then decreased gradually to 2 to 3 cycles, with steady improvement in weld quality. With this short cool time, it was again possible to work with pressures of 400 to 450 psi. The length of weld time per pulse was varied between 2 and 25 cycles; using the short cool time, it proved best to keep the weld time low (2 to 6 cycles per pulse), and increase the number of pulses. Up to 25 pulses were used, each pulse consisting of 2-6 heat cycles followed by 2-3 cool cycles; at this high number of pulses, the weld components were impressed into the surface of the platen electrode, although interestingly they did not stick. With the optimum projection, plated with gold, the best welds were produced using roughly 12 pulses.

The effect of upslope and downslope was evaluated. It was our experience that a downslope of a few cycles is necessary when welding the Kovar seal insert to the cover, in order to temper the weld area. However, when welding the cover to the can, it seemed that less heat was developed in the weldment at a particular transformer setting when using upslope than when weld cycles alone were used. This effect is strong enough that, for example, the weld heat setting might be advanced to 80% and still produce inadequate heat, whereas with no slope but with all other factors equal, a setting of 50% would pit or splatter the electrode. This might be due to softening of the metal or actual formation of nuggets during the upslope portion of the impulse, with consequent shunting of the following weld currents.

Upslope time was varied from 2 to 25 cycles. Within this range, the upslope time : weldtime ratio was varied between 1:1 and 1:4. The same range and ratios were used for upslope together with downslope. In all, no slope settings were found which yielded consistently good welds, and the best of the final welds were done using no slope at all.

Multiple impulses were tried. We did not notice any advantage in repeating the above-described series of 12 pulses. Moreover, with the short cool times that were found to be best, the weldment is cooled very little — and the use of multiple impulses materially decreased the life of the electrodes.

Chilling and tempering appears thus far to have little effect on these welds. The chill time was generally left between 180 and 360 cycles, simply to give the weldment time to cool before it was removed from the welder. No temper was used for the final welds. Final judgment on the value of chill and temper should, however, be withheld pending the gathering of long term cell performance data. The hold time proved to

be unimportant and generally was left at the maximum setting (60 cycles) in the experimental work in order to hasten the dissipation of heat from the welded parts.

The welding characteristics finally determined to be optimum are given in the CONCLUSIONS Section, p. 70. Photographs of the welding equipment and welded components are given in Fig. 20, p. 60.

B. WELDING OF SUPPORTING DIAPHRAGM AND KOVAR SEAL INSERT

Once the diaphragms had been gold plated, welding of the supporting diaphragm of the inner seal to the cover proved to be much easier than the cover/can weld, and there was considerably more latitude in the operating characteristics than was possible with the cover weld. Here again the pressure used was 400 psi, with the squeeze time left at maximum. Current was 82,000 to 95,000 amps (more frequently the higher figure). The major difference from the cover welding was that the weldment was rotated 120° between each of 3 impulses. Each impulse consisted of pulses of 2 cycles of heat and 4 cool cycles, repeated 4 times. No upslope/downslope was used with these settings, although it did appear that upslope/downslope might have some value at certain other settings. As with the cover welding, chill and temper had no discernible effects; the chill time was generally left at 180 cycles or more.

The welding of the Kovar seal insert to the cover was generally similar to the supporting diaphragm weld, though with fewer impulses. Pressure was 400 psi, and current was 102,000 amps. With this weld, upslope/downslope proved to be necessary; this is not surprising, since it does involve welding 2 dissimilar materials, and therefore would be expected to benefit from the tempering effect. The impulses consisted of single pulses of 2 cycles of upslope, 4 of heat, and 2 of downslope; 3 of these impulses were applied, with the weldment turned 120° between each. This technic produced very satisfactory welds without requiring that the inserts be gold-plated prior to the weld. 600 of these inserts were welded into covers and were sent to a local organization for helium leak testing; 2 of the 600 were found to be leakers.

C. DRAWING OF WELDED FLANGE, SECONDARY HELI-ARC WELD

As was mentioned at the beginning of this section, we originally planned that after the cover had been projection welded to the can, the welded flange area would be drawn up from the horizontal into the vertical position, preparatory to the secondary heli-arc weld. This draw proved to be impossible. To begin with, in spite of extremely tight control exerted on the metal and the dies to prevent tearing the metal, countless microfractures were in most cases caused in the weld area. After considerable work on the drawing tools and technics, we were able to draw up the flange of a few cells so that the secondary heli-arc weld could be attempted. This welding was not successful. Stresses are of course set up in the flange area during the drawing process, directed as shown in Fig. 18. The heli-arcing apparently frees the resistance welds sufficiently so that these stresses cause the components to shift, thus destroying the continuity of the weld. This relieving of stress during the heli-arc weld is severe enough that simply keeping the flange aligned under the welding head is a serious problem. We have been unable to conceive a method of heat-treating the flange area that would not do damage to the cell.

FIG. 18. DIRECTION OF STRESSES IN DRAWN FLANGE AREA

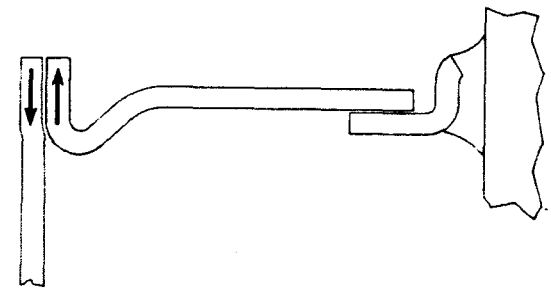

It must be mentioned that these problems were aggravated in that we were, during this phase of the program, working with hydro-formed cell cans, rather than drawn cans. The releasing of internal stress during a welding operation seems to be an inherent problem with hydro-formed cans; we have not been able to effect the same improvement in weld characteristics by annealing these cans prior to welding as can be done with drawn cans. A further problem is the porosity of the metal in hydro-formed cans, which will of course leave gas pockets in the weld area. Our suspicions having been aroused by the bubbling and blowing observed during the welding, we inspected several of the cans with dye-check, and found that the metal was so stretched and porous that the dye-check actually penetrated the can walls. On the basis of this experience we strongly recommended that, at least with the present state of the art, hydro-formed cans be avoided for space use.

Our next approach was to leave the resistance welded flange in the horizontal position and perform the heli-arc secondary weld without attempting to draw the flange up. This was only partially successful. There was to some extent the same positioning problem that had been experienced in trying to heli-arc cells with the flanges drawn upright. The relieving of stress during the weld made it difficult to precisely hold the components under the welding head; it should, however, be possible to resolve this. The welding setup

used in this work involved a lathe chuck holding the cell in a horizontal position with the flange under the welding head, and a variable speed drive on the chuck. The ground connection in this setup was probably insufficient. and the control of the speed and positioning was perhaps inadequate. This experimentation was done during the closing days of the program, and there was insufficient time to resolve these difficulties. Further experimentation would involve a fixture capable of more precise positioning and control of speed, use of a mercury ground, and water cooling applied to the fixture.

We do feel, though, that an alternate consideration would be to leave the flange in the horizontal position. We are quite sure that the projection welds now being made are very close to the level required for space use, without requiring that the secondary heli-arc weld be done in addition. Vacuum performance data on several cells which were closed with projection welds is given in the section on vacuum testing, on page 71, and it will be seen that they performed very well. Using cells with these horizontal flanges would probably waste no more volume in the assembly of a battery than do some present cell types that have been subjected to the helium leak test technics, and have the helium seal nipples projecting from the bottom. In fact, if the cells were arranged alternately as is shown in Fig. 19 (upper view) the lost volume would be cut to an absolute minimum. Wiring of the cells, as can be seen in this figure, would be very simple. In one application that has been brought to our attention by a representative of a firm actively engaged in space development work, the existence of this flange would be an actual advantage. This application requires that the cell be individually mounted on a plate, as is shown in Fig. 19 (lower view). This is for the purpose of heat dissipation. Provided that problems of unevenness in heating during welding could be overcome, cells for this application could be made with cover and flange of square rather than circular configuration, and secured directly to this plate at the corners of the flange.

FIG. 19. POSSIBLE BATTERY ARRANGEMENTS WITH FLANGE CELLS

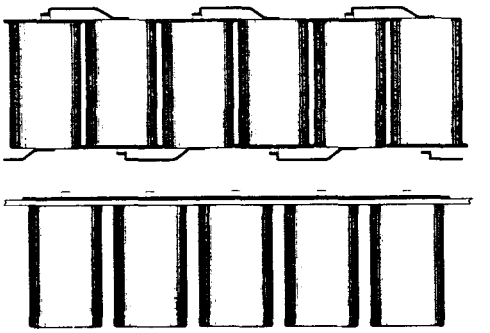

FIG. 20. PROJECTION WELD TECHNIC

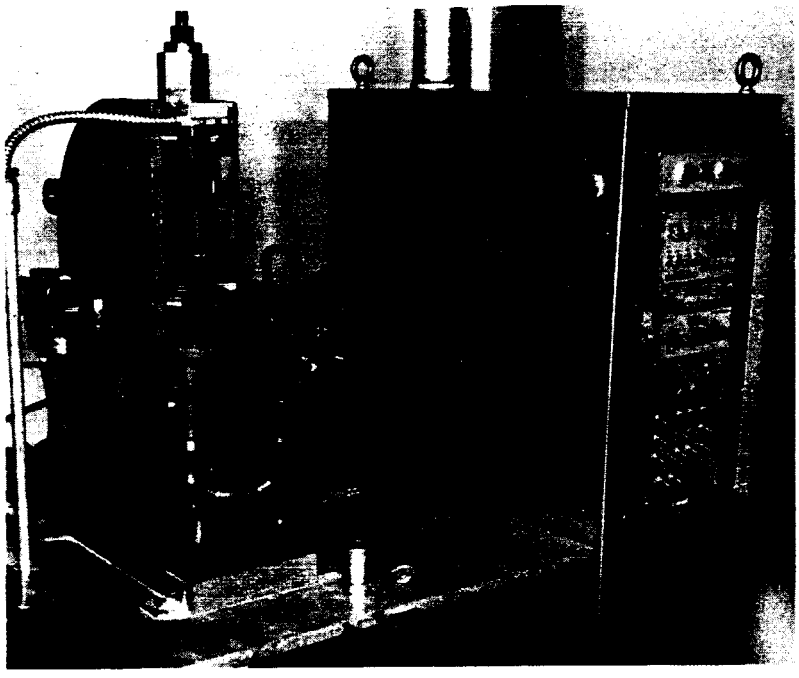

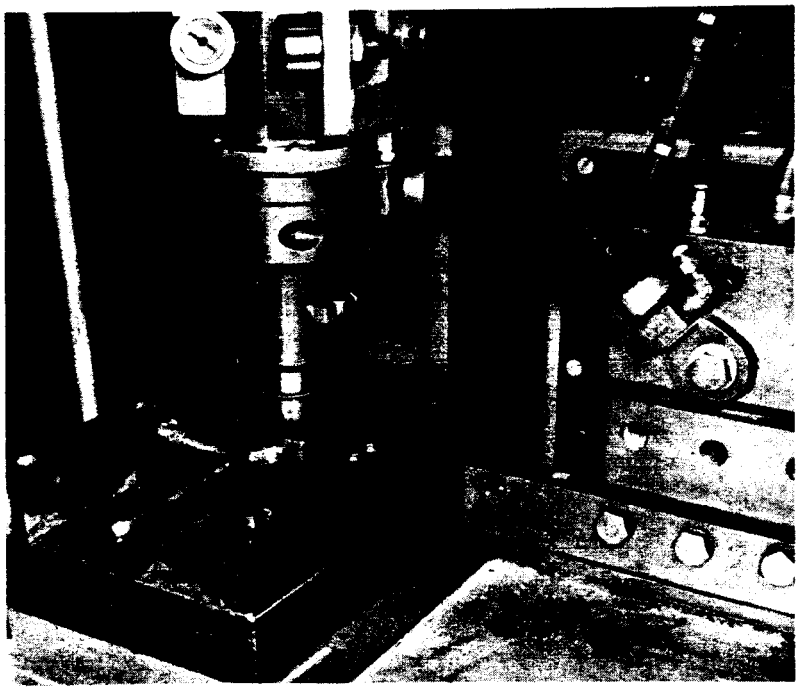

A. TWO VIEWS OF THE WELDING EQUIPMENT USED

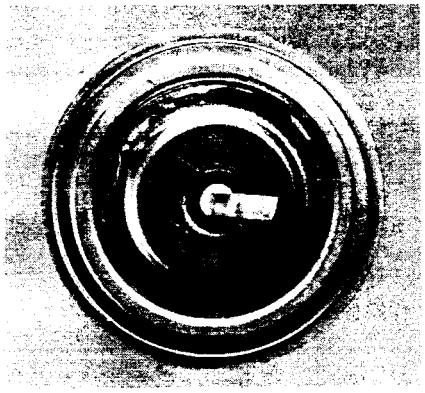

B. COMPLETED COVER ASSEMBLY, SHOWING INNER SEAL WELDED IN PLACE

C. COMPLETED CELL

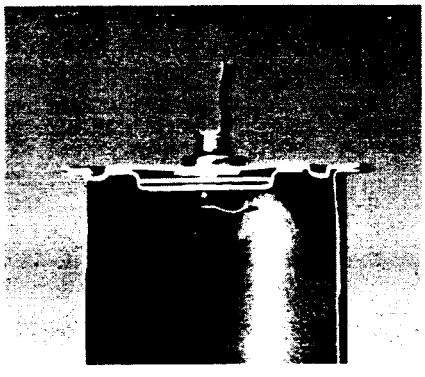

D. CROSS SECTION OF CLOSED CELL CONTAINER, THROUGH SEAL AREA

FIG. 21. COVER FOR PROJECTION WELD

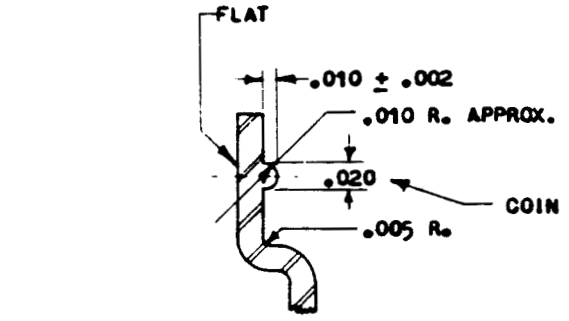

DETAIL "B"

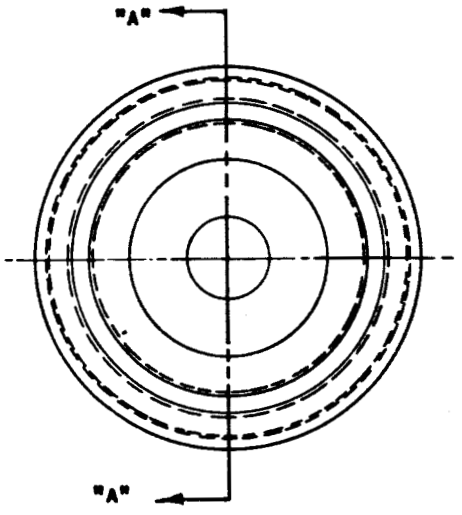

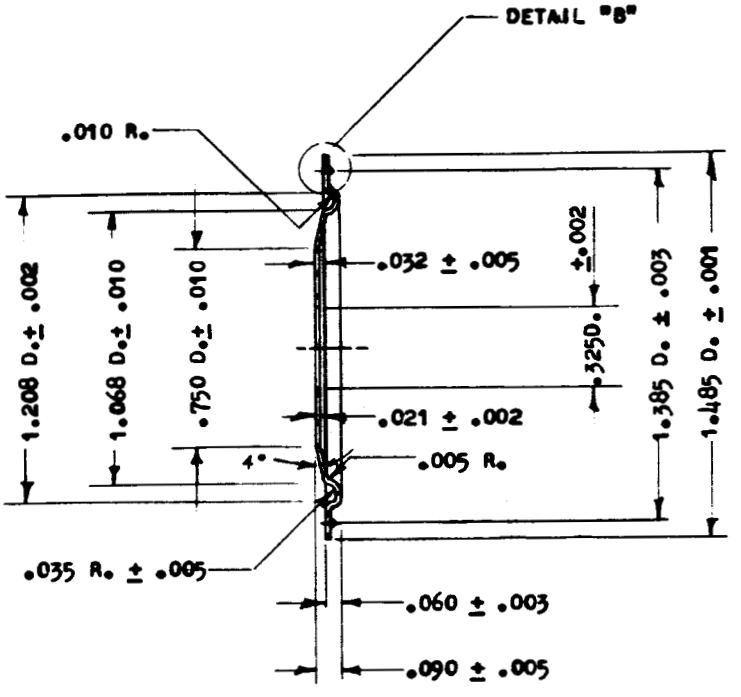

SECTION "A-A"

MATERIAL: ELECTRONIC "A" NICKEL
TO BE HYDROFORMED WITHOUT LUBRICANT.

NOTE: THE 1.485, 1.385, 1.208, 1.068, .750 & .325 DIAS. MUST BE CONCENTRIC WITHIN .005 T.I.R.

ISSUE	DATE	REVISION
A	10-16-61	ADDED 4°

TITLE: COVER
GLASS TO METAL SEAL

ORDER NO. | B/M NO.

GOULD-NATIONAL BATTERIES, INC.

DR. EMB CH.
DATE 3-24-61
PART NO.

DRAWING NO. MHA 101732

FIG. 22. FORMING AND COINING DIE FOR PROJECTION WELD COVER

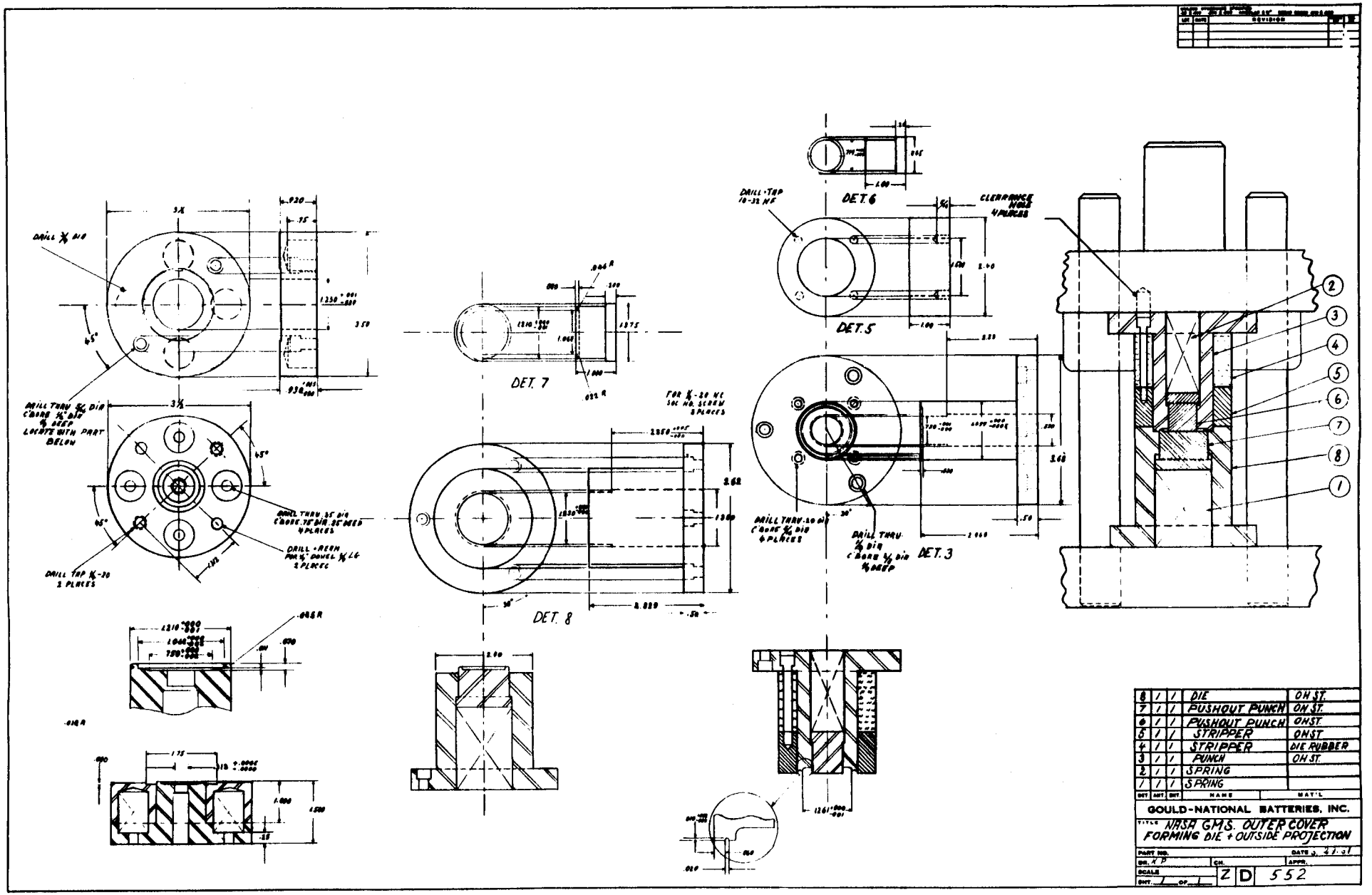

FIG. 23. PROJECTION WELDING ELECTRODES

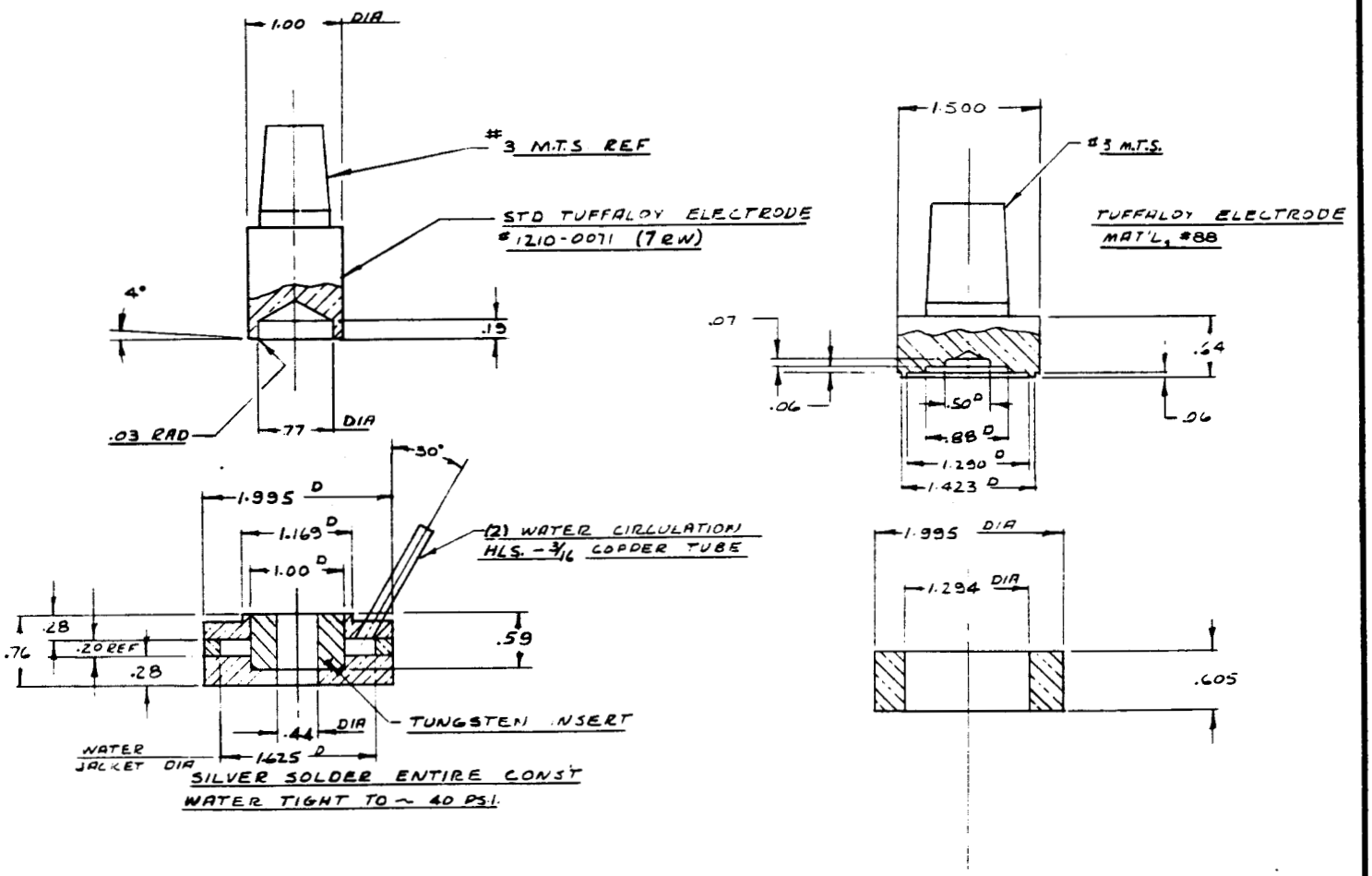

DET.	AMT.	SHT.	NAME	MAT'L
GOULD-NATIONAL BATTERIES, INC.				
TITLE: WELDING ELECTRODES, NASA "D"				
PART NO.				DATE
DR.		CH.		APPR.
SCALE			C	SK-9X
SHT. ____ OF ____				

IV. HELI-ARC WELD

As was mentioned previously, the problems experienced from the beginning of the program in performing the projection weld led us to think that it would be wise to continue the attempt to perform a satisfactory cell seal by heli-arc welding alone.

A. DEVELOPMENT OF TECHNIC

Our experience prior to the NASA program had been with cell cans and covers formed from .016" steel. It was with these components that we experienced the previously-mentioned difficulties of the electrolyte rising up the cell wall and vaporizing in the weld area, and the "breathing" of the metal ahead of the welding tip. Early in the program it was decided that .020" metal would be used for the cans and covers, which of course required greater welding heat. The "blowing" of the electrolyte proved surprisingly to be much less of a problem with these components than with the thinner ones. It may be that the necessary increase in welding heat was sufficient so that a considerable amount of the rising electrolyte was being vaporized off the can wall before reaching the weld area.

As our first attempt to develop a workable heli-arc technic, we attempted to form cans and covers of such dimensions that the cover would fit snugly within the rim of the can and thus would be held in position as the weld was being done. It proved impossible, however, to control these drawn components closely enough to reduce the average gap between cover and can much below .003" to .004". Such a gap is wide enough that it is difficult to adequately bridge it with the melt. Furthermore, as the weld was begun, it frequently happened that the free side of the cover would rise out of position.

As the next approach, we attempted to place the cover in position and then size the rim of the can sufficiently so that it would grip the edge of the cover. It was hoped that this would provide secure positioning during the weld. This sizing, however, is very difficult. For one thing, since the diameter of the drawn cans cannot be controlled as closely as one might wish, it was difficult to provide adequate bearing surface for the sizing post; as the post began to force the cell through the sizing die, it would frequently slip off the edge of the can rim, forcing the cover down into the cell.

An attempt was then made to apply enough force against the can rim with the welding blocks themselves to force the rim inward against the cover edge and thus secure the cover. This also was difficult to achieve. The blocks must be raised almost flush with the can rim in order to provide this kind of support; at this height there is of course the danger of welding the parts to the blocks or of contaminating the weld whenever there is a slight dip in the height of the can rim. Furthermore, with the blocks in this position, the loss of heat was too severe for good welding. This approach was therefore abandoned.

It became apparent that some sort of welding of the cover to the can would be necessary prior to the heli-arc weld. Our problems with the projection welding had not lessened at this point in the program; we therefore turned to spot welding. Initially, the cover was tacked in place with several small spots running around the perimeter of the can. This, however, disturbed the subsequent heli-arcing; the quality of the bead dropped noticeably at each point where a spot weld had been done, even though the spots had been placed somewhat below the edge of the can rim.

The final stage of the work involved developing semi-cylindrical electrodes which produce a spot weld covering about 1/5 or 1/6 of the circumference of the can. The design of these electrodes is given in Fig. 26 on p. 68. Eight or ten over-lapping spot welds are done so that the cover is completely secured to the can in one continuous weld joint. The weld conditions are: 40 lbs. pressure; 14,800 amps; single weld impulses consisting only of 2 cycles of heat. This is doubtlessly not a perfect seal, but it is complete enough that the amount of electrolyte entering the weld area during the subsequent heli-arc weld is very minimal. It solves the problem of holding the cover perfectly in position as the heli-arc weld is done; moreover, the breathing of the weld components due to thermal expansion ahead of the welding head seems no longer to be a problem. This technic has been used on 500 or more cells which have been fabricated during the last several months, some of which have been supplied to NASA and to other establishments engaged in space activities. The technic produces a uniform, high-quality bead — the scrap rate has been reduced far below that experienced with other technics (it has with occasional lots been as low as 8%) — and the welds, some of which have been observed for several months now, seem to leak only in a small minority of cases.

B. INVESTIGATION OF EQUIPMENT

Experimentation was done with the composition, diameter, and positioning of the tungsten welding tip. Rods of pure tungsten, and of 1% thoriated and 2% thoriated tungsten, were tried. The thoriated tips provided a more stable arc — they gave a more even, uninterrupted melt. The 2% thoriated tips would provide longer life, although 1% tips were used through most of this experimentation, since production volume was not

a factor. The diameters used were .020", .040", and .062". We received recommendations that we start with the .040" tips, since this is the combined thickness of the weldment (both can and cover being of .020" nickel). It turned out that the .020" tips performed better, however. They provided a more stable, even melt than the .040" tips; furthermore, the .040" tips, which generate more heat, gave some evidence of dangerously overheating the cells. The heating is now well enough controlled that no discernible damage is done to a nylon insulating disc which lies within the cell immediately under the cover, and extends to the walls of the can, directly under the weld area. It was found that the best distance between tip and work is 1/32", perhaps up to 3/64". The tip projects 1/2" from the torch.

The original torch used was air-cooled, with the power cable extending from its side. It was found that this torch was not being sufficiently cooled; furthermore, the drag of the power cable was enough to pull the torch out of alignment and disturb the weld. The final design is a water-cooled torch (fed with 50° to 60° F. water), and has the cable projecting from the top so as to minimize drag.

A ceramic gas feed cup of superior design was acquired. The upper portion of this cup is a chamber of considerably larger diameter than the lower portion surrounding the tip. As the gas enters the cup, it eddies in this chamber and is heated. The resulting expansion of the gas makes it possible to cut the rate of gas feed virtually in half, with no apparent loss in shielding effectiveness.

It should be mentioned that the use of hydro-formed cans was seriously investigated for heli-arc welding as well as for resistance welding. Roughly 150 welds were attempted, many of which were on empty cans. It was occasionally possible to get a good weld on a hydro-formed can, but the results were very inconsistent. It might happen that one or two welds would be satisfactory and the four or five immediately following would be defective, with no discernible change in any of the welding parameters. A wide range of adjustments of welding current, speed, and flow of inert gas were tried, to no avail. This reinforces the recommendation, made earlier, that hydro-formed cans be avoided for space use.

The welding set-up used and examples of welding components are shown in Fig. 24 on the following page. The characteristics of the optimum welding technic are summarized in the CONCLUSIONS section, on p. 70.

FIG. 24. HELI-ARC WELD TECHNIC

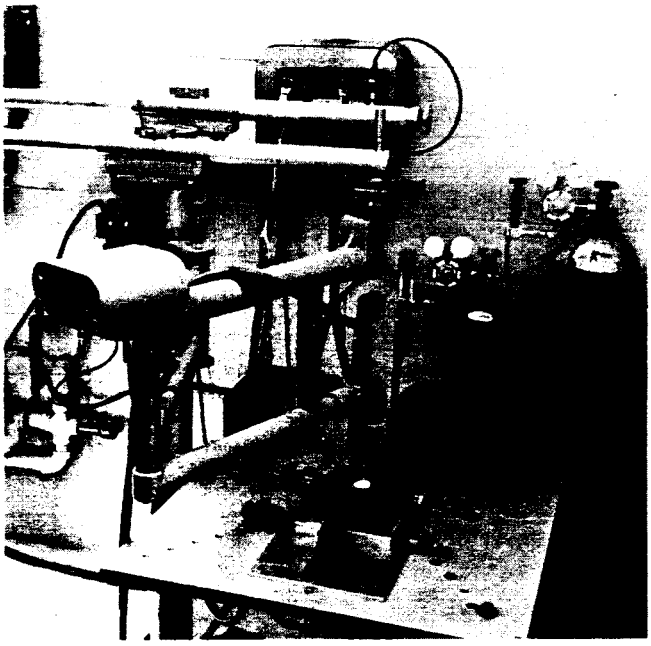

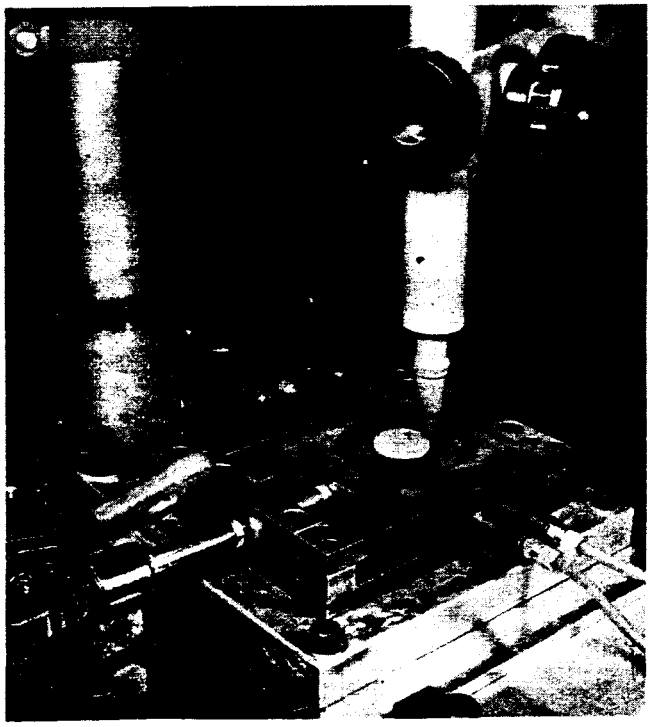

A. TWO VIEWS OF THE WELDING EQUIPMENT USED (CELL COVER HAS BEEN DYED FOR BETTER REPRODUCTION)

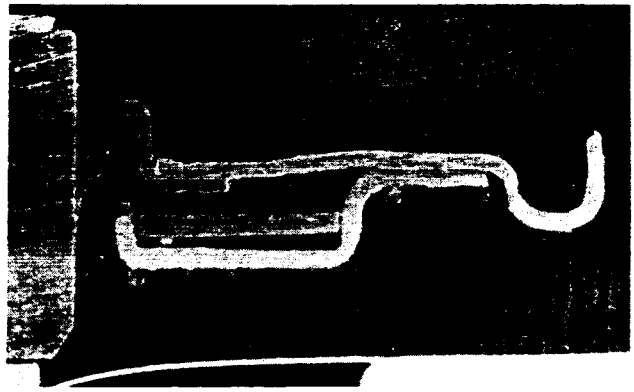

B. COMPLETED COVER ASSEMBLY SHOWING INNER SEAL WELDED IN PLACE

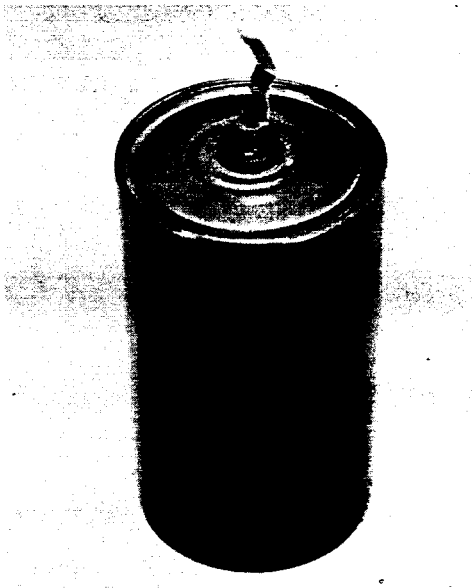

C. COMPLETED CELL

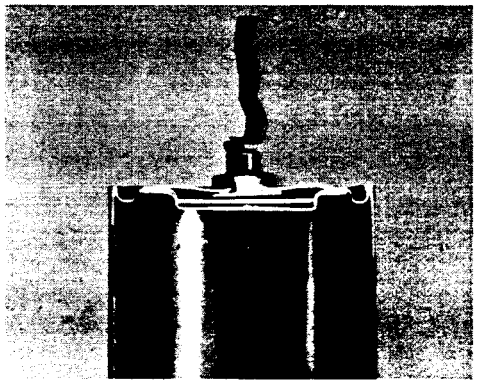

D. CROSS SECTION OF CLOSED CELL CONTAINER, THROUGH SEAL AREA

FIG. 25. COVER FOR HELI-ARC WELD

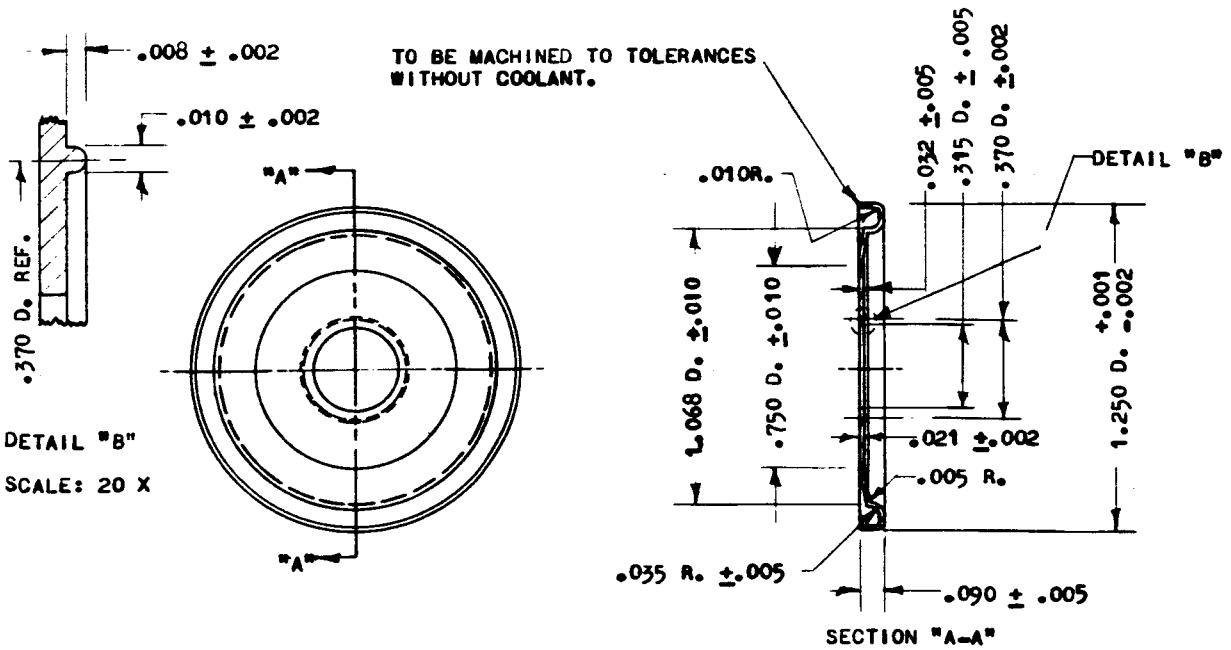

MATERIAL:
NICKEL 233, DEEP DRAWING TEMPER (ROCKWELL 64B MAX.)

NOTE:
THE 1.250, 1.068, .750 & .315 DIAS. MUST BE CONCENTRIC WITHIN .005 T.I.R.

ISSUE	DATE	REVISION
A	4-16-52	MAT'L. CHANGE.

TITLE: COVER GLASS TO METAL SEAL

ORDER NO. | B/M NO.

GOULD-NATIONAL BATTERIES, INC.

DR EMB CH.
DATE 12-7-60
PART NO

DRAWING NO. M H 101435

FIG. 26. ELECTRODES FOR OVERLAPPING SPOT WELD

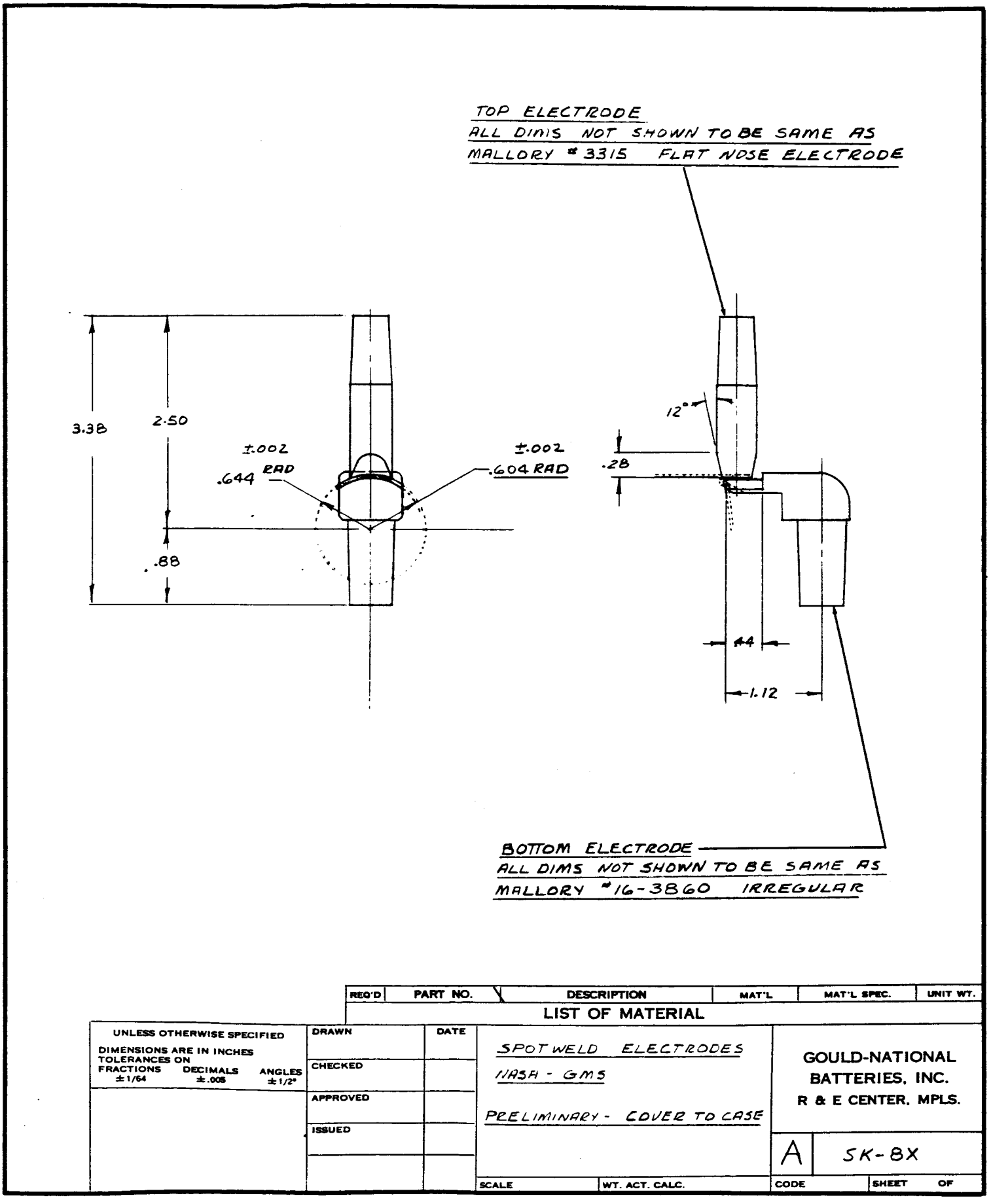

REQ'D	PART NO.	DESCRIPTION	MAT'L	MAT'L SPEC.	UNIT WT.

LIST OF MATERIAL

UNLESS OTHERWISE SPECIFIED DIMENSIONS ARE IN INCHES TOLERANCES ON FRACTIONS ±1/64 DECIMALS ±.005 ANGLES ±1/2°	DRAWN	DATE	SPOT WELD ELECTRODES NASA - GMS PRELIMINARY - COVER TO CASE	GOULD-NATIONAL BATTERIES, INC. R & E CENTER, MPLS.
	CHECKED			
	APPROVED			A SK-8X
	ISSUED			
			SCALE / WT. ACT. CALC.	CODE / SHEET OF

FIG. 27. HELI-ARC WELDING BLOCKS

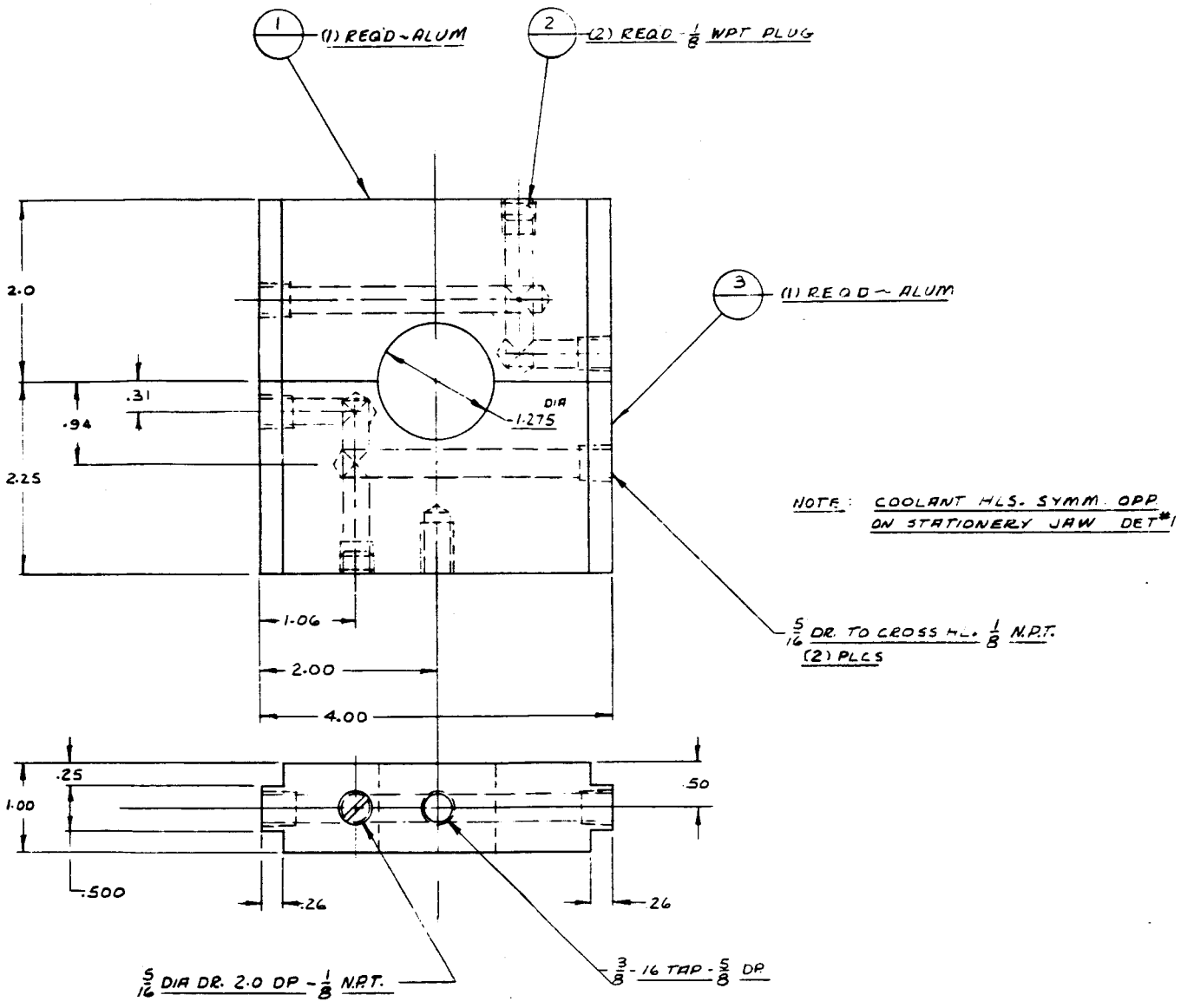

REQ'D	PART NO.	DESCRIPTION	MAT'L	MAT'L SPEC.	UNIT WT.

LIST OF MATERIAL

UNLESS OTHERWISE SPECIFIED	DRAWN	DATE	HEAT DISSIPATING & HOLDING BLOCKS	GOULD-NATIONAL BATTERIES, INC. R & E CENTER, MPLS.
DIMENSIONS ARE IN INCHES TOLERANCES ON FRACTIONS ±1/64 DECIMALS ±.005 ANGLES ±1/2°	KELLY	10-30-72		
	CHECKED			
	APPROVED			C SK - 12X
	ISSUED		SCALE / WT. ACT. CALC.	CODE / SHEET / OF /

V. CONCLUSIONS

Among the conclusions emerging from this phase of the program are the following:

The application of an epoxy coating to the underside of the cover assembly, as an attempt to isolate the glass from the KOH, is wholly unsatisfactory — even when using those epoxies now available on the market which are thought to have the highest resistance to KOH. A cover design has been developed which, it is believed, will provide a more satisfactory barrier between the seal and the KOH. This design involves a nylon seal between the lower portion of the positive post and a supporting diaphragm, which in turn is projection welded to the underside of the cover. Assessment of the actual effectivness of this design awaits the gathering of long-term cell performance data.

The walls of hydro-formed cell cans appear so porous that the use of these cans should be avoided for space use regardless of the method of cell closure.

A projection welding method of cell closure has been developed which is thought to be very close to the level required for space use. It was found that optimum bead configuration differs somewhat from that used for steels — the inclination of the bead walls should be somewhat greater than is commonly used, giving the bead a more triangular cross-sectional shape, with smaller mass. The surfaces of the weld components must be perfectly free from oxides and other contaminants; if a satisfactory method of purging and maintaining the components in an inert atmosphere prior to welding cannot easily be used, the components should be plated with an inert metal. It was also found that projection welding of nickel requires pulse characteristics that are quite different from those used on steels — both the weld time and the cool time should be kept very short, and a fairly high number of pulses should be used. In summary, the following characteristics, when applied on plated "D" covers with optimum projection design as described in Section III, produced strong and leak-free welds:

— Pressure: 400-450 psi. Squeeze time: unimportant
— Current: transformer secondary output of 100,000 amps
— Slope: none
— Weld time: 3-6 cycles
— Cool time: 2-3 cycles
— Total welding pulses: 8-12
— Chilling and tempering: not fully evaluated; 180 cycles chill generally used
— Hold time: 60 cycles

The heli-arc method described is a very workable technic, and consistently produces good welds with a very low incidence of leaks. The method involves securing the cell cover to the can with a seam of overlapping spot welds prior to the heli-arc weld. Weld characteristics have been established which make it possible to form an optimum bead with a single pass of the electrode. The reliability of the technic has been proven through the welding of 500 or more cells, some of which have been observed for several months. Until the reliability of the projection weld described previously has been established through the welding and testing of a larger number of cells than has been possible thus far, the heli-arc method is to be given preference over the projection weld.

The weld is performed as follows: the temperature of the blocks (shown in Fig. 27) is held between 50° and 60° F. The welding head is a .020" 1% thoriated tungsten rod, riding roughly 1/32" above the work. A small heat sink, a cylindrical piece containing roughly 21 g. of copper, is used on the cell cover. The cell can and cover are of .020" nickel. The welder drive is set so that the welding head makes one complete revolution around the perimeter of a "D" cell in roughly 20 seconds; this is roughly $11^{3}/_{4}$" per minute. The current used at this speed is 22 amps; this is straight polarity DC (torch negative). High frequency (2230 KC) is used only to strike the arc. It was found that it is necessary to use pure argon when beginning the weld. A second or two after the arc is struck, helium is mixed in, so as to make it easier to maintain optimum heat; the flow rates of the mixture are 18 ft.^{3}/hr. of helium with 3 ft.^{3}/hr. of argon. A single pass is made around the circumference of the cell, with a slight overlap to cover that portion of the bead which was done before the helium was switched in; the current is gradually tapered off through this overlap.

SEAL TESTING

I. INTRODUCTION

Considerable attention was given in this research program to the problem of developing a more satisfactory seal test method. An attempt was made to develop a method that would be relatively rapid, reliable, and would overcome the disadvantages of the other commonly-encountered leak detection methods.

In planning the program, a careful survey was made of the various possible methods of detecting leaks. The use of radioisotopes is the first of the three methods of leak detection that merit consideration for nickel-cadmium space cells. The tracer element can be sealed within the cell during assembly, although this method is generally avoided since it involves a safety hazard in production areas. More commonly, the completed units are soaked at pressures of several atmospheres in a gas which bears the radioisotopes. The gas will diffuse into the unit through any leaks, the amount diffusing in being proportional to the total leak area. The pressurized medium is then removed, and the amount of detected radioactive material diffusing from the cell is converted to the leak rate. This method is quite sensitive (it can detect leaks down to 10^{-12} atm. cc/sec.), but it does have grave disadvantages. The soak time required to attain a sensitivity satisfactory for space work can extend into several hundred hours. Furthermore, it is quite expensive, and the safety hazard is always present. Isotope-bearing substances may occlude on the surface of the containers; emission from these occlusions would give an erroneously high leak reading. The cardinal disadvantage that led us to eliminate the radioisotope method, however, is the possibility of the radioactive degradation of resins used in the fabrication of the cell.

The second commonly encountered method of seal testing is helium leak detection. This is sometimes done with the same technic that was described for the radioisotope method above: the completed unit is subjected to helium under pressure and the helium diffuses in through the leaks — then the helium environment is removed and the amount of helium emitted from the unit is read and converted to leak rate. However, this technic has the same drawbacks in the case of helium detection that it does with the radioisotope method: The amount of helium placed in the cell is so small and so irregular that both the sensitivity and the reproducibility of the method suffer; because of the small volumes of gas admitted to the cell which are available for testing, the method is inordinately sensitive to the presence of small quantities of the tracer gas in the working atmosphere; and, further, the soak times required are frequently too long to be practicable.

As a result, helium leak detection is usually done by incorporating a larger quantity of helium in the cell before it is completely closed. This can be done either by performing the final cell closure in a helium atmopshere (under pressure or at 1 atmosphere), or it can be done by incorporating an open tube into the cell can, and admitting the helium through this tube after cell closure. One technic used for the latter method involves assembling and sealing the cell in the conventional manner, after which helium is injected into the cell through the open tube and the seal is checked; then the tube is pinched off and the pinch is checked by the method of differences.

With both of these methods — helium atmosphere closure or open tube — it has proven very difficult to develop a practical, reliable, test technic. Performing the complete cell closure operation in a helium atmosphere, especially when done under pressure, is cumbersome and expensive at best. It seems to have been the experience of the industry that the desired sensitivity levels (10^{-9} atm. cc/sec. or better) cannot workably be attained with this method. And a cardinal disadvantage is that, since the amount of helium placed within the cell is finite, it will, if the leaks are serious, be essentially exhausted within a certain time, and this method therefore cannot be used to study cell leak rates over prolonged operational periods (particularly in applications involving overcharge in which the increased internal pressure would drive out the helium at an accelerated rate), or after long periods of storage or inactivity. The testing must be done within a relatively short period of time after closure.

Due to the shortcomings of the helium closure method, much attention has been directed to the open tube method. According to the information available to us, it has proved impossible to bring the method to the levels of reliability and reproducibility required for space work. The joining of the tube to the can has proven to be a serious problem; the initial joint is not an easy one to make, plus the fact that it is difficult to adequately anneal the joint so that it does not develop micro-fractures as the tube is crimped shut and the cell is subsequently cycled and shocked. Secondly, with a test unit that offers the desired test productivity (5 to 10 minutes per test, for example) it has proven difficult to hold sensitivity in the 10^{-9} to 10^{-10} atm, cc/sec. range with good reproducibility. Furthermore, the method is essentially the same as the helium closure method in the sense that it will not, in the case of serious leaks, provide leak information beyond a certain limited time following cell closure, since the amount of helium placed in the cell is limited.

Even should these problems be resolved, there still remains the chronic problem common to all helium leak detection methods — the susceptibility of high-sensitivity units to the traces of helium that will build up in any area where helium testing is being done. Stringent and, in many cases, expensive measures must be taken to minimize the build-up of helium in the environment, particularly when large volumes of testing are involved. The only alternative is to abandon the attempt to read absolute values, and read rates of change instead.

Some investigators have turned from helium to argon in an attempt to resolve some of these problems. Argon offers the advantage, in test systems using glass components, of not diffusing through the glass as helium does; some authorities report a consequent increase in system sensitivity and reliability. It would be expected, though, that when working with seal components in which the typical leak is a large number of microscopic fractures (as seems to be the case with glass-to-metal and ceramic-to-metal seals), the use of argon would be attended with serious disadvantages. For one, argon is a molecule half again as large as helium, and has only $^1/_3$ the average molecular velocity that helium does. As a tracer element, it would not therefore be expected to diffuse as readily through microscopic fractures, and would not provide the ulitmate sensitivity that helium would.

With these thoughts in mind, our decision in planning this program was to work toward a high-vacuum method of cell seal. It was expected that high-vacuum testing would have the following advantages (not necessarily listed in order of their importance):

(1) With the high-vacuum method, testing can be done any time during or following the cell's operational life. There is no finite time, beyond which a tracer element will be lost and testing will be impossible.

(2) The high-vacuum method does not require any changes in cell design or in the production of the cells. Testing can be done on cells of a design which has been optimized for the important performance parameters, without requiring special consideration of the test requirements in the formation of this design, or in the formation of the production technics. The overall reliability of the cells should therefore be improved.

(3) This method is not subject to errors in the incorporation of tracer elements in the cells, or in the cleansing of tracer materials from the cell exterior prior to testing. This should ultimately yield a more reliable test method.

(4) By avoiding the use of tracer elements, this method also circumvents another source of test error: This is the presence of these tracer elements in the test environment at large, the detection of which places a ceiling on the sensitivity and the reliability that can be obtained from such a method.

(5) This method avoids the introduction of materials into the cell which might degrade cell components.

(6) The method involves no safety hazards for production or test personnel.

(7) Few expensive materials are consumed — the material cost for this method is quite low.

The design problems that we anticipated in the development of this method, and the disadvantages of the method, are as follows:

(1) The time involved per test had to be reduced far below that presently required for most high-vacuum testing, which generally involves sealing the component in an evacuated chamber, and observing pressure rise over a prolonged period of time.

(2) With high-vacuum methods involving shorter time intervals, it has not been easy to attain leak rate sensitivities in the order of 10^{-8} to 10^{-10} atm. cc/sec., which we judged to be the level required for space work.

(3) The reproducibility of the results had to be high.

II. DEVELOPMENT OF TEST APPARATUS

Since one of the major aims in the development of this test method was the reduction of time necessary for the performance of each test, the system was fabricated entirely of metal components, which are easily

coupled together. Most of the components are of stainless steel No. 304, a metal which has very low outgassing, and is easily welded and machined. The ultra-high vacuum seals are of the crushed copper type, with a minimum of copper exposed to the system interior. The sealing face of the bellows-type high vacuum valve is a Viton "A" gasket.

Three chambers of increasing size were acquired for use with this system. The smallest of these is a 5" cross, the arms of which have an ID of 1 1/2" (1/4" larger than the diameter of the "D" cell configuration). The test cell is placed directly into one of the arms of the cross. To the ends of the four arms are attached (1) a high-vacuum valve with a roughing pump beyond, (2) a high-vacuum pump, (3) a high-vacuum gauge or electrical inputs feeding to the cell, and (4) a cover plate — this latter arm serves as the entrance port. The medium sized chamber (1 7/8" ID x 5 1/4"), can be mounted on this 5" cross in place of the high vacuum gauge. This is a cylindrical chamber, with electrical inputs borne by the end access plate, and a high-vacuum gauge coupled to the opposite end plate. The large chamber measures 5 11/16" ID x 10", and makes it possible to test larger cells or groups of cells. The 5" cross is removed when using this large chamber; there are four 1 3/8" ID x 1 1/4" stand-offs in the wall of the cylinder for the mounting of the high-vacuum gauge, the high-vacuum pump, the valve to the roughing pump, and electrical inputs. The system is shown in Fig. 29, p. 75.

A. DISCUSSION OF SYSTEM COMPONENTS

The need for absolute cleanliness and simplicity of operation led us to choose a molecular sieve sorption-type roughing pump. The pump is connected to the chamber through a 1" bellows-type high vacuum valve.

The high-vacuum pump chosen after some investigation is a diode-type getter-ion pump. Slotted cathodes are used to increase the pumping rate of noble gases; this was judged advisable since many of the cells to be tested in the system were to be heli-arc welded, and would be expected to release occluded helium and argon. The pump uses a magnetically-confined cold-cathode gas discharge which promotes sputtering of active metals. The pumping rate is 8 l./sec. The connection between the pump and the test chamber was kept as short as possible so as to provide high conductance and minimize pump-down time; the conductance is 40 to 45 l./sec. When using the small test chamber, these values compare favorably with the values recommended in the literature. B. B. Dayton* recommends that for a system operating as low as 5×10^{-5} to 10^{-6} torr, the pumping speed (in l./sec.) should be equal to 2 or 3 times the volume of the system (in liters) in order to provide reasonably short pump-down time and to adequately overcome outgassing. The internal volume of the small chamber plus high-vacuum pump is roughly 0.5 liter; the large chamber plus high-vacuum pump has a volume of roughly 4.5 liters.

FIG. 28. IONIZATION PUMP CURRENT VS. PRESSURE

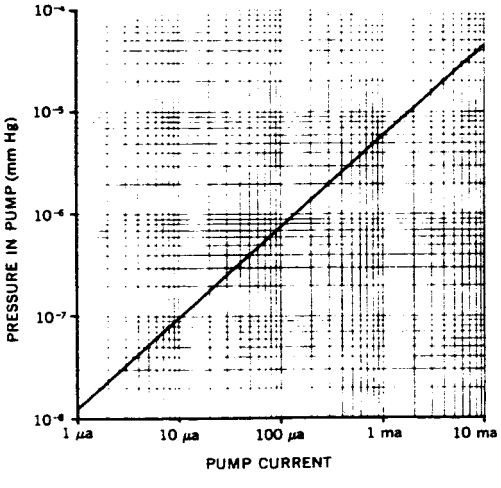

The curve of current drain versus pressure for this pump is given in Fig. 28. It will be seen that the minimum current to which this unit is sensitive corresponds to a pressure of approximately 1.2×10^{-8} torr. In actual practice, the pump current becomes increasingly independent of pressure as the system approaches base pressure, which of course may be considerably higher than 1.2×10^{-8}. That is, as an equilibrium is reached between the pumping rate and the total of leak plus outgassing rates, the pump-down curve becomes increasingly flat, and the changes in current per unit time become too small to detect.

One of the problems in using this type of pump is the re-emission of adsorbed gases into the system when the pump is turned off. This is particularly bothersome when monitoring the pressure rise in a closed static system. This difficulty would be remedied by the addition of a high-vacuum valve between the pump and the chamber.

The high-vacuum gauge chosen is an inverted ionization gauge of the Bayard-Alpert type, using a non-burnout thoria-coated iridium filament. Among the advantages of this gauge type are the following:

(1) This type and the cold-cathode ion gauge with magnetic field (the magnetron) have the widest operating range of any gauge type. Although the magnetron is somewhat more sensitive (can be used

* "Relations Between Size of Vacuum Chamber, Outgassing Rate, and Required Pumping Speed"; Vacuum Symposium Transactions, 1959, 101.

at pressures as low as 10^{-10} or 10^{-12} torr), it is somewhat erratic in its operation and is more tricky to use. It requires a fairly large power supply, which somewhat offsets the advantage it has over the Bayard-Alpert of requiring simpler supporting electronic circuitry.

(2) The Bayard-Alpert is more reliable than many other types of high-vacuum gauges. It has been produced in some quantity, the factors leading to error are fairly well known, and results taken from it are reasonably reproducible.

(3) With the appropriate equipment, the gauge is simple to operate.

(4) The Bayard-Alpert is reasonable in cost and is readily available commercially.

Among the several disadvantages of the Bayard-Alpert gauge, the following are the most relevant for this system:(*,†)

(1) The gauge itself acts as a pump, and thus obscures the reading of test chamber pressure. The conductivity of the tube portion of the glass gauge envelope, which connects to the test chamber, is high enough (15 l./sec.) that virtually all the pumping effect of the gauge will be felt by the system. There are two components of this pumping: (a) electronic pumping, due to the removal, without their being read, of positive ions by bombardment of the electrodes and the glass envelope, and (b) chemisorption of gases on the pump components. This latter type of pumping will continue even when the pump is turned off, to an extent determined partly by the characteristics of the gas molecule involved. The pumping speed of a Bayard-Alpert gauge was found by one investigator to be 2 l./sec. for nitrogen at pressures in the neighborhood of 10^{-4} to 10^{-8} torr. The pumping speed for air is roughly the same. It was found by this investigator that a saturation point was reached and the chemical pumping ceased when 10^{15} molecules of nitrogen had been pumped. The electronic pumping continued until 10^{17} molecules had been pumped, and then rapidly decreased. For a fresh gauge, this saturation of the pumping should occur within one day's operation; our gauge was operated for two days before system readings were attempted, as a safety precaution.

(2) The gauge must be thoroughly outgassed before the performance of each test; this, it is true, is a disadvantage that it shares with most gauges except the magnetron. The degassing can be done by passing a large current (10 amps) through the grids; in addition to degassing the grid, this degasses the collector by radiation. One solution to the pumping problem described above would be to use the gauge only for short periods of time during a test. This, however, is hard to do because of this outgassing problem; large amounts of gas would be re-emitted from the gauge components every time the gauge is turned on. This, as well as the aforementioned re-emission pumping, is a problem which would be resolved by incorporating a high-vacuum valve — in this case, the valve would be placed between the gauge and the test chamber. Degassing of the filament is attended by its own disadvantage: alkaline metal impurities are driven from the interior of the filament, where they are harmless, to the surface, where they can be emitted and may affect the ion current.

(3) A residual current exists at the collector of a Bayard-Alpert gauge which is independent of pressure. This current is caused by subjection of the collector to (a) x-rays generated as the grid is bombarded by electrons, and (b) ultra-violet energy from the filament and from the external environment. This residual current will cause errors in the reading of pressure, particularly at low pressures. The Bayard-Alpert gauge will not reliably provide absolute pressure values below 10^{-8} torr; at these low pressures, it is used only to provide relative pressure information.

(4) There are chemical effects at the hot filament. The disassociation, decomposition, and recombination of the gases being measured, which are due to the high temperature (725°C and over) at which the filament operates, can be serious, particularly for investigators working with hydrocarbons, water, and hydrogen. In our case, it was noticed that when testing cells with very large leaks, there was a reduction in filament current; chemical phenomena at the filament must be considered as one of the more probable causes for this effect.

B. HISTORY OF DEVELOPMENT OF TEST SYSTEM

The original system design recommended by the supplier (Varian Associates), delivered on June 30, 1961, included a back-filling valve on the chamber wall, and a pump without slotted cathodes. We found that as this system was baked out, the system pressure would fall, only to rise again when the system cooled. We were not able to find the source of this pressure rise following bakeout. The supplier suspected the effects of noble gases, which would be presumed to be helium and argon entrained in the cell weld area during the

* "Errors in the Measurement of Pressure with Ionization Gauges," by P. A. Redhead; **Vacuum Technique,** by Saul Dushman; p. 108.

† **Scientific Foundations of Vacuum Technique,** by Saul Dushman; John Wiley and Sons, Inc., 1962, pp. 331-334.

heli-arc welding. The supplier recommended at this point that we try the slotted-cathode type pump, so as to improve the pumping efficiency for noble gases. A slotted-cathode pump was received and mounted on the system, with no improvement in system characteristics. The entire system was then returned to the supplier (August 30, 1961).

The supplier found that the back-fill valve in the test chamber wall was leaking at the weld joint. This valve was not absolutely essential to the operation of the system, and was eliminated. The system continued to behave erratically, and the slotted-cathode pump which had been sent to us to replace the original pump, was in turn replaced with another slotted-cathode pump. It was finally determined that there were leaks in the weld joints of the test chamber (the 5″ cross), and this component was replaced. These changes resolved the problem, and the system was returned to us on November 3, 1961.

The system in its final form, with the large test chamber installed, is shown in Fig. 29, which follows.

FIG. 29. HIGH-VACUUM TEST SYSTEM

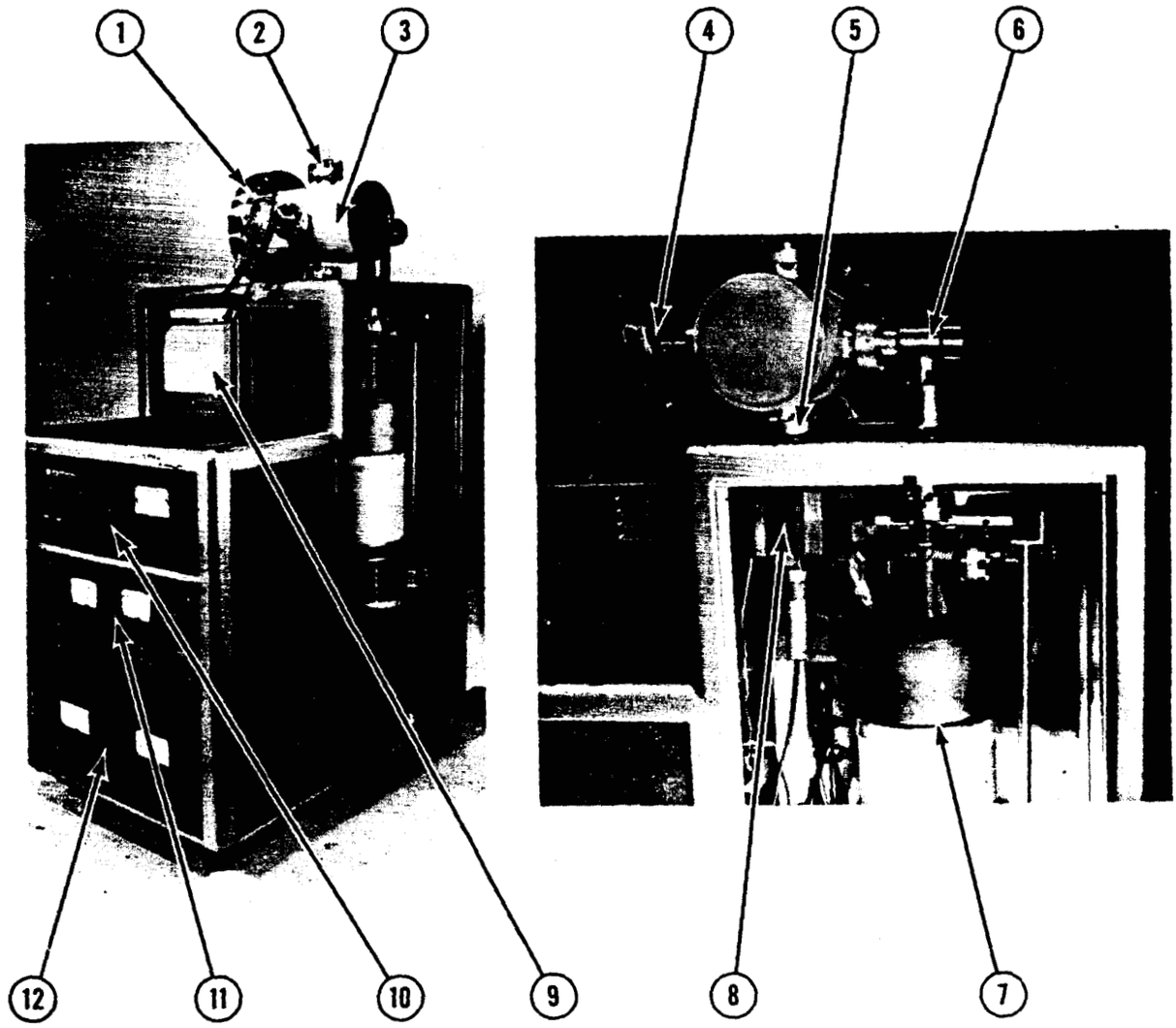

1. Entrance port
2. Electrical lead-ins
3. Test chamber
4. Ionization gauge
5. Port to Vaclon pump
6. High-vacuum valve
7. Roughing pump with DeWar flask
8. Vaclon pump
9. Recorder
10. Vaclon pump control unit
11. Ionization gauge control unit
12. Power supply

III. ALTERNATIVE TEST METHODS — CALIBRATION

A. DISCUSSION OF TEST METHODS

The "elevated base pressure" test method, as originally conceived and described in the program proposal, involves determination of system pressure by reading current drawn by the getter-ion pump. The high-vacuum gauge is used only for system evaluation and calibration purposes. This makes it possible to obtain leak test information within a very short period of time relative to other high-vacuum methods. Most high-vacuum testing involves sealing off the evacuated chamber containing the test article, and observing the rise of chamber pressure over a prolonged period of time. Reading pump current, however, provides leak information within a few hours (in some cases, in less than an hour), while the system is running, without requiring that the chamber be sealed off. The base pressure of the system itself is determined by running the system with no test cells in the chamber. At this base pressure, pumping speed (which is known) is in equilibrium with system leakage and system outgassing (which can now be calculated). A cell is then placed in the test chamber and current drain is plotted against time as the system is pumped down. The system is run until the base pressure has been reached, and the curve of current drain (or pressure) versus time becomes horizontal, as is shown in Fig. 30. At a reasonable length of time after the base pressure has been reached (T_1 in Fig. 30), the cell is overcharged, which will result in an increase of cell internal pressure from 1 atmosphere to roughly 5 or 7 atmospheres. This increase in pressure will greatly accelerate any leak rate that the cell has; system pressure should rise sharply, and would level off at some new, elevated equilibrium pressure. Curves 2, 3 and 4 in Fig. 30 would represent pressure curves obtained from cells with varying leak rates. The difference between this new equilibrium pressure and the base pressure can be calculated against the known pumping rate of the high vacuum pump to give the cell leak rate.

FIG. 30. IDEALIZED PRESSURE VS. TIME CURVE, ELEVATED BASE PRESSURE METHOD

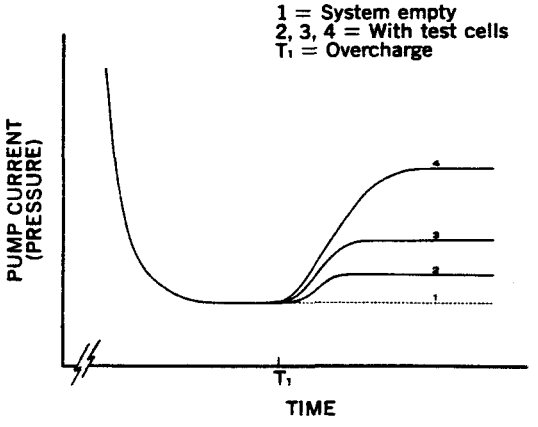

The assumption here is that, with proper cleansing of the cells prior to testing, outgassing from the exterior of the cell is negligible compared with any significant leak. However, if the leaks are small and the difference between the system base pressure and an actual elevated pressure is minor, it would be necessary to distinguish between cell leakage and outgassing from the cell exterior. In this case, a solid dummy would be fabricated from the same metal as the cell cans, to the dimensions of the cells to be tested. Running this dummy in the test system would indicate the amount of cell outgassing, which would then be subtracted from subsequent system readings to give the true cell leakage value.

This method has the advantages of accepting cells of any physical design, of being relatively fast, and of testing cells under the actual operating conditions — that is, while they are being overcharged.

FIG. 31. IDEALIZED PRESSURE VS. TIME CURVE, RATE-OF-RISE METHOD

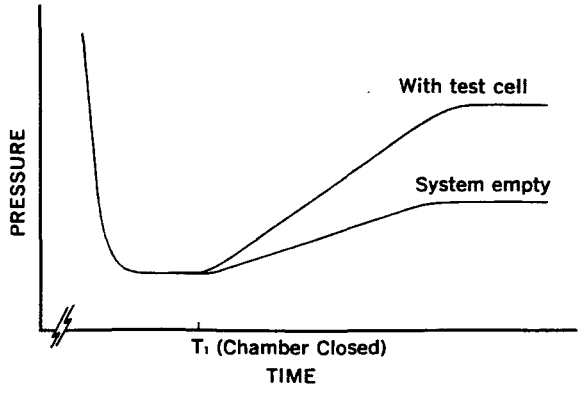

The "rate-of-rise" method is the second general method that can be used with this test system. This method, though slow, can be used either for providing actual leak information, or for system calibration. The first step is to pump down the empty system, close off the test chamber, and monitor the chamber pressure over a prolonged period of time — perhaps several days — as the pressure rises. This is repeated several times until consistent curves are obtained. Then a test cell is placed in the chamber, and the chamber is evacuated, sealed off, and monitored as before. A new rate of pressure rise will be observed, the actual rate depending on the leak rate of the cell, and a new equilibrium pressure will be reached, as illustrated in Fig. 31. As with the previously-described elevated base pressure method, cell leak rate can be calculated from the difference between these 2

equilibrium pressures, or it can be determined from the slope of the pressure rise curves; the latter method will generally prove less time-consuming.

A major problem in most high-vacuum technology is outgassing. It is possible, with this rate-of-rise method, to correct for the effects of system or cell outgassing. As the pressure in the test chamber rises, the rate of outgassing from cell or system walls will decrease exponentially, resulting in a flat pressure/time curve at a certain equilibrium point. However, the supply of gas within a test cell is essentially infinite. The pressure rise due to cell leakage should therefore increase linearly far beyond the point where the outgassing begins to taper off, and should reach an equilibrium pressure significantly above the outgassing equilibrium. Using a solid dummy cell, the amount of outgassing can be calculated from the difference between these 2 curves, as was described above in the discussion of the elevated base pressure method.

One major complicating factor in the performance of this method is the pumping effect of the high-vacuum gauge. Most gauges, other than the magnetic cold-cathode ionization gauge, have this pumping effect. This gauge pumping reduces the sensitivity of the test, by reducing the difference between the pressure rise curves of an empty system and a system containing a test cell — that is, it will flatten out the pressure vs. time curve of the test cell, making it more nearly equal to that of the empty system.

The "pump-down" method is the third general test method that can be performed with this system, and is the fastest of these 3 test methods. Here again, the first step is to run the empty system several times, and determine the slope of the standard pump-down curves, the time at which the knee of the curve is reached (T_1 in Fig. 32), and the equilibrium pressure value. The test cell is then placed in the chamber, and the pressure (via the pump current) is carefully monitored as the system is being pumped down. With leaks of increasing magnitude, the slope of the pump-down curve will decrease, the time required to reach the knee of the curve will increase, and the equilibrium pressure will be of increasingly higher value. The pump-down curve may not exhibit as sharp a knee as has been shown in Fig. 32 for the sake of illustration, but measuring the time necessary to reach a certain empirically-chosen pressure value — say 10^{-7} torr — is quite satisfactory. By running a standard leak or a series of test cells, it is possible to establish a pair of pressure and time values such that any cells which do not reach the given pressure in the required time are known to be leaking at a rate in excess of the acceptable rate. Such a time and pressure are indicated by P_4 and T_4 in Fig. 32. As can be seen, this time can be made considerably shorter than the time required to reach equilibrium, which greatly reduces the time required per test.

FIG. 32. IDEALIZED PRESSURE VS. TIME CURVE, PUMP-DOWN METHOD

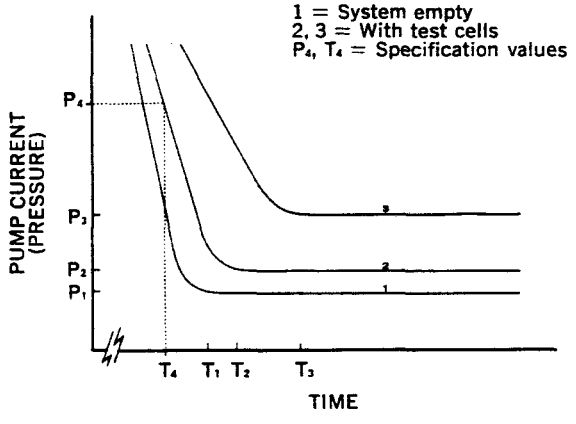

B. CALIBRATION

Calibration was originally attempted with the rate-of-rise method, as described above. As was feared, however, the pumping action of the Bayard-Alpert gauge had an inordinate effect on system pressure. Furthermore, in several of the attempts the system pressure rose at a steady rate for 8 to 10 days before tapering off, which is far too long to be workable. The cell closure technics had by this time been developed to the point where many of the test cells being used in these calibration attempts had very low leak rates, and produced pressure rise curves that were too close to the curve of an empty system for reliable calculation. Also, it was noticed that in some of the longer attempts, the pressure rise curve would reach the equilibrium pressure, flatten out, and then exhibit pronounced fluctuations, which might have been due to imperfect control of room temperature.

These difficulties led us to abandon the rate-of-rise method of calibration. A Granville-Phillips variable leak was acquired and was submitted to Nuline Industries for certified calibration. The leak was then fed into both the small (5" cross) and the large 5 11/16" (ID x 10") test chambers, and system pressure readings were taken; these standard values are given in Table 30. These system pressures were then plotted against the known leak values of the variable leak to give the standard curves of system pressure versus leak rate (shown in Fig. 33). These values are for the leakage of air; air leaks at a rate which is close enough to the leakage of KOH vapor that no conversion of leak values from air to KOH was thought to be necessary in any phase of this program.

TABLE 30. VACUUM SYSTEM CALIBRATION VALUES

TURNS INDICATOR READING	CERTIFIED LEAK RATES (atm. cc/sec.)			SYSTEM PRESSURE (torr)	
	MAX.	MIN.	AVG. OF 5	MAX.	MIN.
0					1.8×10^{-8}
25	1.12×10^{-9}	0	6.72×10^{-10}		
26	5.6×10^{-9}	5.6×10^{-10}	2.8×10^{-9}		
27	1.68×10^{-8}	3.36×10^{-9}	8.29×18^{-8}		
28	5.04×10^{-8}	2.28×10^{-8}	4.0×10^{-8}	3×10^{-8}	2.1×10^{-8}
29	4.14×10^{-7}	2.12×10^{-7}	3.02×10^{-7}	3.5×10^{-7}	2.2×10^{-8}
30	7.33×10^{-6}	3.36×10^{-6}	4.94×10^{-6}	5×10^{-7}	7×10^{-8}
31				1.5×10^{-6}	3×10^{-7}
32				9×10^{-6}	9×10^{-7}
33					9×10^{-6}

FIG. 33. STANDARD CURVE, SYSTEM PRESSURE VS. LEAK RATE

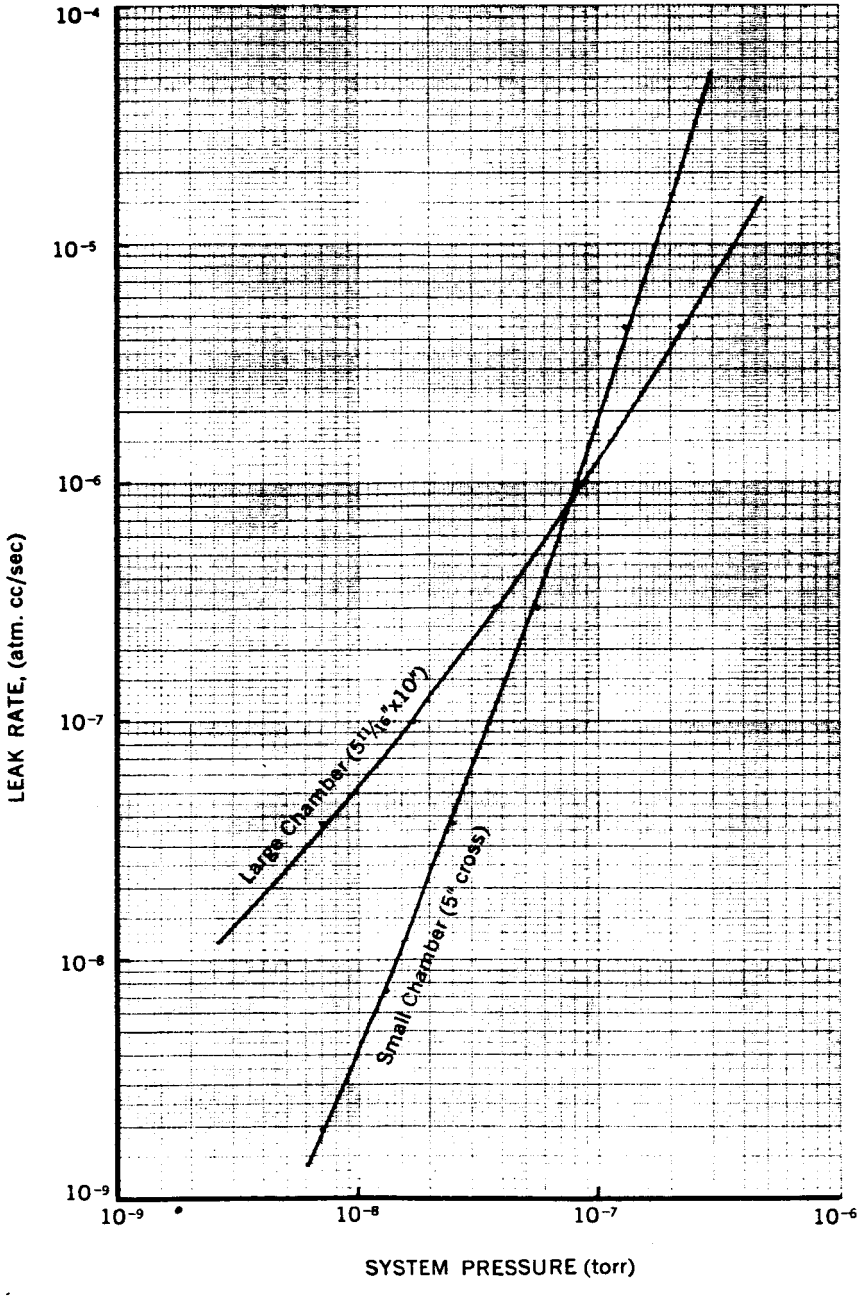

IV. EXPERIMENTAL TEST PERFORMANCE

A. PREPARATION FOR TEST

The preparation of the system itself, after it had been assembled and the valves and seals had been checked out, involved baking at 300°C for 3 to 4 hours. After this bake-out the empty system was pumped down; the base pressure established was 2 to 4 x 10^{-9} torr. This bake-out is necessary whenever significant quantities of ambient air have been allowed to enter the system, or when it has been contaminated by a badly leaking cell. Inability to reach the standard base pressure within a reasonable length of time will indicate when the system requires a bake-out. In the absence of the back-fill valve, contamination of the system as it is opened is prevented by applying a dry nitrogen stream around the flanges to be separated in opening.

The cells to be tested were first evaluated electrically, according to the following schedule:

— Formation cycling (charge; discharge at the 5 hr. rate; repeat for total of 3 cycles)
— Charge
— High rate discharge performance (discharge at the 2 hr. rate)
— Overcharge (charge for 72 hrs. at the 4 hr. rate)
— Open circuit stand (leave on open circuit for 72 hrs., in the discharged state)
— Charge at the 10 hr. rate
— Discharge at 1.8 amps to .8 V (later cells discharged at 1.5 amps)
— Charge
— Final capacity check (discharge at the 5 hr. rate to 1.0 V)
— Charge

Following this electrical evaluation, the test cells were then cleansed. Each cell was cleaned individually. Carbon and other deposits from the heli-arc welding were removed with nitric acid (concentrated). The test cell was then washed in acetone, or in the following carbonate-silicate solution: 6.5 g. sodium carbonate, 40 g. sodium metasilicate, 20 ml I-glyptol (CO-710), in 1 liter water. These cells were then rinsed in water for 15 minutes followed by a rinse in acetone, and were dried in a dry nitrogen stream. There was no discernable difference in test performance between those cells that were cleansed in acetone only following the nitric acid purge, and those that were cleansed in the carbonate-silicate solution.

B. ELEVATED BASE PRESSURE METHOD

Overheating of the test cells proved to be a major obstacle in the development of this method. Cells were placed in the chamber as planned, and the system was pumped down to base pressure. In many cases, base pressures in the order of N x 10^{-8} were reached. The cells were then overcharged at the 10 hour rate; it was expected that this would yield an observable increase in pressure, from which the leak rate of the cell would be calculated.

With most of the cells tested, an increase in system pressure was observed, which was of much greater magnitude in the first test than in subsequent tests; moreover, in any tests beyond the first test done on a particular cell, the pressure rise was more gradual than had been expected, and was not evident for several hours after the overcharge was applied. The most prominent feature of these curves, however, was the sharp decrease in charge voltage as the overcharge was continued, which generally indicates elevated cell temperature. These cells were warm to the touch when removed from the test chamber.

Fig. 34 gives the curves of system pressure and cell on-charge voltage for the first and the third test runs of one of these cells. It will be noted that on the first run, the pressure rise following application of overcharge (at time "A") was considerable. This was assumed to be due to outgassing from the cell exterior, which at an elevated cell temperature would be accelerated, and which would be greatly reduced on subsequent runs since most of the adsorbed gas would by then have been driven off the cell exterior. The correlation between the temperature of a nickel-cadmium cell and its on-charge voltage had previously been roughly established in other test programs; our estimate of the temperature of a cell having an on-charge voltage of 1.324 V (as shown in Fig. 34) was 140°F. On the third trial, the chamber was quickly opened as soon as the charge current was cut off, and a contact thermocouple was applied to the cell can; the temperature recorded was 140°F.

This phenomenon reinforces the findings of other organizations, that overcharging of cells used in space applications is to be held to an absolute minimum. The phenomenon is somewhat puzzling in that cells in our chamber are laying on the wall of the metal test chamber; in some cases there was additional metal-to-metal contact between the cell bottom and one end of the test chamber. It might be expected that this amount of contact to the metal mass of the test system would be enough to outweigh any conductivity effects resulting from the presence or absence of air in the test chamber. This, however, is apparently not the case. There is

serious question whether it would be possible to provide cell heat sinking adequate enough that the elaborate control over the charging of sealed cells now necessary in space applications, could be reduced or eliminated. And, of course, a cardinal problem in the establishment of any design involving thermal conductive paths between the cells and a heat sink, is the electrical isolation necessary to avoid shorting the cells.

Another area of question is the cause for the delay that exists between the application of overcharge current and the beginning of the rise in system pressure, and for the much lower than expected rate of increase of system pressure. There is some indication that, as the nickel-cadmium system is charged, higher oxides are formed than have generally been accounted for in formulations of the cell reactions; it is thought that these higher oxides are unstable, decomposing within a relatively short time following the termination of charge. It may be that the time lapsing between the removal of the cells from the charging circuit and their placement in the test chamber is sufficient for these higher oxides to decompose, and that a certain length of time is required following the application of overcharge current to regenerate them before the evolution of gaseous oxygen rises to a point where system pressure is increased. Moreover, as can be seen from the charge voltage curve, the cell is overheated within a relatively short period of time following the application of overcharge current; the rate of recombination of oxygen and the self-discharge rate in such an overheated cell would be accelerated, both of which mechanisms would have a suppressive effect on the slope of the pressure rise curve.

FIG. 34. CELL CHARGE VOLTAGES AND SYSTEM PRESSURES ON OVERCHARGE

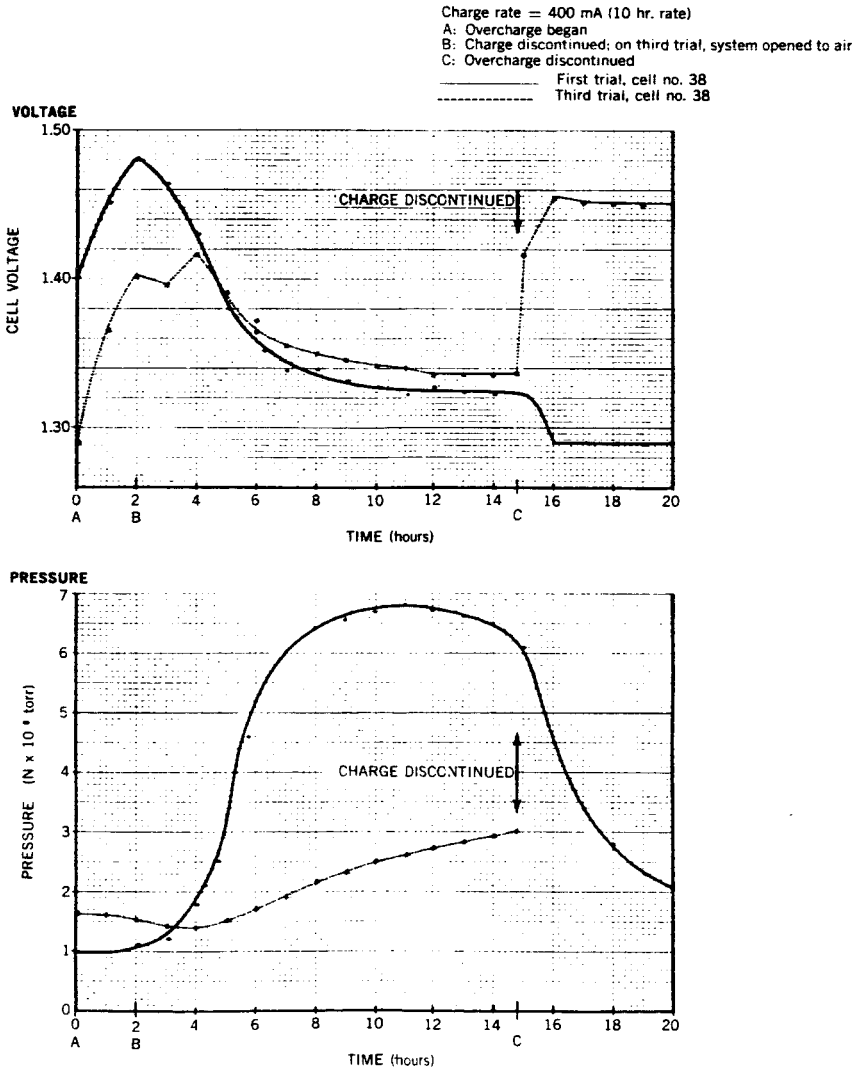

C. RATE-OF-RISE METHOD

The difficulties experienced with the elevated base pressure method led us to actively consider the rate-of-rise technic of cell testing. Rate-of-rise curves of the empty system had been established in the course of system calibration. Calibrating for the performance of seal tests, then, would simply be a matter of performing a rate-of-rise test run with the calibrated leak feeding into the test system at a rate considered to be the maximum allowable for the particular cell design type. Routine testing would then involve comparing the slope of a given test curve with this maximum allowable curve.

Fig. 35 gives the rate-of-rise curves of the empty system, and of three typical cells, one cell with a heli-arc weld closure, one with projection weld closure, and one with our present nylon gasket commercial seal. As can be seen, the curves of the two welded cells are not greatly different from the curve for the empty system. All the curves are somewhat irregular; the slope of the curves in the pressure range of 10^{-4} to 10^{-5} torr does not bear good relationship to the slope in the higher pressure ranges (above 2×10^{-5} torr). Some of these irregularities are assumed to be due to irregularities in the performance of the Bayard-Alpert gauge. Furthermore, as has been discussed previously, the pumping effect of the Bayard-Alpert gauge distorts these pressure rise readings. The final factor that led to the abandonment of this method of seal testing was that the time required to obtain meaningful curves was too long to make it possible to test cells in any significant volume.

FIG. 35. TEST CURVES OBTAINED BY RATE-OF-RISE METHOD

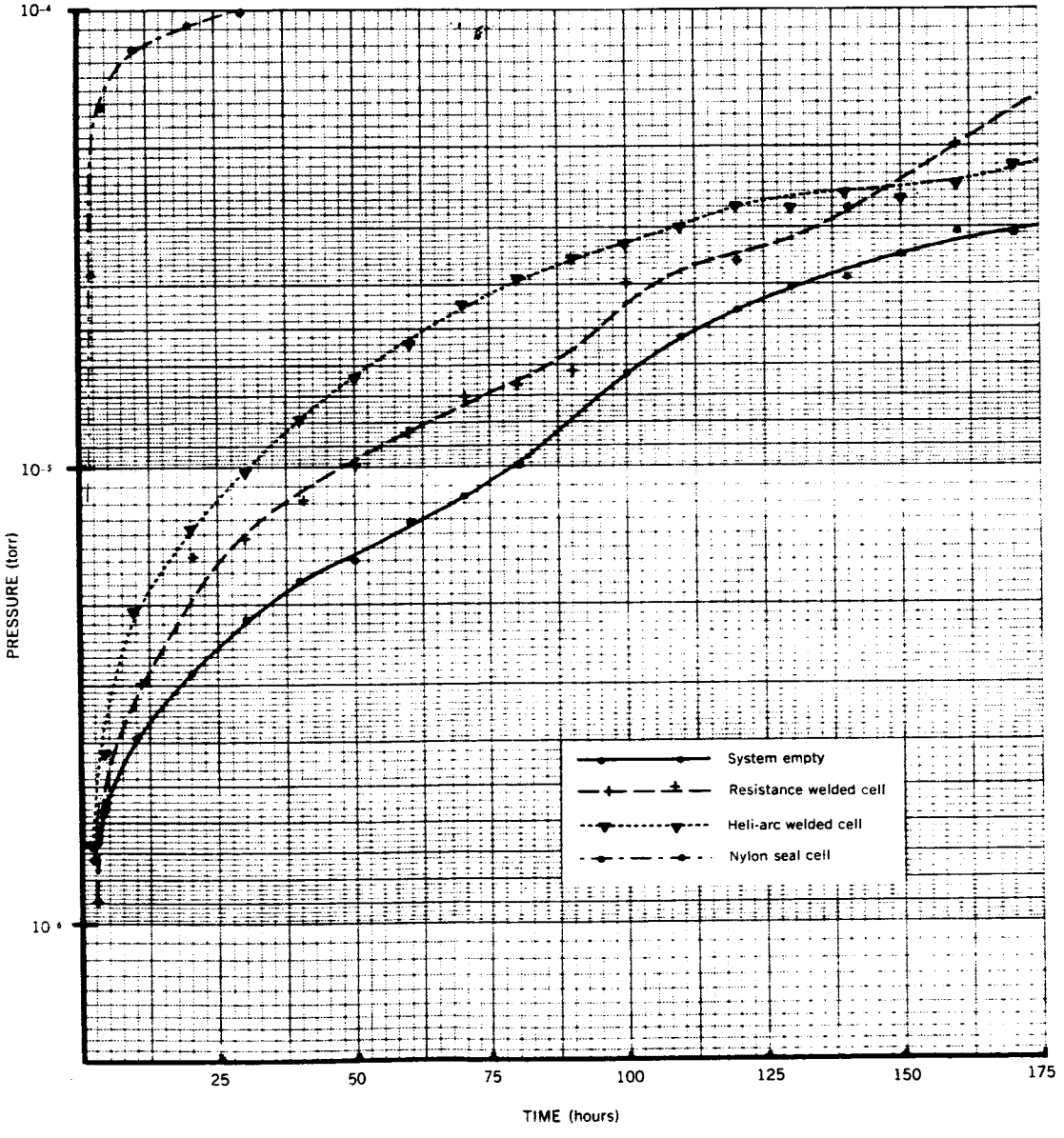

D. PUMP-DOWN METHOD

The most successful of the seal test methods evaluated was that involving the analysis of the curves obtained during pump-down of the system. This method involves establishing the standard pump-down curve of the empty system, and then comparing against this the pump-down curves obtained with test cells in the chamber. Pump-down data gathered from the empty system and from several test cells is presented in Table 31. The preponderant majority of these cells had heli-arc weld closures, since the projection weld technic was not developed to a satisfactory level of performance until quite late in the program.

With the vacuum system at the present level of development, it is generally possible to draw some idea of the quality of the cell seal within one hour after closing the test chamber; it has been empirically established that failure to reach a pressure of 4×10^{-7} torr within 4 hours indicates a leak rate in excess of 5×10^{-7} atm. cc/sec.

Test curves obtained with the empty system and with typical cells in the chamber are presented in Fig. 36.

TABLE 31. SEAL TEST PERFORMANCE, PUMP-DOWN METHOD

DATE	CELL NO.	TIME TO: 10^{-6} (Min.)	TIME TO: 10^{-7} (Hr.)	BASE PRESSURE (Torr)	LEAK† (Atm. cc/sec.)
CELLS WITH HELI-ARC WELD CLOSURE:					
12/7/62	empty	7	1	2×10^{-6}	
2/28/62	empty	2	.5	1.5×10^{-6}	
2/29/62	empty	2	2	1.5×10^{-6}	
2/30/62	empty	2	1	1.5×10^{-6}	
12/8/62	Nylon seal	60		7×10^{-7}	
8/2/62	Nylon seal			7×10^{-6}	7×10^{-7}
12/1/61	3	15	9.66	8×10^{-6}	
12/2/61	3	6	9.66		1×10^{-7}
12/3/62	3			7×10^{-6}	7×10^{-7}
1/30/62	25	10	3	3×10^{-6}	
1/31/62	25			1.5×10^{-6}	$<1.5 \times 10^{-7}$
1/30/62	25	5	3	2.5×10^{-6}	
3/10/62	38	3-4	.66	2×10^{-6}	
3/11/62	38			7.5×10^{-9}	$< 8 \times 10^{-6}$
3/17/62	38	2	.66	1.5×10^{-6}	
12/7/61	41	9	4.75	2×10^{-6}	
1/9/62	41	4	2	2×10^{-6}	
1/10/62	41	5	2	2.5×10^{-6}	
3/1/62	41	5	4.5	1.5×10^{-6}	
3/23/62	51	4	.92	2×10^{-6}	
3/62	51			1×10^{-6}	$< 1 \times 10^{-7}$
3/24/62	51	5	5	2×10^{-6}	
3/62	52		3.5		5×10^{-7}
3/8/62	52	5		2×10^{-6}	
3/18/62	53	6	9	1×10^{-7}	
3/19/62	53			8.6×10^{-6}	9×10^{-7}
3/20/62	53	5	9	8×10^{-6}	
1/25/62	57	5	18	1×10^{-7}	
1/25/62	57	10	18	1×10^{-7}	
1/26/62	57	10	10.25	8×10^{-6}	
1/18/62	64			2×10^{-6}	$< 2 \times 10^{-7}$
1/19/62	64	5	1.5	2.5×10^{-6}	
1/27/62	72	4	1.42	2×10^{-6}	
2/5/62	72	4	.83	2×10^{-6}	
2/9/62	72			1.5×10^{-6}	$<1.5 \times 10^{-7}$
2/1/62	72	5	3.75	3×10^{-6}	
2/21/62	72	5	1.5		
1/29/62	85			1×10^{-7}	1×10^{-6}
CELLS WITH PROJECTION WELD CLOSURE:					
8/13/62	2	20	8		2×10^{-6}
8/27/62	4	18	7	2×10^{-6}	
9/10/62	5	18	6	2×10^{-6}	

†Leak values reported are for air, which leaks at rates roughly comparable to KOH vapor.

This contract did not involve work toward a specific cell design. It might be of benefit to the reader, however, to report the design characteristics of the cell used as a research vehicle. This was a cell of "D" configuration, having a nominal capacity of 3.5 AH (cells of this general configuration having conventional rather than glass-to-metal seals, have a nominal capacity of 4.0 AH). Operating characteristics are as recommended for the majority of Gould-National sealed cell designs:

— Discharge rates: optimum capacity delivered at the C/5 to C/10 rates; roughly 10% of capacity lost at C/1 rate; absolute maximum discharge rate: C/.1 .

— Charge rates: C/10 recommended; cells will take continuous overcharge at this rate.

— Capacities: as produced, the 3.5 AH cells will vary from 3.4 to 4.1 amp-hrs.

Physical design characteristics are as follows:

ITEM	MATERIAL	DIMENSIONS (in.)	
Positive electrode	NiOOH impregnated into a sintered nickel plaque	18.75 x 1.625 x .025	
Negative electrode	Cd impregnated into a sintered nickel plaque	16.50 x 1.750 x .020	
Separator	Pellon 2505	39.75 x 1.937 x .011	
Can	Pure nickel	1.280 O.D. x 2.240	Many of the cells earlier in the program were built with .016" stock. Later, this was increased to .020".
Cover	Pure nickel	See dwgs. MHA 101732, p. 61, and MH 101435, p. 67	
Glass seal insert ring	Kovar	.450 O.D., .285 shoulder I.D.	
Positive terminal pin	Kovar	.155 O.D. x .345	
Glass seal	Proprietary with supplier, Zell Industries (thought to be Corning No. 7025)	—	
Inner seal diaphragm	Pure nickel	See dwg. MHA 101747, p. 50	
Inner seal nylon gasket	Molded 101 nylon	.240 shoulder O.D., .147 I.D. x .060	
Plate connector tabs	Pure nickel	Pos.: 1.625 x .250 x .005 Neg.: 1.375 x .250 x .005	
Positive terminal lug	Pure nickel	1.0 x .125 x .010	
Sub-cover insulator	Molded 101 nylon	1.235 O.D.	
Element insulating discs	Sheet 101 nylon	1.235 O.D. x .015	
Insulating tape	½" 3-M No. 472	—	
Electrolyte	30% KOH	—	

The positive electrode weighs 16-17 gm, the negative 28-29 gm. The completed cell with cover and can of .020" stock weighs 135-140 gm — with .016" stock, 120-125 gm.